UNIVERSITÀ DEGLI STUDI DI MILANO

GRADUATE SCHOOL IN PHARMACOLOGICAL SCIENCES/
SCUOLA DI DOTTORATO IN SCIENZE FARMACOLOGICHE

DIPARTIMENTO DI SCIENZE FARMACOLOGICHE E BIOMOLECOLARI

XXVI CICLO

SYNAPTIC AVAILABILITY OF GLUN2A SUBUNIT OF NMDA RECEPTORS FROM PHYSIOLOGICAL MECHANISMS TO PATHOLOGY: THE ROLE OF RABPHILIN 3A

Settore Scientifico-Disciplinare: BIO/14

DOTT. JENNIFER STANIC
Matr. N. R09365

TUTOR: Prof.ssa MONICA DI LUCA & Dr. FABRIZIO GARDONI

COORDINATORE: Prof. ALBERTO PANERAI

ANNO ACCADEMICO 2012/2013

« Dans la vie rien est à craindre, tout est à comprendre. »[*]

- Marie Curie

[*]Nothing in life is to be feared, it is only to be understood.

Acknowledments

This Ph. D. has been a long journey, which at times seemed longer and uncertain. But the love and support of many people helped me face the difficulties and stride forward with renewed strength. So today when I write the dissertation for the completion of my Ph.D., it is time to express my heartfelt gratitude to all those friends, companions and family members whose invaluable support has smoothened the path till here.

First of all, I would like to thank my thesis advisors, Prof. Monica Di Luca and Dr. Fabrizio Gardoni, for giving me the opportunity to work with them. Their tremendous enthusiasm about my research motivated me to overcome the obstacles and move ahead with undiminished spirit. Their encouragement for independent thinking helped build confidence in my scientific pursuits. Their intense mentoring and valuable inputs in the course of my work have provided a wholesome training for me as a graduate student. Next, I would like to express my sincere gratitude to our close collaborators in this study, Prof. Christophe Mulle and Dr. Mario Carta, University of Bordeaux II, for welcoming me in their lab, teaching me patch-clamp recordings and continuing the experiments needed for this project. My sincere thanks also goes to Prof. Paolo Calabresi, Dr. Barbara Picconi and Valentina Pendolino, IRCCS Santa Lucia Foundation, for teaching us the techniques to obtain and study the rat PD and LID models. I also sincerely acknowledge SyMBaD, International Training Network Marie Curie Actions for the financial support in the form of grant agreement and fellowship with which this Ph.D. has been accomplished as well as for the training opportunities. Many thank to the members of my student advisory panels from the SyMBaD, Dr. Carlo Sala, CNR, and Dr. John Hanley, University of Bristol for their inputs and many suggestions through the course of the program. I would like to also thank Dr. Andreas Frick for his mentoring during my master studies and for his very important advice and encouragements to apply for SyMBaD and follow Prof. Monica Di Luca.

I am thankful to my lab colleagues for a friendly and supportive environment that has been crucial for my work during all these years. More specifically, I am most grateful for Dr. Manuela Mellone, Elisa Zianni and Annalisa Longhi for their tremendous helps as part the PD team. I extend my sincere gratitude to both former and current lab members, including Elena, Csaba, Margarita, Claudia, Stefano, Silvia, Francesca and Luana for their friendly interactions and help that made my work and life easier and enjoyable.

I would like to extend my huge warm thanks to my friends and family without whom life would not be so pleasant and entertaining. In particular, I would like to thank Marine, Ghjuvan and Audrey for their sympathetic support and understanding as old friends from university who are doing a Ph. D. themselves back home in France; Jonathan, my fellow SyMBaD here in Milan; Liora, Josquin and Sebastien for their never failing belief in me; Renaud for infecting me with his passion (you will always be my mentor); my parents for teaching and encouraging me to find answers.

Finally, I take this opportunity to express my profound gratitude from the depth of my heart to my brother Philippe for his unconditional love and unfailing support through the ups and downs of my journey till this point. From the very begining, Philippe, you have always believed in me, always been by my side, always pushed me to attain further goals in my studies and life and always tried to help weither you could or couldn't.

Jennifer

INTRODUCTION

I. N-methyl-D-Aspartate receptors

The amino acid L-glutamate is the principal excitatory neurotransmitter in the mammalian central nervous system (CNS). After its release from presynaptic nerve terminals, it interacts with a variety of receptors located in the neuronal membrane. According to the mechanism by which their activation generates the cellular response, glutamate receptors are classified into two broad categories: ionotropic and metabotropic. Ionotropic glutamate receptors (iGluRs) are nonselective ion channels that flux cations upon agonist binding, thus producing a depolarizing current. Metabotropic glutamate receptors (mGluRs) are G-protein-coupled receptors that, on binding glutamate, trigger intracellular signaling cascades following activation of the coupled G proteins. iGluRs can be subdivided into three large families (Traynelis et al., 2010) on the basis of agonist selectivity: *N*-methyl-D-aspartate (NMDA), α-amino-3-hydroxy-5-methyl-4-isoxazole proprionic acid (AMPA) and kainate (KA). Since their discovery three decades ago, NMDA receptors (NMDARs) have kept fascinating neuroscientists because of their central roles in CNS function. NMDARs are cationic channels permeable to sodium (Na^+), potassium (K^+), and calcium (Ca^{2+}) ions. They constitute the major portal for the entry of Ca^{2+} into the cell, Ca^{2+} being a vital second messenger that affects a wide range of cellular processes. These glutamate-gated ion channels are essential mediators of brain plasticity and are capable of converting specific patterns of neuronal activity into long-term changes in synapse structure and function that are thought to underlie higher cognitive functions (Traynelis et al., 2010). NMDAR dysfunctions are also involved in various neurological and psychiatric disorders (Traynelis et al., 2010; C. G. Lau & Zukin, 2007; Mony, Kew, Gunthorpe, & Paoletti, 2009), including stroke, pathological pain, neurodegenerative diseases and schizophrenia, and there is growing interest in developing new drugs that target these receptors. Recent studies have highlighted the functional diversity of NMDARs (Traynelis et al., 2010; Cull-Candy & Leszkiewicz, 2004; Paoletti, 2011). NMDARs are diverse in their molecular (subunit) composition, their biophysical and pharmacological properties, their interacting partners and their subcellular localization. Subunit composition varies across CNS regions during development and in disease states (Traynelis et al., 2010; C. G. Lau & Zukin, 2007; Mony et al., 2009). There is also evidence that even at fully mature synapses, the NMDAR subunit content changes depending on neuronal activity (Paoletti, Bellone, & Zhou, 2013).

I.1. NMDAR subunits

Functional NMDARs are tetramers composed of different subunits, falling into three subfamilies according to sequence homology, have been identified (Traynelis et al., 2010; Cull-Candy & Leszkiewicz, 2004; Paoletti, 2011) (Fig. 1A): the GluN1 subunit, four distinct GluN2 subunits (GluN2A, GluN2B, GluN2C and GluN2D), which are encoded by four different genes, and a pair of GluN3 subunits (GluN3A and GluN3B), arising from two separate genes (Paoletti et al., 2013). Typically, endogenous NMDARs are di-heteromers comprising two obligatory GluN1 subunits and two regulatory GluN2 or GluN3 subunits, which assemble as a dimer of dimers. However, NMDARs are also able to

assemble as tri-heteromers. Specifically, GluN1/GluN2B/GluN3A or GluN1/GluN2B/GluN2D complexes are expressed at early stages of development and GluN1/GluN2A/GluN2B or GluN1/GluN2A/GluN2C in adult-hood (Al-Hallaq, Conrads, Veenstra, & Wenthold, 2007; Brothwell et al., 2008).

The total number of amino acids per subunit ranges from 900 to over 1,480. The difference in subunit size is almost entirely accounted for by differences in the length of the intracellular carboxyl (C)-terminal domain (CTD), a region that is involved in receptor trafficking and couples receptors to signaling cascades (Traynelis et al., 2010).

The existence of a large repertoire of homologous NMDAR subunits allows for various combinations of subunit assembly, which leads to a multiplicity of receptor subtypes in the CNS (Fig. 1B & C).The GluN1 subunit is encoded by a single gene but has eight distinct isoforms (GluN1-1a–GluN1-4a and GluN1-1b–GluN1-4b) owing to alternative splicing (Fig. 1A) (Paoletti et al., 2013). The GluN1-b isoforms (or exon 5-containing isoforms) possess an additional extracellular 21 amino-acids stretch (known as the N1 cassette) that affects the receptor's gating and pharmacological properties (Rumbaugh, Prybylowski, Wang, & Vicini, 2000; Vance, Hansen, & Traynelis, 2012). The four other splice variants arise from alternative splicing of exon 21 and exon 22, creating CTDs of variable length and differential subunit trafficking properties (Horak & Wenthold, 2009).

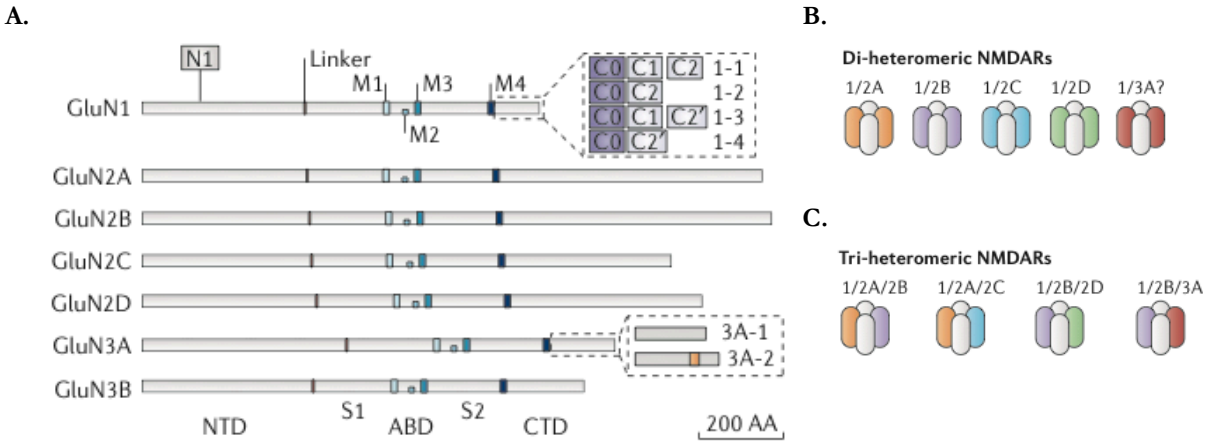

Fig. 1: NMDAR subunit diversity. (A) 7 NMDAR subunits have been identified: GluN1, GluN2A-GluN2D and GluN3A-GluN3B. It exists alternative splicing of GluN1 and GluN3A subunits increasing the NMDAR subunit heterogeneity. M1-M4 indicate membrane segments. (Paoletti, Bellone, & Zhou, 2013).
(B) Di-heteromeric NMDARs thought to exist in CNS. (Paoletti, Bellone, & Zhou, 2013).
(C) Tri-heteromeric NMDARs thought to exist in CNS (Paoletti, Bellone, & Zhou, 2013).

I.2. Subunit architecture and operation

Similar to all other iGluR subunits, NMDAR subunits consist of four discrete modules (Traynelis et al., 2010; Paoletti, 2011; Mayer, 2011) (Fig. 2): in the extracellular region there are a tandem of large globular bilobate (or clamshell-like) domains comprising the amino (N)-terminal domain (NTD), which

is involved in subunit assembly and allosteric regulation, and the agonist-binding domain (ABD) that is formed by two discontinuous segments (S1 and S2), which binds glycine (or D-serine) in GluN1 and GluN3 subunits and glutamate in GluN2 subunits; the transmembrane domain (TMD) made of three transmembrane helices (M1, M3 and M4) plus a re-entrant pore loop (M2) that lines the ion selectivity filter; and an intracellular CTD, which is involved in receptor trafficking, anchoring and coupling to signaling molecules (Paoletti et al., 2013). Although the structure of a full NMDAR is still lacking, several high-resolution crystal structures of isolated NTDs (Karakas, Simorowski, & Furukawa, 2011) and ABDs (Hiroyasu Furukawa, Singh, Mancusso, & Gouaux, 2005) captured in different conformational states are available. Within a tetrameric receptor complex, the NTDs and ABDs assemble as dimers, with the full receptor operating as a dimer-of-dimers. In 'classical' GluN1/GluN2 receptors, the two constitutive GluN1/GluN2 dimers adopt an alternating GluN1/GluN2/GluN1/GluN2 subunit arrangement around the pore (Salussolia, Prodromou, Borker, & Wollmuth, 2011; Riou, Stroebel, Edwardson, & Paoletti, 2012).

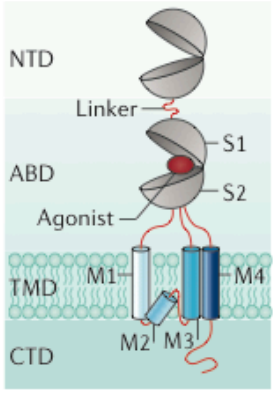

Fig. 2: NMDAR subunit structure. Each GluN subunits are made out of four distinct domains: the N-terminal domain (NTD), the agonist-binding domain (ABD), the transmembrane domain (TMD) containing the ion channel, and an intracellular C-terminal domain (CTD) (Paoletti, Bellone, & Zhou, 2013).

NMDARs probably have a comparable 'layer' organization to that of AMPA receptors (AMPARs) (Sobolevsky, Rosconi, & Gouaux, 2009) in which the ABDs are sandwiched between the TMD at the "bottom" and the NTDs at the "top" (Fig. 3). The basic gating principles that involve agonist-induced closure of the ABDs are also conserved between iGluR families (Paoletti, 2011); Mayer, 2011). By contrast, NMDAR NTDs have a unique twisted clam-shell conformation (Karakas et al., 2011), resulting in looser NTD dimer assemblies than the tightly packed AMPA and kainate NTD dimers. In agreement, structural rearrangements occurring distally at the NTD level can be sensed by the downstream gating machinery (Karakas et al., 2011; Gielen et al., 2008; Gielen, Siegler Retchless, Mony, Johnson, & Paoletti, 2009). The dynamic nature of NMDAR NTDs, together with their ability to recognize a host of small ligands acting as subunit-specific allosteric modulators, confers a central role of the N-terminal region in generating functional and pharmacological diversity in the NMDAR family.

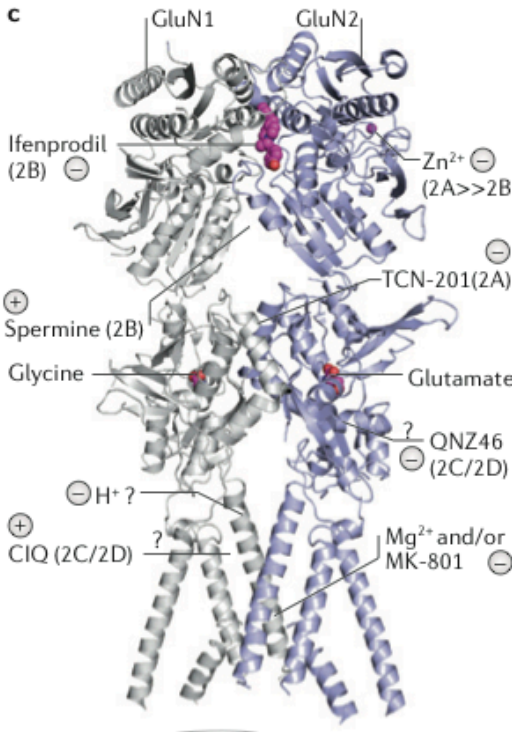

Fig. 3: Multiple binding sites of NMDAR. NMDARs contain multiple binding sites for extracellular small-molecule ligands acting as subunit-selective allosteric modulators. A model of a GluN1/GluN2 heterodimer based on the X-ray crystal structures of GluN1/GluN2B NTDs (Karakas et al., 2011), GluN1/GluN2A ABDs (Furukawa et al., 2005) and the AMPA receptor GluA2 pore region (Sobolevsky, Rosconi, & Gouaux, 2009) is shown. The + and - signs indicate positive and negative allosteric modulators, respectively (Paoletti, Bellone, & Zhou, 2013).

I.3. Subunit expression profile

In accordance with the widespread CNS distribution of NMDARs, the obligatory GluN1 subunit is ubiquitously expressed from embryonic stage E14 to adulthood (Watanabe, Inoue, Sakimura, & Mishina, 1992; Akazawa, Shigemoto, Bessho, Nakanishi, & Mizuno, 1994; Monyer, Burnashev, Laurie, Sakmann, & Seeburg, 1994). There are specific differences in GluN1 isoform expression however (Paoletti, 2011). Whereas GluN1-2 is widely distributed, GluN1-1 and GluN1-4 have a complementary distribution: the former is concentrated in more rostral regions (including the cortex and hippocampus). The GluN1-a and GluN1-b isoforms have largely overlapping expression patterns but their relative abundance varies from one region to another. Notably, in the hippocampus, GluN1-a isoforms are found in all principal cells, whereas the GluN1-b isoforms are largely restricted to the CA3 layer (Laurie & Seeburg, 1994). However, the functional significance of the differential expression of GluN1 isoforms remains unclear.

The four GluN2 subunits, which are major determinants of the receptor's functional heterogeneity, show strikingly different spatiotemporal expression profiles (Akazawa et al., 1994; Monyer et al., 1994; Sheng, Cummings, Roldan, Jan, & Jan, 1994) (Fig. 4). In the embryonic brain, only GluN2B and GluN2D subunits are expressed, and the latter is mostly found in caudal regions. Major changes in the expression patterns of the GluN2 subunits occur during the first 2 postnatal weeks. GluN2A expression starts shortly after birth and rises steadily to become widely and abundantly expressed in virtually

every CNS area in the adult. Concomitant to this progressive rise in GluN2A expression, GluN2D expression drops markedly, and in the adult, it is expressed at low levels mostly in the diencephalon and mesencephalon. In sharp contrast to GluN2D expression, GluN2B expression is maintained at high levels following birth, peaks around the first postnatal week and becomes progressively restricted to the forebrain. Lastly, expression of GluN2C appears late in development (postnatal day 10 (P10)), and its expression is mainly confined to the cerebellum and the olfactory bulb. The GluN3A and GluN3B subunits also display differential ontogenetic profiles (Henson, Roberts, Pérez-Otaño, & Philpot, 2010; Pachernegg, Strutz-Seebohm, & Hollmann, 2012) (Fig. 4). GluN3A expression peaks in early postnatal life and then declines progressively. Conversely, GluN3B expression slowly increases throughout development, and in the adult, it is expressed at high levels in motor neurons and possibly other regions. The specific expression of GluN2B, GluN2D and GluN3A subunits early in development strongly suggests that these subunits are important for synaptogenesis and synaptic maturation (Henson et al., 2010; Pachernegg et al., 2012; Paoletti et al., 2013). In the adult CNS, particularly in higher brain structures (such as the hippocampus and cortex), GluN2A and GluN2B are the predominant subunits (Watanabe et al., 1992; Akazawa et al., 1994; Monyer et al., 1994), indicating that they have central roles in synaptic function and plasticity.

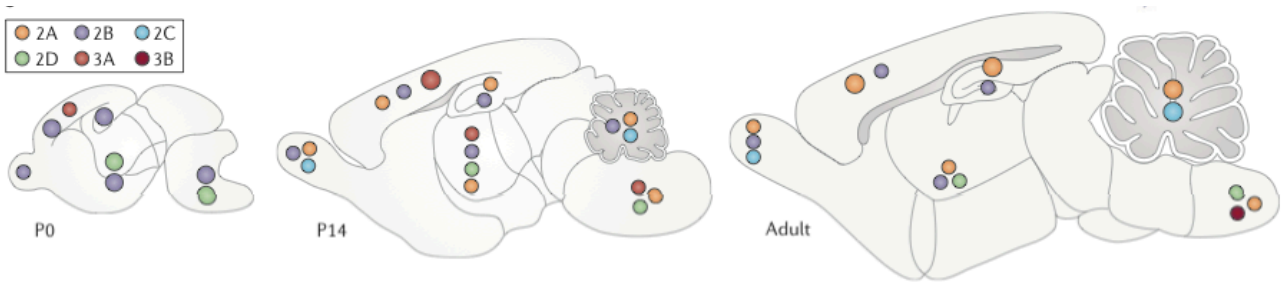

Fig. 4: NMDAR subunit expression from birth to adulthood. The development profile of GluN subunit expression in the mouse brain at day of birth (postnatal day 0 (P0)), 2 weeks following birth (P14) and at adult stage (Paoletti et al., 2013).

The developmental increase in the GluN2A/GluN2B ratio (also referred to as "GluN2B to GluN2A switch") is thought to play a critical role in postnatal brain development, by optimizing the threshold for synaptic plasticity induction at different developmental points via the unique biophysical and signaling properties of GluN2A and GluN2B (Yashiro & Philpot, 2008). GluN2A/GluN2B ratios can be bidirectionally regulated by experimental manipulations in neuronal activity levels *in vitro* (Ehlers, 2003; Bellone & Nicoll, 2007) and *in vivo* sensory experience (Nase, Weishaupt, Stern, Singer, & Monyer, 1999). For instance, visual deprivation reduces the developmental shift in the GluN2A/GluN2B ratio in the primary visual cortex (Quinlan, Olstein, & Bear, 1999a; Philpot, Sekhar, Shouval, & Bear, 2001). Several studies indicate that the elevation in the GluN2A/GluN2B ratio regulates the end of the critical period plasticity across various brain areas (Carmignoto & Vicini, 1992; X.-B. Liu, Murray, & Jones, 2004; Erisir & Harris, 2003). Given the differential characteristics of GluN2 subunits, it is likely that a synapse with a high GluN2A content exhibits a reduced window for spike-timing plasticity, inte-

grating stimuli received in a shorter period of time than a synapse with a reduced GluN2A/B ratio. This may limit the formation of inappropriate synapses by reducing synaptic response time. In addition, the threshold for LTP induction is elevated in these synapses, making their potentiation more difficult. It may be that the elevated threshold for LTP could play a role in the pruning of excess synapses formed in the initial developmental stages, as it has been reported that synapses that are not activated are eliminated (M. Yasuda et al., 2011).

There are also important differences in the subcellular expression of the NMDAR subunits. For example, GluN1 exists in two pool: a population in the plasma membrane, assembled with GluN2 or GluN3 subunits, and another pool retained in the ER with a short half-life. GluN1 retention in the ER is modulated by alternative splicing and PKC phosphorylation. In contrast, GluN2 subunits are mainly localized at the plasma membrane. Although there are some reports of presynaptic NMDARs (Corlew, Brasier, Feldman, & Philpot, 2008), typically NMDARs are localized at postsynaptic sites throughout the CNS. The current simplified model is that GluN2A-containing NMDARs are predominantly expressed at synaptic sites, whereas GluN2B-containing NMDARs are enriched at extrasynaptic sites in the adult CNS (Groc, Bard, & Choquet, 2009).

I.4. NMDAR functional properties

NMDARs exhibit a number of properties that are unique among glutamate receptors. First, their activation requires simultaneous binding of glutamate and a coagonist. Although glycine was first identified as a coagonist of NMDARs (Johnson & Ascher, 1987), D-serine has been proposed as the major endogenous coagonist of synaptic NMDARs at several CNS synapses (Henneberger, Papouin, Oliet, & Rusakov, 2010; Mothet et al., 2000). Recently, Papouin et al. (2012) used enzymatic degradation of either coagonist in hippocampal slices from adult rats to demonstrate that D-serine is the coagonist at synaptic receptors while glycine acts at extrasynaptic NMDARs (Papouin et al., 2012). Second, NMDAR currents display strong voltage dependency due to a channel blockade by physiological concentrations of extracellular Mg^{2+} (Ascher & Nowak, 1988; Mayer & Westbrook, 1987). Mg^{2+} block is relieved upon strong membrane depolarization. Because of the strong voltage-dependence of the block, NMDARs act as coincident detectors, sensing postsynaptic depolarization at the same time as or shortly after release of glutamate from presynaptic terminal. This enables NMDARs to mediate synaptic plasticity and associative learning. Third, NMDAR channels are highly permeable to Ca^{2+} (Moriyoshi et al., 1991), which acts as a second messenger in diverse intracellular signaling pathways. Excess Ca^{2+} is also toxic to neurons, and hyperactivation of NMDARs is thus thought to contribute to a variety of neurodegenerative disorders. Fourth, NMDARs display slow activation and deactivation kinetics, compared to other ionotropic glutamate receptors. Overall, these properties confer crucial roles to NMDARs, in particular those of coincidence detectors capable of synaptic integration and of activation of intracellular signaling cascades.

Despite these commonalities, the particular subunit composition will confer variable biophysical and signaling properties to the different NMDAR subtypes. These properties include channel permeation and gating as well as protein-protein interactions, trafficking and plasma membrane localization.

I.4.1. Channel permeation

Permeation properties that differ between NMDAR subtypes are their single-channel conductances, Ca^{2+} permeability and block by extracellular Mg^{2+} (Stern, Béhé, Schoepfer, & Colquhoun, 1992; Dingledine, Borges, Bowie, & Traynelis, 1999; Cull-Candy, Brickley, & Farrant, 2001; Table 1). NMDARs show a pair of conductance states, the amplitude and relative frequency of which depends on the GluN2 subunit integrating the channel. Receptors composed of GluN2A or GluN2B subunits display large conductances while receptors containing GluN2C or GluN2D subunits show smaller conductances. Voltage-dependent inhibition by extracellular Mg^{2+} of GluN1/GluN2A or GluN1/GluN2B responses is at least four-fold stronger than inhibition of GluN1/GluN2C or GluN1/GluN2D responses at all voltages tested (Kuner & Schoepfer, 1996; Qian, Buller, & Johnson, 2005); (Qian & Johnson, 2006). Ca^{2+} permeability also differs: it is higher in GluN2A- and GluN2B-containing receptors than in GluN2C- and GluN2D-containing receptors (Burnashev, Zhou, Neher, & Sakmann, 1995; Schneggenburger, 1996).

	GluN1-1a+			
	N2A	N2B	N2C	N2D
Conductance (pS)				
Main	50	50	37	37
Sub	38	38	18	18
Mean open time (ms)	3–5	3–5	0.5–1	0.5–1
EC_{50} (Glycine), μM	1.7	0.4	0.3	0.1
EC_{50} (Glutamate), μM	4	2	1	0.4
P_f (Ca^{2+}), %	18	18	8*	n.d.
IC_{50} (Mg^{2+}), μM (V_m = −100 mV)	2	2	12	12

Table 1. GluN2 subunit-specific permeation properties. P_f, fractional Ca^{2+} current; EC_{50}, half maximal effective concentration; IC_{50}, half maximal inhibitory concentration; V_m, membrane potential (Paoletti, 2011).

The structural determinants that control the conductance and permeation properties of NMDARs reside in the re-entrant M2 loop, which lines the inner cavity of the channel pore (Kuner, Wollmuth, Karlin, Seeburg, & Sakmann, 1996; Sakurada, Masu, & Nakanishi, 1993; Kuner & Schoepfer, 1996; Mori & Mishina, 1995). One key determinant is the identity of the residue occupying a functionally critical position at the apex of the M2 loop, the "QRN" site, that is an asparagine in GluN1 and GluN2 subunits (Burnashev et al., 1992; Mori, Masaki, Yamakura, & Mishina, 1992). The asparagine in the QNR site of the GluN1 and an adjacent asparagine (i.e., QRN+1 site) in GluN2 form a narrow constriction within the channel pore (Wollmuth, Kuner, Seeburg, & Sakmann, 1996) and influences single-channel conductance, Ca^{2+} permeability (Burnashev et al., 1992) as well as Mg^{2+} sensi-

tivity (Burnashev et al., 1992; Mori et al., 1992). In addition to residues at or near the QNR sites, a glutamine residue located six positions C-terminal to the QNR site in GluN2A regulates Ca^{2+} permeability (Vissel, Krupp, Heinemann, & Westbrook, 2002), suggesting that this position may underlie GluN2 subunit-specific differences in Ca^{2+} permeability. A highly conserved GluN2B tryptophan residue (W607) in the M2 loop also has been proposed to contribute to the narrow constriction (Williams et al., 1998). Occupancy of permeant ion-binding sites in the external and internal cavities of the channel pore by Na^+ or K^+ alters the association and dissociation rates of Mg^{2+} from its blocking site (Qian, Antonov, & Johnson, 2002). The nature of these ion-binding sites differs between GluN2 subunits and hence, may underlie some GluN2-specific effects on Mg^{2+} block (Qian & Johnson, 2006; Kuner & Schoepfer, 1996). Moreover, the rates for Mg^{2+} unblock and reblock depend on the GluN2 subunit; receptors containing GluN2C or GluN2D unblock more rapidly than those containing GluN2A or GluN2B (Clarke & Johnson, 2006). Although considerably less attention has been dedicated to the GluN3 subunits, it is known that they have unique properties. For example unlike GluN2 subunits, GluN3 binds to glycine and not to glutamate. Therefore, NMDARs containing exclusively GluN1/GluN3 subunits can as excitatory glycine receptors, which are impermeable to Ca^{2+}. Tri-heteromers containing GluN2 and GluN3 subunits, however, are sensitive to glutamate, but they show a decrease in open probability, Ca^{2+} permeability, and Mg^{2+} sensitivity in comparison with GluN1/GluN2 NMDARs (Henson et al., 2010). Insensivity to Mg^{2+} may explain why GluN3- and GluN2C-containing NMDARs expressed on oligodendrocytes (Piña-Crespo et al., 2010; Burzomato, Frugier, Pérez-Otaño, Kittler, & Attwell, 2010) can be active while the membrane (myelin sheath) on which they reside experiences little depolarization.

I.4.2 Channel gating

Depending on their subunit composition, NMDAR subtypes display distinct gating properties, including sensitivity to agonists, activation and deactivation kinetics and channel mean open time and maximal open probability. Although the GluN1 glycine/D-serine binding site is common to all NMDAR subtypes, the identity of the GluN2 subunit influences their affinity for D-serine versus glycine (Matsui et al., 1995; Madry et al., 2007; Priestley et al., 1995). GluN1/GluN2B subtypes bind glycine with a 10-fold better affinity than do GluN1/GluN2A subtypes, and exhibit a stronger affinity for glycine than for D-serine (EC_{50}, concentration producing half-maximal response, being ~0.057 versus 0.15 μM, respectively) (Priestley et al., 1995; Madry et al., 2007). On the contrary, GluN2A-containing NMDARs exhibit a slightly stronger affinity for D-serine over glycine (EC50 ~0.22 versus 0.53 μM, respectively) (Priestley et al., 1995; Matsui et al., 1995). Also, affinity for glutamate, measured as the steady-state EC_{50} varies with the GluN2 subunits in the following order: GluN2A < GluN2B ~ GluN2C < GluN2D.

A similar ranking of subunits is found for measurements of glutamate deactivation kinetics, i.e. The time course of the macroscopic current decay following a brief pulse of glutamate (Monyer et al.,

1994; Vicini et al., 1998; Yuan, Hansen, Vance, Ogden, & Traynelis, 2009; Fig. 5). The time course of decay of NMDAR currents is crucial for synaptic transmission because it governs the duration of the slow, NMDAR-mediated component of excitatory postsynaptic currents (EPSCs) (Lester et al., 1990). GluN1/GluN2A receptors have the fastest decay with a time constant of tens of milliseconds. GluN1/GluN2D receptors are the slowest (in the order of seconds) (Wyllie, Béhé, & Colquhoun, 1998). The molecular determinants responsible for the difference in glutamate sensitivity and deactivation kinetics between GluN1/GluN2 receptor subtypes are yet to be identified.

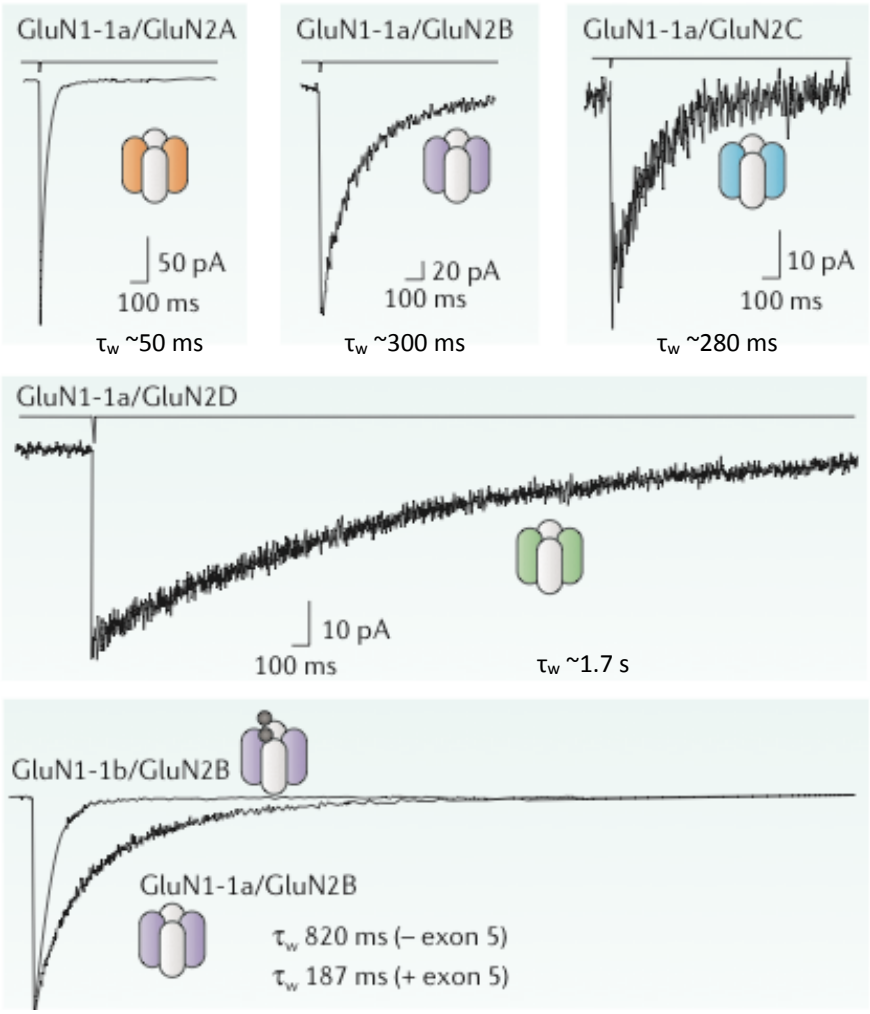

Fig. 5: Decay of NMDAR currents. Macroscopic recombinant NMDARs in response to glutamate, illustrating GluN2 subunit-dependent deactivation. τ_w, weighted deactivation time constant; higher τ_w signifies slower decay. (Data from Vicini et al., 1998; image from Paoletti et al., 2013)

The maximal open probability (P0), that is the probability of the ion channel being in an open state while the agonist binding sites are fully occupied, is another key gating parameter that varies between NMDAR subtypes. P0 is high for GluN1/GluN2A receptors, intermediate for GluN1/GluN2B receptors and very low for GluN1/GluN2C and GluN1/GluN2D receptors (Wyllie et al., 1998; G. Q. Chen, Cui, Mayer, & Gouaux, 1999; Erreger, Dravid, Banke, Wyllie, & Traynelis, 2005; Dravid, Prakash, & Traynelis, 2008). Moreover, the channel mean open time, that reflects the stability of the open state of a channel, is higher for GluN2A- or GluN2B-containing channels than for GluN2C- or GluN2D-

containing ones. The higher open probability and faster deactivation at single-channel level result in the faster rise and decay times observed macroscopically for GluN2A-containing NMDARs in response to glutamate release compared to GluN2B-containing ones. Although GluN1/GluN2B channels may have lower peak currents, they carry about two-fold more charge for a single synaptic event than GluN1/GluN2A channels because the deactivation of GluN2B channels is slow enough to compensate for their low open probability (Erreger et al., 2005). Unfortunately, little is known about gating properties of tri-heteromeric receptors containing more than on type of GluN2 subunit or a GluN2 subunit and a GluN3 subunit. To date, our understanding of how NMDAR channel properties are defined by the GluN2 subunit composition is mostly based on studies of recombinant receptors. Further studies on native NMDARs in an intact neuronal preparation are needed to confirm these conclusions. Recently, an elegant study using conditional deletion of GluN2A and GluN2B in single neurons in the hippocampal CA1 region of mice determined the biophysical properties of pure di-heterometric NMDARs (GluN1/GluN2A or GluN1/GluN2B) (Gray et al., 2011). The subtype dependence of current kinetics and open probability of these native NMDARs was similar to the findings in heterologous systems.

I.4.3. Synaptic localization

There is a long-standing paradox that NMDA (N-methyl-d-aspartate) receptors (NMDARs) can both promote neuronal health and kill neurons. NMDAR-induced responses depend on the receptor localization: stimulation of synaptic NMDARs, acting primarily through nuclear Ca^{2+} signaling, leads to the build-up of a neuroprotective 'shield', whereas stimulation of extrasynaptic NMDARs promotes cell death. These differences result from the activation of distinct genomic programs and from opposing actions on intracellular signaling pathways. Perturbations in the balance between synaptic and extrasynaptic NMDAR activity contribute to neuronal dysfunction in acute ischemia and Huntington's disease, and could be a common theme in the aetiology of neurodegenerative diseases (Hardingham & Bading, 2010; Fig. 6).

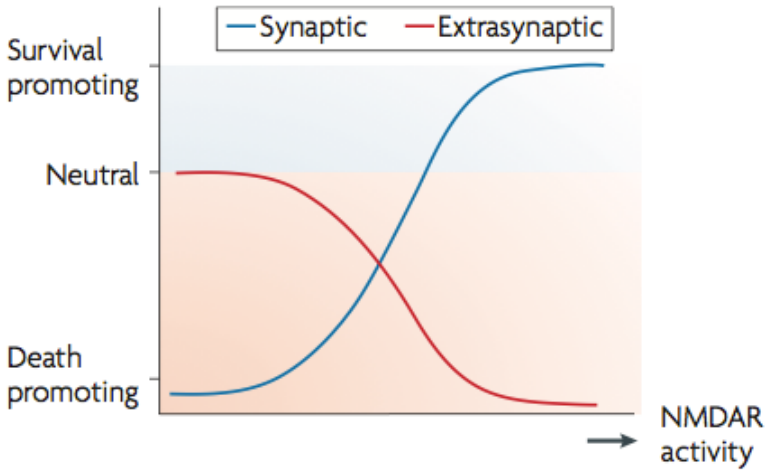

Fig. 6: χ-shaped model of NMDAR-dependent excitotoxicity. The schematic illustrates the opposing effects of increasing synaptic and extrasynaptic NMDAR (N-methyl-d-aspartate receptor) activity on neuronal survival and resistance to trauma. Hypoactivity of synaptic NMDARs is harmful to neurons. Enhancing synaptic NMDAR activity triggers multiple neuroprotective pathways and this promotes neuronal survival. Low levels of activation of extrasynaptic NMDARs have no effects on neuronal survival but increasing the level of extrasynaptic NMDAR activity activates cell death pathways and exacerbates certain neurodegenerative processes, thus reducing neuronal survival ({Hardingham & Badding, 2010).

At the neuronal surface and at the synapses, NMDAR distribution is not homogenous and highly depends on their GluN2 subunit composition. Growing evidence suggests that GluN2A-containing NMDARs occupy the central portion of the mature synapse while GluN2B-containing NMDARs are preferentially targeted to perisynaptic and extrasynaptic sites (Stocca & Vicini, 1998; J. H. Li et al., 1998; Tovar & Westbrook, 1999; Groc et al., 2006). For instance, in the visual cortex, NMDAR-EPSCs lose their sensitivity to GluN2B-specific antagonists by P7, but the extrasynaptic receptors are still blocked, suggesting that GluN1/GluN2B receptors are restricted to extrasynaptic sites beyond a certain stage of development (Stocca & Vicini, 1998). Moreover, electrophysiological characterization in acute hippocampal slices obtained from adult rats indicates that synaptic receptors at CA3-CA1 synapses are predominantly composed of GluN2A-containing NMDARs (Papouin et al., 2012). The GluN2B-NMDARs antagonist Ro25-6981 did not affect the slope of NMDAR-field excitatory postsynaptic potentials (fEPSPs) but free zinc, a highly specific allosteric inhibitor of GluN2A-NMDARs, strongly reduced synaptic NMDAR-fEPSPs. Further, immunocytochemical analysis revealed that GluN2B clusters occur both at synaptic and extrasynaptic sites in cultured cortical neurons, while GluN2A clusters are almost exclusively synaptic (J. H. Li et al., 1998).

Ultrastructural studies using immunogold labeling also showed a preferential localization of the GluN2B subunit in the perisynaptic area and of the GluN2A subunit at the center of the synapse (Shinohara et al., 2008; J. Zhang & Diamond, 2009). Investigation of surface mobility of native GluN2A and GluN2B subunits in cultured neurons using single-molecule and -particle approaches revealed that GluN2A-NMDARs are less mobile and more retained within synapses than GluN2B-NMDARs because of differential lateral diffusion at the neuronal surface (Groc et al., 2006).

However, the segregation of GluN2A and GluN2B to synaptic and extrasynaptic sites is not absolute, as has been shown in many studies (Mohrmann, Köhr, Hatt, Sprengel, & Gottmann, 2002; C. G. Thomas, Miller, & Westbrook, 2006). For instance, the sensitivity to GluN2B-specific antagonists has been shown to be comparable between synaptic and extrasynaptic sites (A. Z. Harris & Pettit, 2007; C. G. Thomas et al., 2006). It is to be noted that the synaptic content of NMDAR subtypes changes during brain development (Kew, Richards, Mutel, & Kemp, 1998; Kirson & Yaari, 1996), sensory experience (Quinlan et al., 1999a; (Quinlan, Philpot, Huganir, & Bear, 1999b; Philpot et al., 2001) or synaptic plasticity (Bellone & Nicoll, 2007; Matta, Ashby, Sanz-Clemente, Roche, & Isaac, 2011). Therefore, some of the apparent discrepancies may be resolved when taking into account developmental and regional differences in the localization of NMDAR subtypes as well as the experimental paradigms used for its study (Köhr, 2007).

I.4.4. Protein-protein interactions.

Proteins interacting with NMDAR subunits are important in determining the direction of synaptic plasticity as they couple NMDARs to distinct downstream signaling pathways (Kennedy, Beale, Carlisle, & Washburn, 2005). GluN2A and GluN2B, each with an extended C-terminus (630 and 650 amino acids, respectively), interact with different intracellular proteins. Ca^{2+}-calmodulin-dependent protein kinase II (CaMKII), a key mediator of long-term potentiation (LTP), binds with high affinity to GluN2B (A. S. Leonard, Lim, Hemsworth, Horne, & Hell, 1999; Strack & Colbran, 1998) as well as to the GluN2A subunit (Gardoni et al., 1998). CaMKII activation and its association to GluN2B are required for LTP induction (Lisman, Schulman, & Cline, 2002; Barria & Malinow, 2005). Other unique binding partners of GluN2B include Ras-guanine nucleotide-releasing factor (Ras-GRF1) (Krapivinsky et al., 2003) and Ras GTPase activating protein (RasGAP) (J. H. Kim, Liao, Lau, & Huganir, 1998); associations which might also affect the induction of plasticity (Zhu, Qin, Zhao, Van Aelst, & Malinow, 2002). GluN2B binds the cytoskeletal protein α-actinin and the clathrin adaptor protein AP2 through a common binding site (YEKL) near the distal end of its C-terminus (Lavezzari, McCallum, Lee, & Roche, 2003; (Nakazawa et al., 2006). Interactions with these two proteins bidirectionally regulate the synaptic localization of GluN2B. On the other hand, the neuronal nitric oxide synthase, Homer and β-catenin are synaptic proteins that bind GluN2A more effectively than GluN2B (Al-Hallaq et al., 2007), although these interactions seem to be direct.

Both GluN2A and GluN2B, through PDZ-binding motifs (ESDV) in their extreme C-termini, interact with members of the membrane-associated guanylate kinase (MAGUK) family of synaptic scaffolding proteins, such as PSD-93, PSD-95, SAP97, SAP102. These interactions are involved in anchoring NMDARs at the synapse (Kennedy, 2000), and studies suggested that differential interaction of each GluN2 subunit with MAGUKs might determine the distinct synaptic localization of each subtype (Townsend, Yoshii, Mishina, & Constantine-Paton, 2003; Sans et al., 2000). However, a recent report indicates that the MAGUK proteins interact with GluN1/GluN2A and GluN1/GluN2B receptors at

comparable levels (Al-Hallaq et al., 2007). Thus, further studies are required to understand the association of NMDAR subunits with these scaffolding proteins and its influence on their subcellular localization. Both GluN2A and GluN2B directly interact with flotillin-1, a lipid raft-associated protein, via analogous regions in their distal C-termini (Swanwick, Shapiro, Yi, Chang, & Wenthold, 2009), and this interaction potentially recruits NMDARs to signaling microdomains within lipid rafts.

II. Modulation of NMDA receptor localization in neurodegenerative diseases and other disorders.

Mislocalization and abnormal trafficking of NMDAR subunits have been reported in several brain disorders and neurodegenerative diseases. Excessive calcium influx through NMDARs triggers excitotoxic cell death mediated by downstream signaling cascades (Lynch & Guttmann, 2002). The mode of calcium entry depends on not only the number but also the subtype of NMDARs present at the cell surface, given the distinct biophysical properties of the individual subunits. Furthermore, the excitotoxicity of NMDR activity is not only dependent on the degree of activation or specific subtype but also on the synaptic or extrasynaptic localization of those NMDAR subtypes (Hardingham & Bading, 2010).

Beyond the traditional view of excitotoxic cell death, recent studies suggest that disruptions in NMDAR trafficking and targeting may be the culprit for NMDAR dysfunction in various neuropathological conditions (C. G. Lau & Zukin, 2007). Dynamic trafficking of NMDARs to and from the cell surface or to and from extrasynaptic sites is a powerful mode of controlling the abundance and composition of surface and/or synaptic NMDARs. Thus, dysregulation of NMDAR trafficking would contribute to impairment of synaptic function, that may eventually result in the collapse of the synaptic functional unit in the absence of excitotoxic cell death.

In this part, examples of some neurodegenerative diseases and other disorders will be summarized although more attention will be put on the modulation of NMDAR in Parkinson's disease (PD) and L-DOPA-Induced Dyskinesia (LID) as it was the focus of our study.

II.1. Ischemia and stroke

Calcium influx through extrasynaptic NMDARS has been associated with the induction of cell death, while that through synaptic receptors mediates induction of synaptic plasticity and has pro-survival effects (Hardingham, Fukunaga, & Bading, 2002). Thus, synaptic or extrasynaptic localization determines whether NMDAR activation prevents or promotes neurotoxicity because of coupling to either anti- or pro-apoptotic downstream signaling cascades, respectively. Perturbations in the balance between synaptic and extrasynaptic NMDAR activity has been implicated in ischemic stroke. For instance, enhanced activity of extrasynaptic NMDARs has been shown to contribute to the acute neu-

ronal dysfunction during an ischemic episode following extracellular accumulation of glutamate (Tu et al., 2010).

II.2. Alcohol abuse

Regulation of NMDAR trafficking by ethanol underlies the plastic modifications of neural circuitry associated with alcohol abuse. In the hippocampus, acute ethanol administration promotes selective internalization of GluN2A through H-Ras activation and inhibition of Src, thereby changing the synaptic NMDAR complement from a mixture of GluN2A- and GluN2B-containing receptors to exclusively GluN2B ones (Suvarna et al., 2005). On the other hand, chronic exposure to ethanol has been shown to induce synaptic incorporation of NMDARs without affecting extrasynaptic (Carpenter-Hyland, Woodward, & Chandler, 2004).

II.3. Alzheimer's disease

Alzheimer's disease (AD) is a progressive neurodegenerative disorder characterized by impairments in memory and cognition. The pathogenesis of the disease is linked to abnormal production of β-amyloid (Aβ) peptide and formation of neurofibrillary tangles and plaques having neurotoxic effects. Recent studies show that elevated levels of Aβ impair glutamatergic transmission and inhibit synaptic plasticity, suggesting a glutamatergic synaptic dysfunction at early stages of the disease (Selkoe, 2002). Mechanistically, NMDARs have been implicated in the loss of synapses in the AD brain (Shankar et al., 2007). Discrepant results regarding alterations in NMDAR subunit expression suggest that additional mechanisms may be involved in the neuropathological changes observed in the susceptible brain regions (Hynd, Scott, & Dodd, 2004). One such mechanism is the increased endocytosis of NMDARs stimulated y Aβ in cultured cortical neurons and in transgenic mice expressing mutant amyloid precursor protein (APP), the precursor of Aβ (Snyder et al., 2005). Altered striatal enriched tyrosine phosphatase (STEP) activity has been associated with cognitive impairments in AD. STEP61 expression and activity are significantly increased in transgenic AD mice and human AD brain (Kurup et al., 2010). Although STEP is normally ubiquitinated, it is not degraded efficiently due to proteosome inhibition by Aβ. High-affinity binding of Aβ to α-7-nicotinic acetylcholine receptor results in increased Ca^{2+} influx, calcineurin activation and dephosphorylation and activation of STEP61. Increased STEP61 activity leads to Fyn inaction and reduced NMDAR exocytosis, as well as enhanced GluN2B Y1472 dephosphorylation and increased NMDAR internalization (Kurup et al., 2010). Thus, increased expression and activity of STEP61 alters synaptic glutamatergic signaling and may contribute to AD cognitive dysfunction. Also, Aβ production is enhanced by chronic extrasynaptic NMDAR activation, which is blocked by the NMDAR antagonist memantine (Bordji, Becerril-Ortega, Nicole, & Buisson, 2010). In summary, AD neuronal dysfunction involves an imbalance between synaptic and extrasynaptic NMDAR localization and function; whereas synaptic NMDARs are depleted, extrasynaptic NMDAR-mediated signaling

is sustained, facilitating detrimental Aβ synthesis and downstream pathogenesis. (Gladding & Raymond, 2011).

II.4. Huntington's disease

Huntington's disease (HD) is an autosomal dominantly inherited neurodegenerative disorder characterized by cognitive deficits, motor decline, and mood dysfunction (Harper, 1992). The disease involves extensive and selective cell death in GABAergic projection medium-sized spiny neurons (MSNs) of the neostriatum and, to a lesser extent, cell death in the cortex (Vonsattel & DiFiglia, 1998). The pathology is caused by an expansion of the CAG repeats in the huntingtin (htt) gene that leads to an expanded polyglutamine repeats in the protein (Landles & Bates, 2004). Normal htt binds to PSD-95, resulting in the inhibition of NMDAR activity and significant attenuation of neuronal toxicity induced by both NMDA and a mutated form of htt (Sun, Savanenin, Reddy, & Liu, 2001). Mutated htt (mhtt) has an abnormal conformation and can be cleaved to generate toxic fragments that form aggregates and interfere with vital cellular processes, such as mitochondrial function, Ca^{2+} signaling and homeostasis, gene transcription and vesicular trafficking (Zuccato, Valenza, & Cattaneo, 2010). Recent evidence indicates that aberrant glutamatergic transmission involving altered NMDAR activity and trafficking contributes to HD neuropathology. In the YAC128 transgenic mouse model of HD, that expresses mhtt with a 128-length polyglutamine expansion, striatal NMDAR activation and excitotoxicity is enhanced, NMDAR currents and surface expression are increased in these mice with specific increases in the extrasynaptic NMDAR activity, dominated by GluN2B-containing NMDARs, due at least in part to enhanced NMDAR forward trafficking to the plasma membrane that contribute to the phenotype onset (Cepeda et al., 2001; M. M. Y. Fan, Fernandes, Zhang, Hayden, & Raymond, 2007; Fernandes, Baimbridge, Church, Hayden, & Raymond, 2007; Graham et al., 2009; L. Li, Murphy, Hayden, & Raymond, 2004; Milnerwood & Raymond, 2007; Shehadeh et al., 2006; Zeron et al., 2002; H. Zhang et al., 2008). In HD transgenic models, an alteration of membrane-associated neuronal nitric oxide synthase (nNOS) and a decrease in PSD-95, which link nNOS to the NMDAR was observed (Luthi-Carter et al., 2003; Jarabek, Yasuda, & Wolfe, 2004). Overall, NMDAR/PSD-95 complex can be considered a key factor contributing to excitotoxicity in preclinical models of HD, specifically striatal PSD-95 localization is shifted to non-synaptic membranes, as the PSD-95/htt association decreases in the presence of mhtt, presumably increasing the availability of unbound PSD-95 to anchor and stabilize NMDAR on the surface (Sun et al., 2001; J. Fan, Cowan, Zhang, Hayden, & Raymond, 2009). It results in an enhanced formation of GluN2B/PSD-95 complex at non-postsynaptic density fractions (J. Fan et al., 2009). Alterations in synaptic and extrasynaptic NMDAR localization can lead to imbalance of pro-survival and pro-apoptotic signaling (Hardingham & Bading, 2010) and is a critical element in neuronal cell survival in HD (Levine, Cepeda, & André, 2010).

II.5. Parkinson's disease and L-DOPA-induced dyskinesia

Parkinson's disease (PD) is a progressive neurodegenerative disorder characterized by the accumulation of α-synuclein inclusions (Lewy bodies) and progressive dysfunction and death of the dopaminergic (DA) neurons projecting from the substantia nigra to the striatum, and consequently, the depletion of dopamine in the striatum (Shulman, De Jager, & Feany, 2011). The dopamine deficit can be mimicked in animal models by inducing nigrostriatal denervation with injections of the neurotoxin 6-hydroxydopamine (6-OHDA) (Ungerstedt & Arbuthnott, 1970). The degeneration of the nigrostriatal dopaminergic pathway in PD leads to significant morphological and functional changes in the striatal neuronal circuitry, including overactivity of the corticostriatal glutamatergic pathway. The alteration in the nigrostriatal pathway results in the motor symptoms characteristic of PD as dopaminergic and glutamatergic signaling interact to control motor function.

Among the various modifications in the glutamatergic striatal synapses in PD, several studies reported alterations in NMDA receptor subunit composition at the dendritic spines of medium spiny neurons (MSNs) (Gardoni, Ghiglieri, Luca, & Calabresi, 2010; Sgambato-Faure & Cenci, 2012; Mellone & Gardoni, 2013; Fig. 7). Changes in subcellular localization of NMDARs have been reported in 6-OHDA mouse models of PD. The amount of GluN1 and GluN2B, but not GluN2A, in membrane fractions decreased in the 6-OHDA lesioned striatum relative to the unlesioned striatum (Dunah et al., 2000). Further studies indicated that alterations in NMDAR subunit composition at synapse correlated with the reduction of corticostriatal synaptic plasticity (Picconi et al., 2003; Picconi et al., 2004; Gardoni et al., 2006). In particular, GluN2B-containing NMDAR are specifically reduced in synaptic fraction purified from parkisonian rats (Gardoni et al., 2006). Similar results were found in a monkey model of PD, the MPTP-treated macaques. Interestingly, alterations of NMDAR subunit localization at synapse are associated with a decreased interaction with PSD-95 (Picconi et al., 2004; Gardoni et al., 2006). Furthermore, other studies reported that experimental parkisonism in rats is related to a decreased synaptic membrane localization and increased vesicular localization of members of the PSD-MAGUK family (Nash, Johnston, Collingridge, Garner, & Brotchie, 2005) which may account for the observed dysregulation of NMDAR at the synapse (Mellone & Gardoni, 2013).

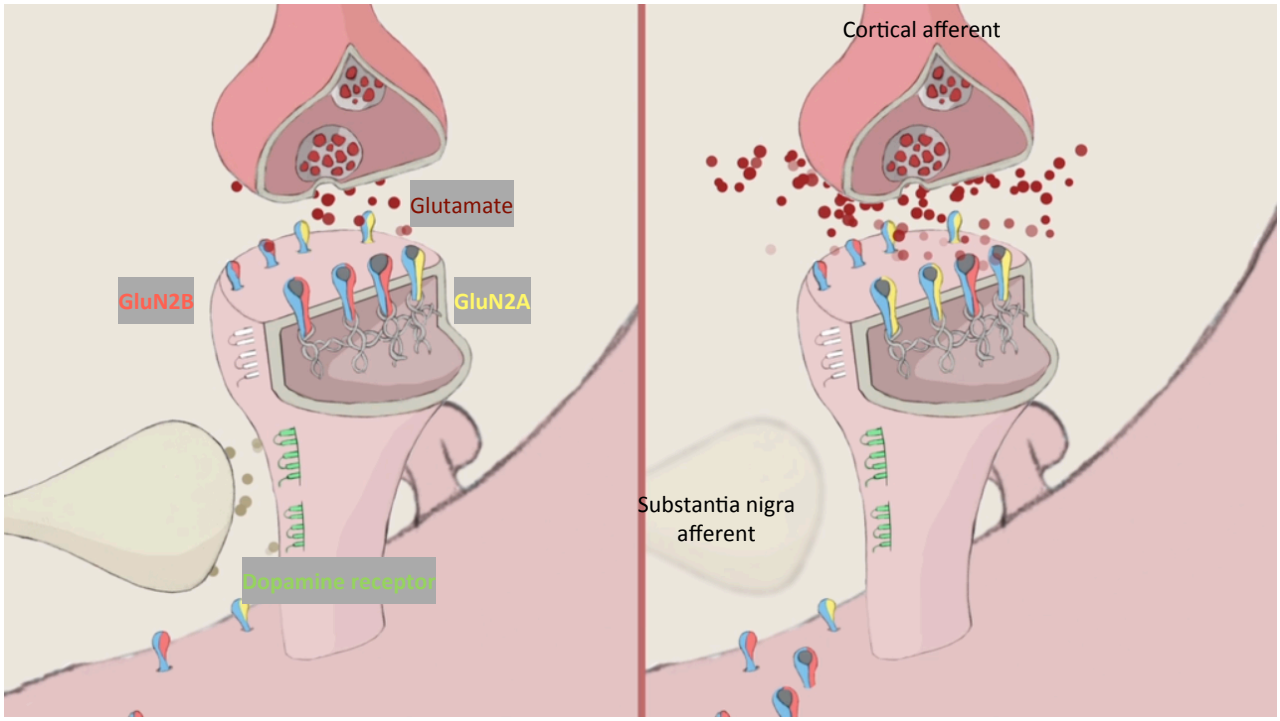

Fig. 7. Alterations of NMDA receptors at striatal spines in Parkinson's disease. At the striatal level, glutamatergic and dopaminergic inputs converge to the spines of medium spiny neurons where it is for the output responsible for motor skills among many. In PD, the dopaminergic afferents are lost inducing an increase un glutamate release, a redistribution of GluN2B to extrasynaptic sites and an increase of GluN2A at the synapse.

An important feature in PD is the onset of dyskinetic movements as a consequence of chronic L-DOPA treatment. L-DOPA-induced dyskinesias (LID) represent the main side effect of the therapeutic strategy clinically used in PD (Calabresi, Di Filippo, Ghiglieri, Tambasco, & Picconi, 2010). Although its discovery constitutes a major milestone in the modern neuropharmacology (Birkmayer & Hornykiewicz, 1961; Mercuri & Bernardi, 2005), the beneficial "honeymoon" phase of the treatment is followed by the appearance of motor fluctuations in the drug efficacy ("on-off" state) and dyskinesias (Calabresi et al., 2010; Cotzias, Papavasiliou, & Gellene, 1969). Among the numerous players involved in the onset of dyskinesia, excessive striatal glutamatergic transmission exerts a central role (Gardoni et al., 2010; Sgambato-Faure & Cenci, 2012). After chronic L-DOPA treatment the glutamatergic signaling from cortex to the striatum undergoes further adaptive changes, resulting in an abnormal NMDAR composition and function at dendritic spines of striatal medium spiny neurons (Gardoni et al., 2006). L-DOPA-treated dyskinetic rats have significantly higher levels of GluN2A subunit, while GluN2B is reduced at the postsynaptic compartment and redistributed to extrasynaptic membranes (Gardoni et al., 2006). Similar data was found in dyskinetic MPTP-monkeys as well as in PD patients treated with L-DOPA (Gardoni et al., not published; Fig. 8). These events are paralleled by modifications in the association of GluN2B subunit with members of the PSD-MAGUKs family (Gardoni et al., 2006). Notably, it has been demonstrated that these molecular alterations are strictly correlated to abnormal synaptic plasticity and motor behavior in L-DOPA-treated dyskinetic rats (Picconi et al., 2003). Treatment of non-dyskinetic animals with a cell-permeable peptide (TAT-GluN2B9c), able to affect the synaptic lo-

calization of GluN2B-containing NMDAR by interfering with its binding to PSD-MAGUK proteins, caused a worsening of motor symptoms with the appearance of dyskinetic behaviors (Gardoni et al., 2006). Overall, these data further support the idea that molecular disturbance of the glutamatergic synapse, initially caused by dopamine denervation, create a pathological substrate that may have causal role in the development of dyskinesia (Gardoni et al., 2010; Mellone & Gardoni, 2013).

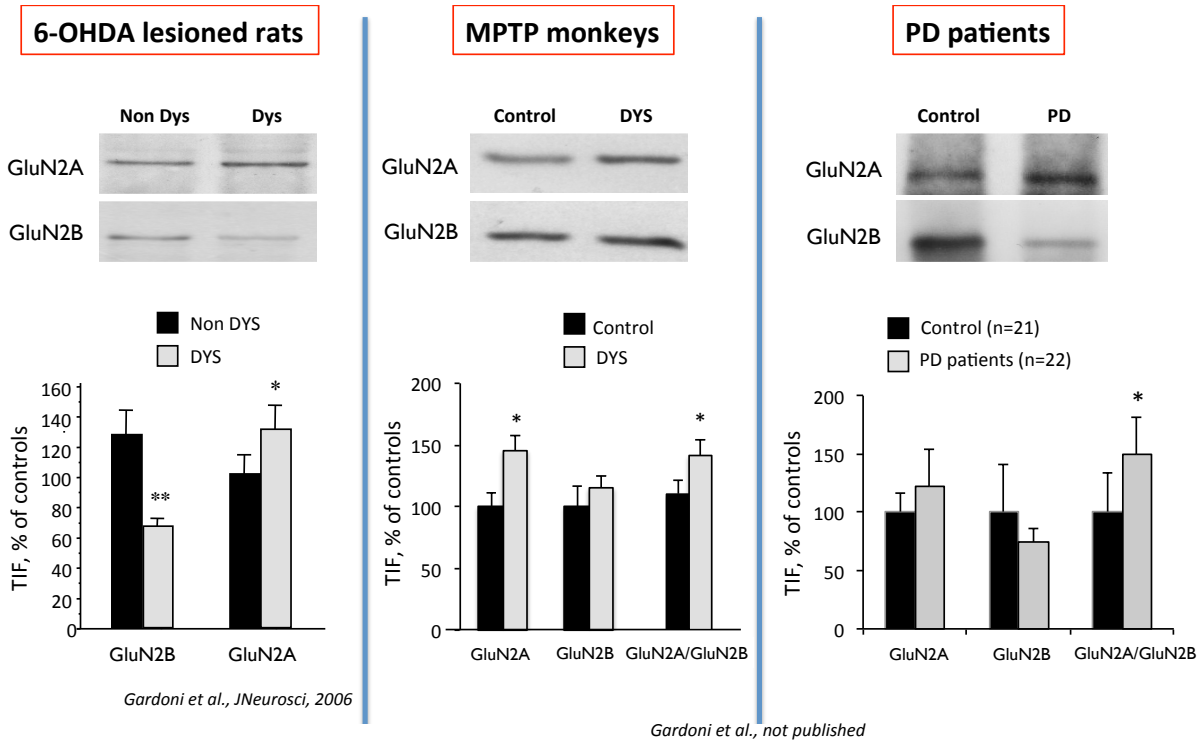

Fig. 8: NMDAR composition at the synapse in LID. Gardoni et al. Have demonstrated that there is a increase of GluN2A/GluN2B ratio in the 6-OHDA lesioned rat model of LID compared to the dyskinetic conterpart (Gardoni et al., 2006), the MPTP monkey model of LID but also in PD patients treated with L-DOPA compared to aged-matched healthy subjects (Gardoni et al., not published).

The efficacy of NMDAR antagonists in blocking the onset of dyskinesia without influencing the beneficial effects of the treatment on parkinsonian symptoms was examined in animal models of PD (Nash et al., 2000; Löschmann et al., 2004; Hadj Tahar et al., 2004; Wessell et al., 2004). Overall, there is a general agreement that NMDAR blockade attenuates parkinsonian motor symptoms and improves dopaminergic therapy. However, classical NMDA agents are not well tolerated by primates because of numerous side effects. Therefore, recent research has focused on low-affinity or subunit-specific NMDAR antagonists in order to ameliorate parkinsonian symptoms in absence of major adverse effects (Mellone & Gardoni, 2013).

Amantadine is a low-affinity, non-competitive antagonist of NMDAR (Kornhuber, Bormann, Hübers, Rusche, & Riederer, 1991). Several studies demonstrated that amantadine exhibits anti-dyskinetic activity even if the beneficial effects is attenuated after a few months (Verhagen Metman et al., 1998; Luginger, Wenning, Bösch, & Poewe, 2000; Snow, Macdonald, Mcauley, & Wallis, 2000; A. Thomas et al., 2004; da Silva-Júnior, Braga-Neto, Sueli Monte, & de Bruin, 2005). However, a random-

ized, placebo-controlled, parallel-group study recently demonstrated a long-term (>1 year) anti-dyskinetic effect of amantadine in a limited cohort of patients (Wolf et al., 2010). Furthermore, a meta-analysis based on 11 randomized, placebo-controlled clinical trials confirmed at least the short-term benefits of amantadine therapy in the treatment of dyskinesia (Elahi, Phielipp, & Chen, 2012).

GluN2B-selective antagonist ifenprodil, together with its derivatives, seemed well suited for treatment of PD as well as LID as they induced reduced parkinsonian symptoms in different animal models (Steece-Collier, Chambers, Jaw-Tsai, Menniti, & Greenamyre, 2000; Nash et al., 2004; Hadj Tahar et al., 2004; Morissette et al., 2006). However, contradictory results have been provided by recent studies on the the effects of GluN2B-selective antagonists on the onset of LID in experimental models of parkinsonism (Rylander et al., 2009; Nash et al., 2000; Wessell et al., 2004) as well as dose-related dissociation and detrimental side effects like amnesia in randomized, double-blind, placebo-controlled clinical trial (Nutt et al., 2008).

While there is an increasing research on GluN2B-specific compounds, few studies have been performed on GluN2A-selective agents. A recent work, which applied a cell-permeable peptide disrupting GluN2A/PSD-MAGUKs interaction, demonstrated that a decrease in synaptic GluN2A-containing NMDA receptors induces a significant reduction in the onset of LID (Gardoni et al., 2011) in parkinsonian rats (Mellone & Gardoni, 2013).

III. GluN2A/B trafficking and targeting to synapses

It is believed that the protein-protein interactions in the cytoplasmic C-terminus and the extracellular N-terminus of the receptor determine the precise localization of GluN2 subunits. For example, the PDZ binding motif at the extreme C-terminus of both GluN2A and GluN2B subunits binds to the second PDZ domain of MAGUK proteins, which act as scaffolding proteins. Members of this family (PSD-93, PSD-95, SAP97 and SAP102) show differential subcellular localization, with PSD-95 predominantly expressed at the postsynaptic density and SAP102 being distributed more evenly between synaptic and extrasynaptic sites. In addition, a preferential association of GluN2A/PSD-95 and GluN2B/SAP102 has been reported (Sans et al., 2000; although see Al-Hallaq et al., 2007). Therefore, a working model proposes that binding of GluN2 subunits to different MAGUK proteins controls NMDAR localization. Current data support this scenario for GluN2B because the disruption of the GluN2B PDZ binding domain results in a lost of synaptic GluN2B as demonstrated by electrophysiological and confocal imaging approaches (H. J. Chung, Huang, Lau, & Huganir, 2004; Prybylowski et al., 2005). In contrast, the literature for GluN2A is less consistent because GluN2A expressing a point mutation disrupting its PDZ binding domain has similar NMDA-mEPSCs compared to GluN2A wild-type in transfected cerebellar granule cells (Prybylowski et al., 2005, but see Barria & Malinow, 2002). However, a genetically modified mouse line expressing GluN2A lacking the C-terminus (GluN2A$^{\Delta C/}$

$^{\Delta C}$) (Sprengel et al., 1998) shows a reduced synaptic GluN2A expression, as revealed by biochemical subcellular fractionation and electron microscopy (Steigerwald et al., 2000). Consistently, GluN2A$^{\Delta C/\Delta C}$ mice display slower NMDAR kinetics, indicating a decrease in synaptic GluN2A (Steigerwald et al., 2000). A possible explanation for these data is the existence of additional protein binding domains, other than the PDZ binding, in the GluN2A C-terminus that act to stabilize the receptor at synaptic sites. Recent reports identifying PDZ-independent binding sites between GluN2 and MAGUKs support this model (B.-S. Chen, Thomas, Sanz-Clemente, & Roche, 2011; Cousins, Kenny, & Stephenson, 2009). The extracellular domain of NMDARs also plays a role in controlling their subcellular localization via interaction with postsynaptic proteins such as the activated EphB receptor (Dalva et al., 2000) and with components of the extracellular matrix such as reelin (Groc et al., 2007). Other proteins are likely to modulate NMDAR localization via indirect processes, including neuroligins or integrins (Jung et al., 2010).

The cytoplasmic C-tails of GluN2A and GluN2B contain distinct motifs that control their trafficking (Fig. 9). Evidence supports a model in which GluN2B is more mobile than GluN2A, and it is subject to regulated lateral diffusion, endocytosis, and recycling. With two different approaches, it has been demonstrated that NMDARs move in and out of synapses and that GluN2B-containing NMDARs have a much higher (250-fold) surface mobility (Tovar & Westbrook, 2002; Groc et al., 2006). A possible molecular explanation of these data emerges with a report showing that GluN2B is phosphorylated by casein kinase 2 (CK2) within its PDZ-binding domain, which disrupts the association with scaffolding proteins, whereas GluN2A is not (Sanz-Clemente, Matta, Isaac, & Roche, 2010). The phosphorylation of the PDZ ligand domain, however, is NMDAR-activity dependent, whereas the coefficient of diffusion for GluN2B is not modified by synaptic activity. Also, GluN2B shows a higher ratio of endocytosis than GluN2A in adult neurons (Lavezzari, McCallum, Dewey, & Roche, 2004). Another important difference in GluN2 subunit trafficking is postendocytic sorting. Whereas GluN2B is sorted to recycling endosomes (Rab11-positive) and reinserted into the plasma membrane, GluN2A colocalizes better with Rab9 in late endosomes following endocytosis and is subjected to lysosomal degradation (Lavezzari et al., 2004; Tang, Badger, Roche, & Roche, 2010).

GluN2A and GluN2B are subject to differential regulation by several posttranslational mechanisms, including palmitoylation and nitrosylation. However, the best characterized example is the modulation of NMDARs by phosphorylation (B.-S. Chen & Roche, 2007; Fig. 9). For example, it has been shown that the phosphorylation of the GluN2A C-terminus by cyclin-dependent kinase 5 (cdk5) increases NMDAR currents and cdk5 inhibition has protective effects against ischemic insults (J. Wang, Liu, Fu, Wang, & Lu, 2003). However, no cdk5-mediated phosphorylation has been reported so far for GluN2B. Conversely, CK2 and calcium- and calmodulin-dependent kinase II (CaMKII) phosphorylate GluN2B on S1480 (within its PDZ binding domain) and S1303 (within the CaMKII binding site), re-

spectively, but not GluN2A (Omkumar, Kiely, Rosenstein, Min, & Kennedy, 1996; Sanz-Clemente et al., 2010). It should be noted, however, that S1291 on GluN2A and S1096 on GluN2C (analogous to S1303 on GluN2B) are phosphorylated by PKC and PKB, respectively (B.-S. Chen & Roche, 2009; M. L. Jones & Leonard, 2005). Other kinases, such as PKA, PKC, and several protein tyrosine kinases (Fyn and Src), phosphorylate both GluN2A and GluN2B subunits, although the precise residues and the consequences of their phosphorylation also differ.

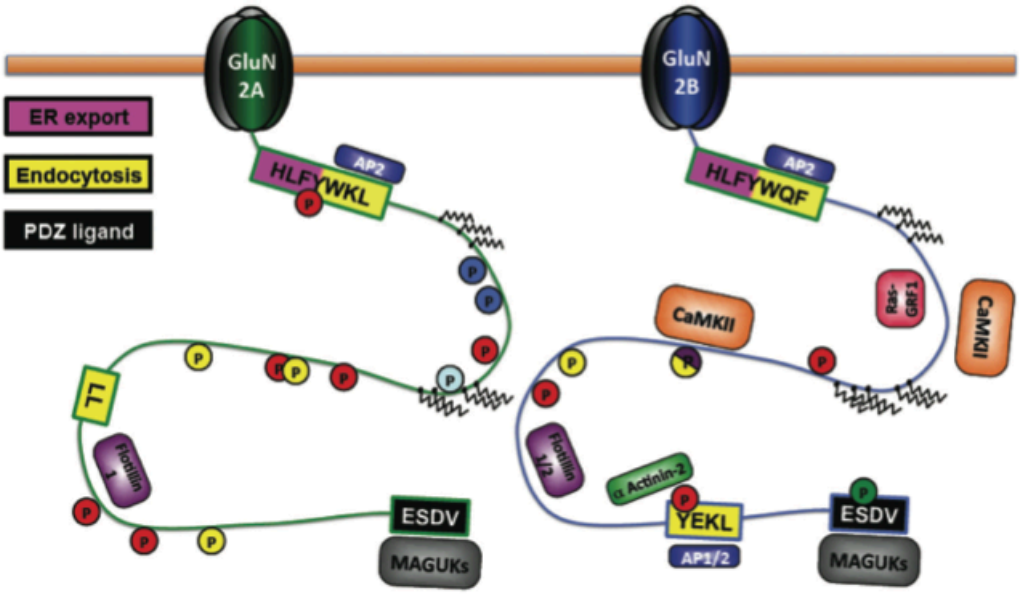

	GluN2A	GluN2B
PKA	S900 ; S929	
PKC	S1291 ; S1312 ; S1416	S1323
CK2		S1480
Cdk5	S1232	
PKC/CaMKII	S1303	
Src/Fyn	Y842 ; Y1105 ; Y1267 Y1292 ; Y1325 ; Y1387	Y1252 ; Y1336 ; Y1472
Palmitoylation	C848 ; C853 ; C870 C1214 ; C1217 ; C1236 ; C1239	C849 ; C854 ; C871 C1215 ; C1218 ;C1239 ; C1242 ; C1245

Fig. 9: GluN2A and GluN2B intracellular C-terminal tail. The GluN2A and GluN2B C-termini contain distinct regulatory motifs, phosphorylation sites, and protein-protein interaction domains (Sanz-Clemente, Nicoll & Roche, 2012).

As discussed above, the interaction of GluN2 subunits with MAGUKs and other synaptic proteins defines their differential subcellular localization. Similarly, many other parameters are determined by their distinct protein-protein interactions, including trafficking regulation and activation of intracellular pathways. One of the classic examples is the binding of CaMKII to NMDARs. It has been reported that CaMKII binds to GluN2A in vitro, but this interaction is much weaker than the well-documented association between CaMKII and GluN2B (Bayer, De Koninck, Leonard, Hell, & Schulman, 2001). Calcium entry through NMDARs activates CaMKII that can then bind to GluN2B (residues 1290 - 1310). This CaMKII-GluN2B association is regulated by the CaMKII/PKC phosphoryla-

tion of S1303 within the CaMKII binding site (Raveendran et al., 2009). The presence of CaMKII bound to GluN2B at synaptic sites is believed to be an important requirement for the maintenance of LTP, since disrupting this interaction reverses the potentiation (Sanhueza et al., 2011).

In the end, the proteins and mechanisms involved in the targeting to the synapse are much more studied and understood concerning the GluN2B subunit of NMDAR unfortunately they still remains a lot of questions concerning the GluN2A subunit. In fact, compared to GluN2B C-terminal tail, there is very informations on proteins interacting with the C-terminal tail of GluN2A. Based on these considerations, our lab has concentrated its focus in studying the modulation of GluN2A at synapses starting from the identification of new interactors of the C-terminal tail of GluN2A involved in its targeting or stabilization at synaptic sites. Consequently, a yeast two-hybrid screening has been performed using as bait the intracellular C-terminal sequence of GluN2A without the PDZ-binding sequence (aa 831 to aa 1461) and 16 positive clones were found among which was a Rab-binding protein involved in endocytosis and calcium-dependent vesicle exocytosis, Rabphilin3A.

IV. Rabphilin3A

Rabphilin3A (Rph3A) was first identified as a vesicle-associated protein involved in the vesicular trafficking machinery. Rph3A was studied as a binding partner of GTP-bound Rab3A (Shirataki et al., 1992; Shirataki et al., 1994), a member of the Rab family of GTPases implicated in vesicle docking/fusion reactions in many systems (Simons & Zerial, 1993; Takai, Sasaki, Shirataki, & Nakanishi, 1996). In mice, Rph3A is a protein of 681 aa and has two functionally different domains: the N-terminal Rab3A-binding domain (1–179 aa) and the C-terminal two C2-like domains (C2A [380–503 aa] and C2B [540–672 aa] domains) interacting with Ca^{2+} and phospholipids (Yamaguchi et al., 1993; Fukuda, Kanno, & Yamamoto, 2004; Fig. 10). The NH_2-terminal half of Rabphilin-3A binds to the cytoskeletal protein, α-actinin, and enhances its ability to bundle actin filaments (Kato et al., 1996) and the other half binds the GTP-bound form of Rab3A (Yamaguchi et al., 1993), maintaining Rab3A in this state by preventing a GTPase-activating protein from catalyzing GTP hydrolysis by Rab3A (Kishida et al., 1993). At least two Rab3s bind to Rabphilin: the abundant Rab3A and the less abundant Rab3C (C. Li et al., 1994), but Rab27 has also been shown to bind Rph3A (Fukuda, 2005). The central domain of Rph3A is phosphorylated, as a function of stimulation, by Ca^{2+}-calmodulin dependent protein kinase II (CAMKII) and by cAMP-dependent protein kinase (PKA) (Fykse, Li, & Südhof, 1995; Lonart & Südhof, 1998). Phosphorylation is regulated in a brain region-specific manner. The C_2-like domains are homologous to the C_2 domains of Synaptotagmin I, a calcium sensor that triggers vesicle fusion (DeBello, Betz, & Augustine, 1993; Südhof, 1995), and contain the residues that mediate Ca^{2+} binding in synaptotagmins (Südhof & Rizo, 1996). Recent nuclear magnetic resonance experiments confirmed that Ca^{2+} binds to Rabphilin with a relatively high affinity (Ubach, García, Nittler, Südhof, & Rizo, 1999). Thus, rabphilin is a bona fide Ca^{2+}-binding protein. Although Rab3A is found in all the cells

with a Ca^{2+}-regulated secretion pathway, rabphilin3A is expressed only in neurons and neuron-like cells, such as adrenal chromaffin cells and PC12 cells (Mizoguchi et al., 1994; C. Li et al., 1994). In addition, the C2 domains of Rph3A bind to the cytoskeletal protein ß-adducin (Miyazaki et al., 1994), which functions in the assembly of spectrin–actin complexes at the plasma membrane (Hughes & Bennett, 1995), as well as CASK (calcium/calmodulin-dependent serine protein kinase), a PDZ-containing protein of the MAGUK family (Y. Zhang, Luan, Liu, & Hu, 2001). Moreover, the C_{2B} domain of Rph3A has been shown to bind SNAP-25, a member of the SNARE (soluble *N*-ethylmaleimide-sensitive factor attachment protein receptor) proteins, fundamental fusion machinery of vesicle exocytosis (Tsuboi & Fukuda, 2005). Although Rph3A is associated with synaptic vesicles (Shirataki et al., 1994; C. Li et al., 1994), the protein lacks a membrane-spanning region. Instead, Rph3A is thought to associate with synaptic vesicles by binding to another vesicular protein whose identity is not yet clear (Shirataki et al., 1994; McKiernan, Stabila, & Macara, 1996; Stahl, Chou, Li, Südhof, & Jahn, 1996).

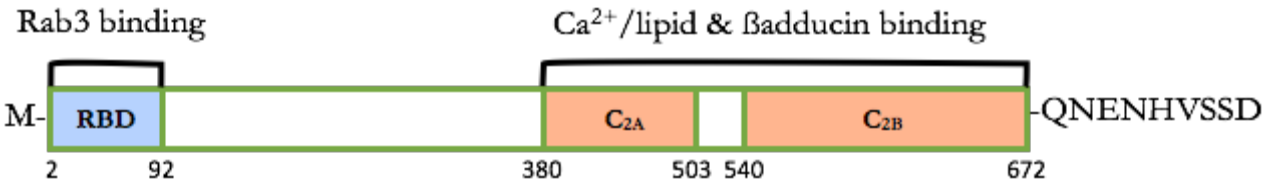

Fig. 10: Schematic of Rabphilin3A domains. Rph3A has a Rab binding domain (RBD) at its N-terminus, two C2 domains (C2A and C2B), and the last 4 amino acids (VSSD) resemble a putative PDZ-binding site.

The biochemical properties of Rph3A, in particular its ability to bind calcium, Rab3A, and the cytoskeleton, make it a prospective participant in synaptic vesicle trafficking (Südhof, 1997). Burns et al. have examined the function of this protein in the synaptic vesicle cycle showing that Rph3A regulates both exo- and endocytosis, (Burns, Sasaki, Takai, & Augustine, 1998). Rph3A's implication in endocytosis was recently confirmed with the discovery of the interaction between Rph3A and Phosphatidylinositol-4,5-bisphosphate (PIP2), a key player in the neurotransmitter release process (Montaville et al., 2008). PIP2 represents <1% of the lipids in the plasma membrane and forms microdomains to regulate several signaling events (Osborne, Wen, & Meunier, 2006). More specifically, PIP2 is involved in different stages of the neurotransmitter release process: it is required for clathrin-mediated endocytosis (Haucke, 2005), for specific stages of exocytosis, and synaptic vesicle trafficking (Osborne et al., 2006).

Rph3A is, so far, the only known C_2 domain tandem containing protein where both C_2 domains bind PIP2 (S. H. Chung et al., 1998). Montaville, P. et al., (2008) investigated the interactions of the two C_2 domains with the PIP2 headgroup IP3 (inositol-1,4,5-trisphosphate) by NMR, that showed a well-defined binding site on the concave surface of each domain. The binding models of both C_2 domains of Rph3A to the IP3 differ in affinity as well as in Ca^{2+} dependency. The binding of IP3 to the C_{2A} domain is strongly enhanced by Ca^{2+}. Reciprocally, the binding of IP3 increases the apparent Ca^{2+}-

binding affinity of the C_{2A} domain in agreement with a Target-Activated Messenger Affinity (TAMA) mechanism. The C_{2B} domain binds IP3 in a Ca^{2+}-independent fashion with low affinity. These different PIP2 headgroup recognition modes suggest that PIP2 is a target of the C_{2A} domain of Rph3A while this phospholipid is an effector of the C_{2B} domain (Montaville et al., 2008).

A further confirmation of a putative Rph3A's implication in endocytosis comes from recent studies showing that Rph-3A is one of the binding partners of BR-MyoVa (Brozzi et al., 2012). The brain-spliced isoform of Myosin Va (BR-MyoVa) plays an important role in the transport of dense core secretory granules (SGs) to the plasma membrane in hormone and neuropeptide-producing cells. Activity-dependent secretion of hormones and neuropeptides is critical for the execution of various endocrine functions, neurotransmission and neuronal plasticity (Park & Loh, 2008). Despite the diverse functions of these cells, they share some degree of similarities in the transport of their SGs which involves microtubules (Rudolf, Salm, Rustom, & Gerdes, 2001; Varadi, Ainscow, Allan, & Rutter, 2002) and cortical actin filaments (Steyer & Almers, 1999). The active transport along actin filaments is driven by the motor protein myosin Va (MyoVa) (Rosé et al., 2003; Rudolf et al., 2003; Varadi, Tsuboi, & Rutter, 2005). The SGs are transported from the cell center to the cell cortex primarily by the microtubule-based motor protein conventional kinesin (Varadi et al., 2002; Varadi, Tsuboi, Johnson-Cadwell, Allan, & Rutter, 2003). The short-range movements in the cortical regions of the cell that carry SGs over the last few hundred nanometers to the cell surface involve myosin Va (MyoVa) (Varadi et al., 2005; Ivarsson, Jing, Waselle, Regazzi, & Renström, 2005). Current studies identified novel protein-complexes that bind BR-MyoVa to SGs, like Rph3A that enhanced their interaction when secretion is activated (Brozzi et al., 2012). These findings were rather unexpected because this was the first time that direct interaction between these C_2 domain–containing proteins and MyoVa was demonstrated. The inhibition of its (and the other proteins) interaction with MyoVa nearly completely abolishes stimulated secretion. Interestingly, in rat hippocampus, myosin Va regulates also the insertion of AMPA receptors (AMPARs) into spines during synaptic plasticity (Correia et al., 2008). Myosin Va associates with AMPARs through its cargo binding domain. This interaction was enhanced by active, GTP-bound Rab11, which is also transported by the motor protein. In particular, Myosin Va mediated the CaMKII-triggered translocation of GluA1 receptors from the dendritic shaft into spines. In summary, Myosin Va catalyzes the directional transport of AMPARs into dendritic spines during activity-dependent synaptic plasticity.

Mice that lack Rph3A are viable and fertile without obvious physiological impairments. Moreover, no abnormalities in synaptic transmission or plasticity were observed; notably, synaptic properties that are impaired in rab3A knock-out mice were unchanged in Rph3A knock-out mice. Furthermore, Rph3A is endowed with the properties of a Rab3 effector but is not essential for the regulatory functions of Rab3 in synaptic transmission (Schlüter et al., 1999).

Overall, all these results indicate that Rph3A regulates synaptic vesicle traffic and appears to do so at distinct stages of both the exocytotic and endocytotic pathways. Thus, even if a large amount of information on Rabphilin is available, there is no consensus on the precise role of Rph3A in the presynaptic terminal. Finally, Rph3A interaction with Myosin Va put forward also a possible role for Rph3A in regulating receptor trafficking within the postsynaptic terminal.

V. Modulation of Rph3A in CNS disorders

Schlüter *et al.*, (1999) therefore suggested that it is plausible that Rph3A may have no fundamental role in the execution or regulation of neurotransmitter release under normal conditions but could play a specialized role under, as yet unidentified, possibly more "extreme" physiological conditions; this hypothesis was partially confirmed when Rph3A has been shown to be involved in Huntington's Disease (Smith, Petersén, Bates, Brundin, & Li, 2005, Smith et al., 2007). Rph3A was found to be depleted from synapses throughout the brain in the R6/1 transgenic mouse model of HD (Smith et al., 2005). The depletion of Rabphilin-3A started at an age when weight loss, motor dysfunction, and cognitive deficits begin (Mangiarini et al., 1996), gradually became more pronounced, and was not apparent before there were clearly overt motor symptoms. The reduction of Rph3A was not due to recruitment into protein aggregates, since there was no colocalization of Rph3A and huntingtin aggregates but could be due to changes at both the transcriptional and post-translational levels. Mutant huntingtin can interrupt normal transcription (J.-Y. Li, Plomann, & Brundin, 2003; Sugars & Rubinsztein, 2003) and could be involved in causing the reduction in Rph3A mRNA in the cortex of R6/1 mice (Smith et al., 2005). Using in situ hybridization, it was demonstrated that Rph3A mRNA expression was substantially reduced in the R6/1 mouse cortex compared to wild-type mice. This is interesting especially because changes in the corticostriatal pathway has been suggested to play an important role in the pathogenesis of HD and dysfunctional release of neurotransmitter at this level, such as glutamate, may also cause excitotoxicity (as presented earlier in *II.4. Huntington's disease*). These results indicate that a decrease in mRNA levels underlie the depletion of protein levels of Rph3A and this reduction may be involved in causing impaired synaptic transmission in R6/1 mice that contributes to the development of HD-like symptoms in R6/1 mice (Smith et al., 2005).

A recent study found specific reductions of Rph3A immunoreactivity in AD patients compared with aged controls. Rph3A loss correlated with dementia severity, cholinergic deafferentation, and increased βamyloid (Aβ) concentrations. Furthermore, RPH3A expression is selectively downregulated in cultured neurons treated with Aβ peptides. This data suggest that presynaptic SNARE dysfunction forms part of the synaptopathology of AD (Tan et al., 2013).

Subsequent studies suggested an involvement of Rph3A in the pathological events preceding overt neuronal degeneration in Parkinson's disease (PD) and α-synucleinopathy (C. Y. Chung, Koprich, Siddiqi, & Isacson, 2009). With a model of slow α-synucleinopathy in rat, Chung, C.Y. et al., (2009) in-

vestigated predegenerative changes (at 4 weeks and 8 weeks) long before cell death and striatal dopamine loss, aiming to identify pathogenic changes that are most likely causal to the disease, and not a by-product of the cell death process. They demonstrated that before neuronal loss, significant changes occurred in levels of proteins relevant to synaptic transmission and axonal transport in the striatum. It was detected a decrease in levels of proteins involved in synaptic vesicle exocytosis, including Rph3A and syntaxin, by 2 months. Interestingly, characterization of striatal tissue at different times after α-synuclein overexpression revealed dynamic changes in presynaptic and axonal transport related proteins. For example, levels of Rph3A, KIF3A and myosin Va were elevated at 4 weeks followed by a reduction at 8 weeks raising the possibility that compensatory changes occurred at 4 weeks to counteract the effects of A53T α-synuclein overexpression. It is plausible that such compensatory mechanisms were overcome by 8 weeks with progression of the disease process. In contrast to the results in the striatum, the expression levels of most of these proteins were not altered in the Substantia Nigra (SN), suggesting that the decreased protein levels seen in the striatum was not a result of general reduction of protein production in the cell body, but most likely due to trafficking disruption. These results demonstrate that changes in proteins relevant to synaptic transmission and axonal transport, precede α-synuclein-mediated neuronal death, and these findings can provide ideas for antecedent biomarkers and presymptomatic interventions in PD (C. Y. Chung et al., 2009).

AIM

NMDARs are key mediators of excitatory synaptic transmission in the brain. Their subunit composition is determinant for several physiological functions in the brain, i.e., synaptic plasticity. On the other hand, there is a general agreement that modulation of NMDAR complex subunit composition plays a key role in mediating at least some aspects of glutamate neurotoxicity that is thought to be a major mechanism in several CNS disorders.

Based on these considerations, understanding in minute details the mechanisms governing the localization of NMDAR subunits at synaptic sites is necessary for a complete understanding of the physiology and pathology of the excitatory synapse.

In this context, even if the literature reported extensive studies describing the differential role of GluN2B-containing receptors at synaptic and extrasynaptic sites and identified relevant protein partners regulating their synaptic localization, much less is known for GluN2A-containing receptors.

It is known that the GluN2A subunit binds PSD-MAGUK family members (PSD-95, SAP97 and SAP102) by means of a well-described interaction of GluN2A-SDV C-terminal motif with PDZ domains of PSD-MAGUKs (C. G. Lau & Zukin, 2007; Gardoni, Marcello, & Di Luca, 2009). Although the interaction with these important scaffolding elements plays a key role in the synaptic clustering of GluN2A, the molecular mechanisms regulating the synaptic targeting of GluN2A-containing receptors are far from being understood.

At present, there is few information about other putative proteins which could interact with the very long GluN2A intracellular C-tail. Based on these considerations, we decided to study the modulation of the GluN2A subunit in the synapse starting from the identification of new GluN2A-interacting proteins. A yeast two hybrid screening performed by using GluN2A(839-1461) as bait, without the last 3 aa (SDV) of the PDZ-binding domain, revealed 16 new putative GluN2A-interacting proteins. One of them was Rabphilin3A (Rph3A).

Rph3A is mainly known as a presynaptic protein involved in the regulation of the vesicle trafficking (both in the exo- and endocytosis). In addition, it has been demonstrated that Rph3A interacts with the Myosin Va cargo protein, known to catalyze the transport of AMPARs into dendritic spines during activity-dependent synaptic plasticity. Interestingly, Rph3A involvement in CNS disorders such as Huntington's disease, α-synucleinopathy and possibly Parkinson's disease has been put forward.

Overall, the main aim of this study is to investigate the subcellular distribution of Rph3A in neurons, its interactions with GluN2A and with a PDZ-containing protein like PSD-95, and the role of these interactions in the synaptic localization of GluN2A in physiological conditions, in the hippocampal glutamatergic synapse, and in the pathology of Parkinson's disease and L-DOPA induced dyskinesia, in the striatal glutamatergic synapse.

These studies will be instrumental for the analysis of a possible novel role for Rph3A in the glutamatergic synapse, involved in the regulation of NMDA receptor trafficking within the postsynaptic terminal.

MATERIAL & METHODS

I. Animals

Animals used in this project were male C57/BL6 mice of 6 weeks, male Sprague-Dawley rats of 6 weeks, E18 embryos from Sprague-Dawley rats for primary hippocampal neuron cultures, P6-P21 Sprague-Dawley rat pups and 125-175g male Sprague-Dawley rats for 6-OHDA lesions. All the experiments were approved by the OHSU Institutional Animal Care and Use Committee and by the Italian Health Ministry.

II. Cell cultures and transfections

II.1. Cell lines (COS7)

COS7 cells were grown on 100 mm dishes and maintained in Dulbecco's Modified Eagle's Medium containing Glutamax (DMEM + Glutamax, GIBCO) supplemented with 10% Fetal Bovine Serum and penicillin-streptomycin (GIBCO). Cells were allowed to grow till confluence before passaging every 3-4days using trypsin. The day before transfection, COS-7 cells were placed in a 6 wells multiwell (for cells lysis) or 12 wells multiwell (for imaging), then cells were transfected with 250-500 ng of plasmid DNA (for RFP-Rph3A, kind gift from Prof. Mitsunori Fukuda; RFP-Rph3A(673), was created by site-directed mutagenesis of Q673 into a stop codon; GluN2A-eGFP; GluN2A(1049)-eGFP, provided by Dr. Margarita Dinamarca from University of Milan; and/or PSD-95) using the lipofectamine method. After 36 hours COS-7 cells were lysed or fixed for immunostaining/imaging.

II.2.1. Primary hippocampal neurons

Hippocampal neuronal primary cultures were prepared from embryonic day 18-19 (E18-E19) rat hippocampi as previously described (Piccoli et al., 2007). Neurons were transfected at DIV9 with 2-4 μg of plasmid DNA for RFP-Rph3A, kind gift from Prof. Mitsunori Fukuda; GluN2A-eGFP; GFP,a kind gift from Dr. Maria Passafaro from the University of Milan; shRph3A-tGFP, from Thermoscientific or shScramble-tGFP, from Thermoscientific, using calcium-phosphate method. Neurons were treated at DIV15, lysed or fixed and then immunostained.

III. Triton Insoluble Fraction (TIF) and crude membrane fraction (P2) purifications

From adult rat forebrain, hippocampus or striatum, Triton Insoluble Fraction (TIF), a fraction highly enriched in all categories of postsynaptic density proteins (i.e., receptor, signaling, scaffolding, and cytoskeletal elements) absent of presynaptic markers, was isolated. To obtain the TIF fractions, samples were homogenized at 4°C in an ice-cold buffer with protease inhibitors (*Complete*™, GE Healthcare, Mannheim, Germany), phosphatase inhibitors (*PhosSTOP*™, Roche Diagnostics GmbH, Mannheim, Germany), 0.32 M Sucrose, 1 mM Hepes, 1 mM NaF, 0.1 mM PMSF, 1 mM $MgCl_2$ using a hand held glass-teflon (for forebrain samples) or glass-glass homogenizer. An aliquot of homogenate (Homo) was kept for Western Blot (WB) analysis. Homo were then centrifuged at 1,000 g for 5 min at 4°C, to remove nuclear contamination and white matter. The supernatant was collected and centrifuged

at 13,000 g for 15 min at 4°C. The resulting pellet (crude membrane) was resuspended in hypotonic buffer (1 mM Hepes with protease inhibitors (*Complete™,* GE Healthcare)). An aliquot of P2 was kept to perform coImmunoprecipitation (coIP) assay. P2 were then centrifuged at 100,000 g for 1 h at 4°C. Triton-X-100 extraction of the resulting pellet was carried out at 4°C for 20 min in an extraction buffer (1% Triton-X-100, 75 mM KCl and protease inhibitors (*Complete™,* GE Healthcare)). After extraction, the samples were centrifuged at 100,000 g for 1 h at 4°C and the TIFs obtained were resuspended in 20 mM HEPES with protease inhibitors (*Complete™,* GE Healthcare).

To get only the crude membrane fraction (P2), samples were homogenized at 4°C in an ice-cold buffer with protease inhibitors (*Complete™,* GE Healthcare), phosphatase inhibitors (*PhosSTOP™,* Roche Diagnostics GmbH, Mannheim, Germany*),* 0.32 M Sucrose, 1 mM Hepes, 2 mM EDTA, 0.1 mM PMSF using a hand-held glass-teflon (for forebrain samples) or glass-glass homogenizer. Homo were then centrifuged at 1,000 g for 10 min at 4°C, to remove nuclear contamination and white matter. The supernatants were collected and centrifuged at 100,000 g for 1 h at 4°C. The resulting pellet (crude membrane) obtained corresponds to the P2 fraction and the supernatant was discarded.

IV. Post-Synaptic Density purification

To isolate PSDs from rat forebrain and hippocampus, a modification of the method of Carlin et al. (1980) was used. In brief, forebrain (from 4 rats) and hippocampus (from at least 12 animals) were rapidly dissected and pooled. Animals were killed, and brain areas were dissected within 2 min (Suzuki et al., 1994). Homogenization was carried out by 10 strokes in a hand-held glass-teflon (for forebrain samples) or glass-glass homogenizer in 4 volumes of cold 0.32 *M* sucrose containing 1 mM HEPES, 1 mM MgCl2, 1 mM NaHCO3 and 0.1 mM phenylmethylsulfonyl fluoride (PMSF) (pH 7.4) in the presence of a complete set of protease inhibitors (*Complete™*; Boehringer Mannheim GmbH, Mannheim, Germany) and Phosphatase inhibitors (*PhosSTOP™,* Roche Diagnostics GmbH, Mannheim, Germany). The homogenized tissue was centrifuged at 1,000 *g* for 10 min. The resulting supernatant was centrifuged at 3,000 g for 15 min to obtain a fraction containing mitochondria and synaptosomes. The pellet was resuspended in 2.4 volumes of 0.32 M sucrose containing 1 mM HEPES, 1 mM NaHCO3, and 0.1 mM PMSF, overlaid on a sucrose gradient *(0.85—1.0—1.2 M),* and centrifuged at 82,500 g for 2 h. The fraction between 1.0 and 1.2 *M* sucrose was removed, diluted with an equal volume of 1% Triton-X-l00 in 0.32 M sucrose containing 1 mM HEPES, 1 mM NaHCO3, and 0.1 mM PMSF, and stirred at 4°C for 15 mm. This solution was spun down at 82,500 g for 30 min. The pellet was resuspended, layered on a sucrose gradient (1.0—1.5—2.1 *M),* and centrifuged at 100,000 g at 4°C for 2 h. The fraction between 1.5 and 2.1 M was removed and diluted with an equal volume of 1% Triton-X-100 and 150 mM KC1. PSDs were finally collected by centrifugation at 100,000 g at 4°C for 30min and stored at -80°C.

V. Co-immunoprecipitation

Rat forebrain/hippocampus/striatum aliquots of 150 μg of homogenate or of 50 μg of P2 fraction or 5μg of TIF were incubated for 1 h at 4ºC in RIA buffer containing 200 mM NaCl, 10 mM ethylene-diamine-tetra-acetic acid (EDTA), 10 mM Na_2HPO_4, 0.5% NP-40, 0.1% sodium dodecyl sulphate (SDS) and 25 μl of protein A/G-agarose beads (Santa Cruz) in a final volume of 225 μl to preclean the samples. The beads were then let to sediment at the bottom of the tube and the supernatant was collect. An antibody (Ab) against Rph3A or GluN2A was added to the supernatant before leaving to incubate overnight at 4ºC on a wheel. Protein A/G-agarose beads (Santa Cruz) were added and incubation was continued for 2 hours, at room temperature on a wheel. Beads were collected by gravity and washed three times with RIA buffer before adding sample buffer for SDS-PAGE and boiling for 5 minutes. Beads were collected by centrifugation, all supernatants were applied onto 7%-10% SDS-PAGE and revealed by either anti-GluN2A, anti-GluN2B, anti-GluA1, anti-PSD-95, anti-Rph3A, anti-SAP97, anti-MeOx2, anti-Rab3A, anti-Rab8, anti-Rab11, etc.

VI. Cloning, expression and purification of glutathion-S-transferase (GST) fusion proteins

The GluN2A subunit was subcloned downstream of glutathione S-transferase (GST) in the BaMHI and HindIII sites of the expression plasmid pGEX-KG by PCR using the Pfu polymerase (Stratagene) on a GluN2A cDNA template (kind gift from S. Nakanishi). Glutathione S-transferase (GST)-GluN2A C-terminal domain fusion protein containing the cytoplasmic domain of GluN2A (1049-1464 or 1349-1461 or 1244-1389) were expressed in Escherichia coli and purified on glutathione agarose beads (Sigma Aldrich, St. Louis, MO, USA) as previously described (Gardoni et al., 1999). Briefly, overnight cultures from single colonies of E. coli transformed with the plasmid were grown in 50 ml of Luria-Bertani medium (Sigma, St. Louis, MO, USA) containing 100 μg/ml ampicillin (Sigma, St. Louis, MO, USA) at 37°C, diluted 1:10 with Luria-Bertani medium containing 100 μg/ml ampicillin and incubated under the same conditions for 2 h. Synthesis of recombinant proteins was induced by 0.1 mM isopropyl-L-D-thiogalactopyranoside (Sigma, St. Louis, MO, USA), the bacteria were grown for another 4 h and harvested by centrifugation. Bacterial pellets were resuspended with ice-cold PBS (8.4 mM Na2HPO4, 1.9 mM NaH2PO4, 150 mM NaCl, pH 7.4) containing 5 mM dithiothreitol (DTT), 100 μg/ml lysozyme, 0.1 mM PMSF and incubated on ice for 15 min. Lysis was achieved by the addition of 1.5% N-laurylsarcosine (sarkosyl) from a 10% stock in PBS. Bacteria were sonicated on ice for 1 min and the lysate was clarified by centrifuging at 10,000 g (5 min, 4°C) in a SS-34 rotor (Sorvall). Supernatants were adjusted to 2% Triton X-100 and incubated with glutathione-agarose beads (50% v/v in PBS) for 2 h at room temperature. The beads were then extensively washed with ice-cold PBS.

VII. Pull-down assay

250 μg of proteins were incubated with Tris Buffered Saline (TBS, 10 mM Tris and 150 mM NaCl) and 20 μl of GST to a final volume of 1 ml for 1 hour on the rotator at room temperature.

Samples were centrifuged at 3,000 rpm for 90 seconds and then the supernatant was collected (proteins that did not bind to GST). Proteins were incubated for 2 hours with 30-40 μl of GST fusion proteins of the C-terminal domain of GluN2A, PDZ1-2 or PZ3 domains of PSD-95 (plasmid DNA were generously provided by Prof. Yutaka Hata from Tokyo Medical and Dental University in Japan) or GST alone. After incubation beads were washed four times with TBS and 0.1% Triton X-100. Bound proteins were resolved by SDS-PAGE and subjected to immunoblot analysis with polyclonal anti-Rph3A antibody or monoclonal anti-GST antibody.

VIII. Western Blotting

15-30 μg of proteins from rat homogenate, subcellular fractions from brain or primary cultured hippocampal neurons or samples from coIP or GST-Pulldown Assay were separated on 7% or 10% SDS-PAGE gel, transferred to a nitrocellulose membrane and probed with the corresponding primary Ab, followed by incubation with horseradish peroxidase-conjugated secondary Ab. Membranes were developed using *Clarity*™ reagent (Biorad).

IX. Immunofluorescence

Cells were fixed with 4% Paraformaldehyde (PFA)-4% sucrose in PBS solution at 4ºC and washed several times with PBS. Cells were either blocked with 5% BSA in PBS for 30min at room temperature and then labeled with primary anti-Nterminal GluN2A antibody (Invitrogen), anti-Nterminal GluN2B (Neuromab) or anti-Nterminal GluA1 (Invitrogen) for surface labeling of GluN2A for 1 h at room temperature or permeabilized with 0.1% Triton-X-100 in PBS for 15min at room temperature and then blocked with 5%BSA in PBS for 30min at room temperature. Cells were then labeled with antibodies for intracellular epitopes (anti-Nterminal GluN2A, anti-Nterminal GluN2B or anti-Nterminal GluA1 for total labeling; anti-Rph3A, EMC or Novus biological; anti-PSD-95, Neuromab; anti-Pan-shank, Neuromab) for 1 h at room temperature or overnight at 4ºC. Cells were washed and secondary antibody against appropriate specie conjugated with Alexa-488, Alexa-555 or Alexa-633 (invitrogen) for 1 h at room temperature. Cells were then wash in PBS and mounted in Fluoromount (Sigma) or permeabilized for total labeling (following step are the same).

X. Point mutations

RFP-Rph3A plasmid was a kind gift from Prof. Mitsunori Fukuda, from Tohoku University. This plasmid was used to perform point mutation inserting a stop codon for the codon corresponding to aa 673 using following primers: 5'-CGCTGGCACCAACTGTAGAACGAGAACCACGTG-3' (Forward) and 5'-CACGTGGTTCTCGTTCTACAGTTGGTGCAAGCG -3' (Reverse).

XI. Electrophysiology

Patch-clamp recordings of isolated NMDA-EPSCs or AMPA-EPSCs were performed of CA1 hippocampal neurons from DIV12-16 organotypic cultured hippocampal slices from P7 rat pups using

a previously described protocol (Bellone & Nicoll, 2007). NMDA-EPSCs were isolated pharmacologically by adding 10 μM NBQX, 50 nM CPA and 10 μM Bicuculin to oxygenated ACSF bath solution and recordings were performed at +30mV to remove Mg^{2+} block of NMDAR. AMPA-EPSCs were isolated pharmacologically by adding 50 nM CPA and 10 μM Bicuculin to oxygenated ACSF bath solution and recordings were performed at -70mV were NMDAR are block by Mg^{2+}. 1μM Scr or 2A-40 peptide was added to the intracellular solution contained in the patch pipette. After obtain giga seal, to minimize run-up of baseline responses we waited 5min before entering whole-cell. Before breaking in, stimulation intensity was calibrated just below the threshold required to elicit an action potential monitored in while in cell attached configuration (Bellone & Nicoll, 2007). After entering whole-cell, in the first 1-2min the intensity of stimulation was adjusted to have a similar staring amplitude with both peptide. Recording was then started using 180 0.1Hz stimulation (30min). Electrophysiology experiments were carried out in the laboratory of Prof. Christophe Mulle and under the supervision of Dr. Mario Carta from IINS/Neurocentre Magendie, University of Bordeaux II (France).

XII. DiI labeling for spine morphology

Carbocyanine dye DiI (invitrogen) was used to label neurons as it is a lipophilic fluorescent molecule. Protocol used for labeling has been previously described (B. G. Kim, Dai, McAtee, Vicini, & Bregman, 2007). DiI crystals were applied using a thin needle by delicately touching region of interested on both sides of 2 mm cortical slices prepared with cardiac perfusion of 1.5% PFA in PB 0.1 M. DiI was left to diffuse for 1 day in the dark at room temperature, then slices were fixed with 4% PFA in PB 0.1 M for 45min at 4ºC. 150 μm cortical slices were then obtain using a vibratome. The first slice was discarded. Slices were then mounted on glass slides with Fluoromount (Sigma) for confocal imaging.

XIII. Rat model of PD and LID

XIII.1. 6-OHDA unilateral lesion in MFB (nigrostriatal)

Male Sprague-Dawley rats were deeply anesthetized with Isofluorane and were injected with 6-hydroxydopamine (6-OHDA, 12 μg/4 μl of saline containing 0.1% ascorbic acid) via a Hamilton syringe into the medial forebrain bundle, at a rate of 0.38 μl/min (AP = -4.4, L = + 1.2, VD = -7.5). Fifteen days later, the rats were tested with 0.05 mg/kg s.c. injection of apomorphine, and the contralateral turns were counted for 40 min. Only the rats consistently making at least 200 contralateral turns (Schwarting & Huston, 1996) were used two months after the lesion, to avoid possible interference of apomorphine treatment with the plastic changes occurring in dopamine D2 receptors function following chronic dopaminergic denervation. It has been demonstrated previously that rats meeting this screening criterion have 95% depletion of striatal dopamine (Schwarting & Huston, 1996).

XIII.2. AIMs

At 2 months after the 6-OHDA lesion, rats started to receive daily subcutaneous (s.c.) injections of 6 mg/kg L-DOPA plus 6 mg/kg benserazide for 14 days. L-DOPA-induced abnormal involuntary movements (AIMs) were recorded on alternate days three times per week using a validated rat AIM scale, as described previously (Cenci, Lee, & Björklund, 1998; Lundblad et al., 2002; Picconi et al., 2003). Briefly, rat AIMs were classified into three subtypes: axial AIMs (i.e., dystonic posturing of the upper part of the body toward the side contralateral to the lesion), limb AIMs (i.e., abnormal movements of the forelimb contralateral to the lesion), and orolingual AIMs (i.e., empty jaw movements and tongue protrusion). Each of these subtypes was scored on a severity scale from 0 to 4: 1, present during less than half of the observation time (1 min); 2, present during more than half of the time; 3, present all the time but was arrested by extern stimuli; 4, present all the time without possibility to arrest it. Ratings were performed at 20 – 180 min after L-DOPA injection.

Each rat could reach a theoretical maximum AIM score of 80 in one session; each session consisted of five monitoring periods, with a maximal score in each period of 16, and the total AIM score for each session was obtained by summing the monitoring period scores. The rats that reach more than AIM score of 20 per session were included in the dyskinetic group.

Behavioral assessments of TAT-2A-40 treated dyskinetic rats and their controls were performed in double-blind conditions as some animals from the control dyskinetic group were stereotaxically injected in ipsilateral striatum with sterile deionized H_2O and operators were not aware of the status of the treatments.

XIV. Cell-permeable peptides design and use

Each cell-permeable peptide (CPP) was manufactured by Bachem according to our designed sequences. Lyophilized CPPs were resuspended in sterile deionized H2O to a stock concentration of 1 mM and stored at -20ºC. For treatment in cells, CPPs were simply added to the medium for a final concentration of 10 μM. In vivo treatments, were performed by injecting CPPs, as is, by subcutaneous (s.c.) or intraperitoneal (i.p.) at 3 nmol/g.

Intrastriatal injection was performed stereotaxically using 5 μl of the 1 mM stock (5 nmol) at a rate of 0.5 μl/min (AP=+0.2, L=+3.5, DV=-5.7).

RESULTS & DISCUSSION

I. Physiological conditions

I.1. Rph3A is part of the postsynaptic density

As Rph3A was found as a new putative interactor of GluN2A after yeast two-hybrid screening and is believed to be, from the literature, a presynaptic protein, it was important to first assess its subcellular localization in order to confirm its interaction with GluN2A. If true, this interaction could only take place at the PSD since GluN2A is a postsynaptic protein. We found that Rph3A is widely present in different rat brain areas such as Cortex (Cx), Striatum (St), Hippocampus (Hp) and Cerebellum (Cb). We found comparable Rph3A protein levels in total homogenate and in a triton insoluble fraction (TIF), a postsynaptic density elements fraction, purified from all analyzed brain areas (Fig. 11A). To determine Rph3A enrichment into different subcellular compartments, we used a biochemical fractionation approach to isolate purified postsynaptic densities (PSD) from rat brain tissues. We found the presence of Rph3A and P234-Rph3A (phosphorylated form of Rph3A at Ser234) in all subcellular fractions and the enrichment in synaptosomes (Syn), TIF and PSD fractions in both rat forebrain and hippocampus (Fig. 11A) similar to those of GluN2A, PSD-95 and Rab8, which are proteins present at the PSD. As expected, synaptophysin and Rab3A were present in all subcellular compartments analyzed but not in the TIF and PSD purified fractions as they are strictly presynaptic proteins. Similar data was found using fluorescent immunocytochemistry of primary cultured hippocampal neurons and confocal imaging, Rph3A was found co-localizing with PSD-95 (Fig. 11B) and endogenous GluN2A (Fig. 11C). Moreover, in neurons overexpressing Rph3A fused with RFP and GluN2A fused with eGFP, RFP-Rph3A is found co-localizing with endogenous PSD-95 and GluN2A-eGFP (Fig. 11D). This result suggests that Rph3A is not a solely presynaptic protein, as described in the literature, but also a postsynaptic protein where it could in fact interact with GluN2A and PSD-95.

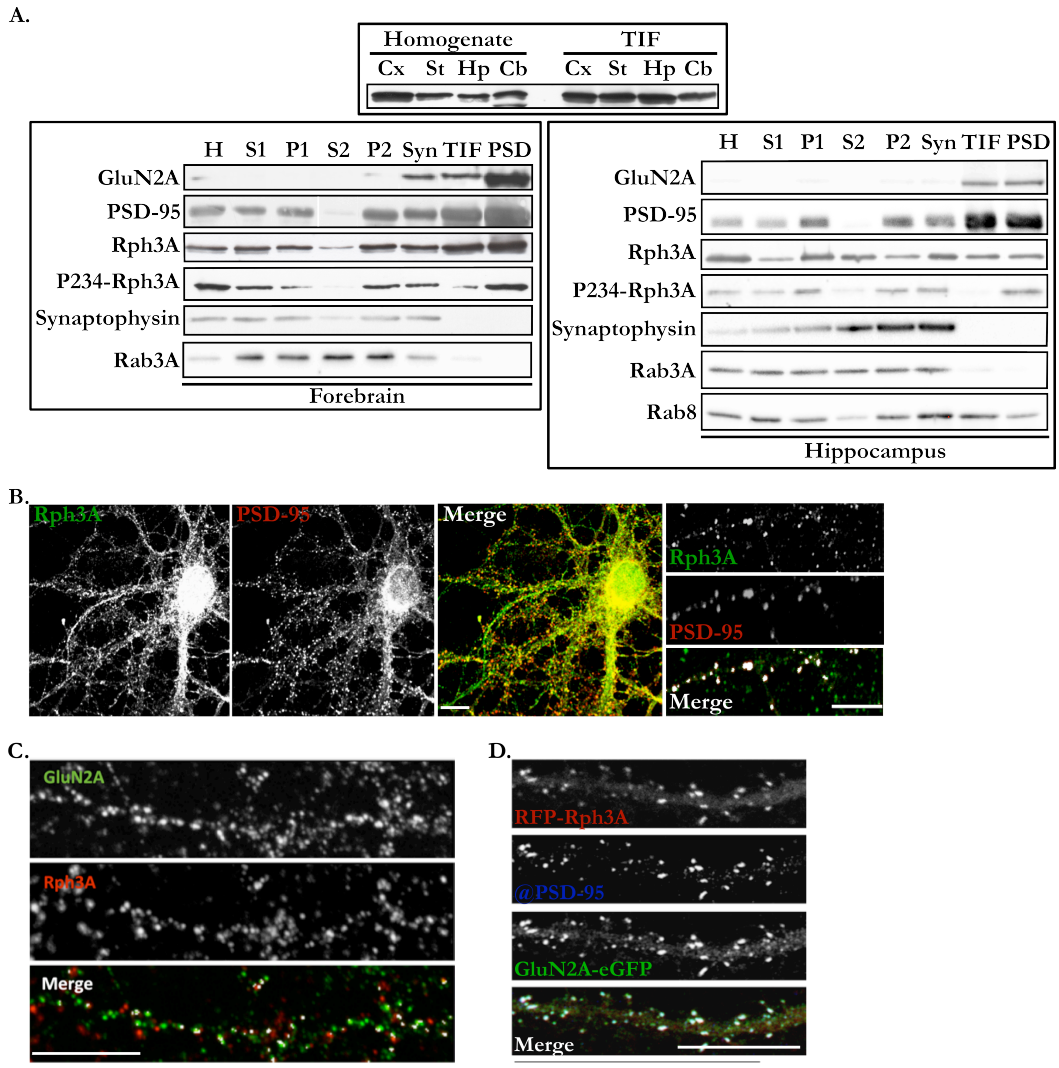

Fig. 11: Rph3A expression at PSD in rat brain. (A) Distribution of Rph3A expression in rat brain and subcellular expression in rat forebrain and hippocampus. H, homogenate; S1/2, supernatant 1/2; P1/2, pellet 1/2; Syn, Synaptosomal fraction; TIF, TritonX Insolyble Fraction; PSD, PostSynaptic Density fraction. (B) Fluorescent immunocytochemistry of Rph3A (green) and PSD-95 (red) in primary hippocampal neurons DIV15. On 6th panel (Merge) the colocalization points between Rph3A and PSD-95 are shown in white. Scale bars: 10µm. (C) Fluorescent immunocytochemistry of Rph3A (Red) and GluN2A (gree) in primary hippocampal neurons DIV15. Co-localization points are shown in whte on the merge panel. Scale bars: 10µm. (D) Fluorescent immunocytochemistry of PSD-95 (blue) in primary hippocampla neurons transfected with GluN2A-eGFP (green) and RFP-Rph3A (red). Co-localizing points between all three protein are seen in white on the merge panel. Scale bar: 5µm.

I.2. Rph3A/GluN2A interaction

The next step of our study was to characterize the interaction between Rph3A and GluN2A and assess the effect of its modulation. Firstly, clustering assay in heterologous COS7 cells was used to confirm the capability of GluN2A to interact with Rph3A and then co-immunoprecipitation assay was used to highlight the interaction in neurons. Secondly, a GST pull-down assay was used to identify the interaction domain of GluN2A with Rph3A. Thirdly, knowing the Rph3A interaction domain of GluN2A enabled use to design a cell-permeable peptide (CPP) able to disrupt the interaction to study the modulation of the interaction.

I.2.1. Characterization of Rph3A/GluN2A interaction

As previously shown (Gardoni et al., 2003), in single transfection in COS7 cells GluN2A-eGFP and GluN2B-eGFP form perinuclear aggregates in the cytoplasm (Fig. 12A, top panels), without the GluN1 subunits GluN2s are incapable of trafficking to the plasma membrane. Co-transfection of RFP-Rph3A with GluN2A-eGFP caused a redistribution of GluN2A-eGFP throughout the cell. In fact, quantification of GluN2A-eGFP co-clustering with RFP-Rph3A shows a high co-localization value when compared with RFP-Rph3A/GluN2B-eGFP transfected cells (Fig. 12A & B; two-tailed t test, p=0.0003 *** n=9 cells). Accordingly, no effect on GluN2B-eGFP distribution was observed when co-transfected with RFP-Rph3A (Fig. 12A).

To further confirm the interaction in neurons, we performed co-immunoprecipitation experiments in total homogenate from rat primary hippocampal cultured neurons (Fig. 12C, PSD-95), P2 or TIF fractions from adult rat hippocampus (Fig. 12C). Anti-Rph3A immunoprecipitates were challenged in WB with GluN2A antibody showing the capability of Rph3A to interact with GluN2A specifically as no immunoreactivity was found with GluN2B. Interestingly, we found Rph3A to interact as well with PSD-95 (PSD-MAGUK family member, this interaction will be looked into further later on see *I.3 of Results & Discussion*) and Rab8, member of the Rab family of GTPases present at postsynaptic terminals (Fig. 12C). Other Proteins were revealed to interact with Rph3A in this assay: CASK, MAGUK family member, known Rph3A interacting protein); CAMKII, known Rph3A interactor; and SAP-97. As a control for purity of the P2 fractions, Meox2, a nuclear protein, was used. It was not present in the input and no interaction was highlighted. As a control for purity of TIF fractions, Rab3A, a presynaptic interactor of Rph3A, was used. It was not present in the input and no interaction was highlighted. Also, no interaction was found between GluA1 (AMPAR subunit) with Rph3A.

Co-transfection in COS7 cells and pull-down assay were used to detect the GluN2A domain involved in the binding with Rph3A. Co-transfection of RFP-Rph3A with a mutant plasmid of GluN2A where a stop codon was inserted at the position 1049 fused with eGFP (GluN2A(1049)-eGFP) revealed a significant decrease of the co-localization degree when compared with co-transfection with the full length GluN2A-eGFP (Fig. 12E & F; two-tailed t test, p=0.0006 *** n=5-9 cells), suggesting that the GluN2A domain of interaction is comprised between aa 1049 and aa 1461. GST pull-down assay of Rph3A with fusion proteins with different length of the C-tail of GluN2A indicated that the aa 1349-1389 region as key GluN2A domain involved in the interaction with Rph3A (Fig. 12D).

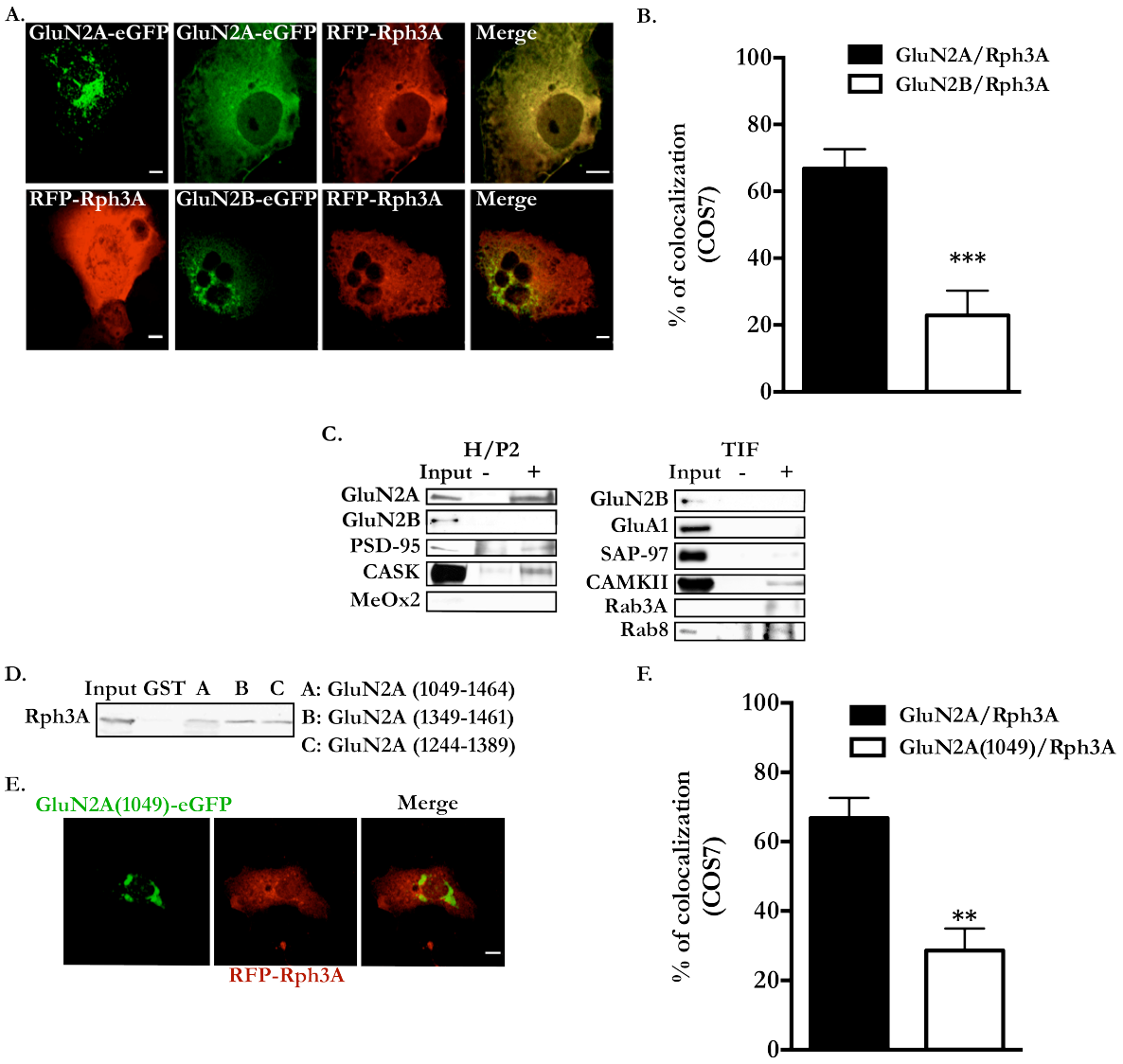

Fig. 12: Characterization of Rph3A/GluN2A interaction. (A) Clustering assay in heterologous COS7 cells. Single transfection of GluN2A-eGFP, GluN2B-eGFP or RFP-Rph3A are shown in top panels. Co-transfection of RFP-Rph3A with GluN2A-eGFP is illustrated in middle panels and co-transfection of RFP-Rph3A with GluN2B-eGFP in bottom panels. (B) Bar graph representing percentage of GluN2s co-localizing with RFP-Rph3A. GluN2B-eGFP/RFP-Rph3A co-localization (two-tailed t test, p=0.0003 *** n=9 cells). (C) Co-Immunoprecipitation assay. Rph3A was immunoprecipitated, from primary hippocampal neurons homogenate (WB: PSD-95, left panel), rat hippocampus homogenate (WB: CASK, left panel), rat hippocampus P2 purifications (left panel) and rat hippocampus TIF purification (right panel) and its interacting proteins were revealed by WB. (D) GST pull-down assay of Rph3A using C-terminal GluN2A GST fusion protein of 3 different sizes. (E) Co-transfection of RFP-Rph3A and mutant GluN2A(1049)-eGFP containing a stop codon at the 1049 aa position in COS7 cells. (F) Bar graph representing the percentage of GluN2A-eGFP or GluN2A(1049)-eGFP co-localizing with RFP-Rph3A (two-tailed t test, p=0.0006 *** n=5-9 cells).

I.2.2. Modulation of Rph3A/GluN2A interaction

To assess the function of the Rph3A/GluN2A interaction, we firstly thought to use a specific shRNA (shRph3A) to knockdown the expression of Rph3A in hippocampal neurons. As Rph3A is a presynaptic and postsynaptic protein, using shRph3A would affect both pre- and postsynaptic Rph3A and therefore we wouldn't be able to segregate the results from a pre- or postsynaptic effect of Rph3A. As shown above, we managed to narrow domain the Rph3A interaction domain of GluN2A to aa 1349 to aa 1389. Thus, we decided to use a different approach by designing a CPP containing that 40 aa sequence along with part of the HIV TAT sequence give the cell-permeability to the peptide (Fig. 13A)

that will called TAT-2A-40. This peptide is capable of disruption Rph3A/GluN2A interaction by binding Rph3A where GluN2A should have been able too as shown by co-immunoprecipitation assay of mice brain treated with CPP at 3nmol/g in i.p. for 1 h (Fig. 13B). After treating DIV 15 rat primary hippocampal neurons with 10µM of CPP for 30min, we found that the co-localization percentage between GluN2A and Shank (marker of the PSD) was significantly reduced in neurons treated with the active TAT-2A-40 compared to the control peptide containing the TAT sequence and a scramble of the Rph3 interaction domain of GluN2A sequence (TAT-Scr) (Fig. 13 C, left panel, & D; two-tailed t test p=0.0012 ** n=10-12 neurons). This effect was specific to GluN2A subunit as TAT-2A-40 had no effect on GluN2B/Shank co-localization (Fig. 13 C, right panel, & D; two-tailed t test p=0.6568 n=7-14 neurons). These datas suggest that disrupting Rph3A/GluN2A interaction affects the synaptic localization of GluN2A.

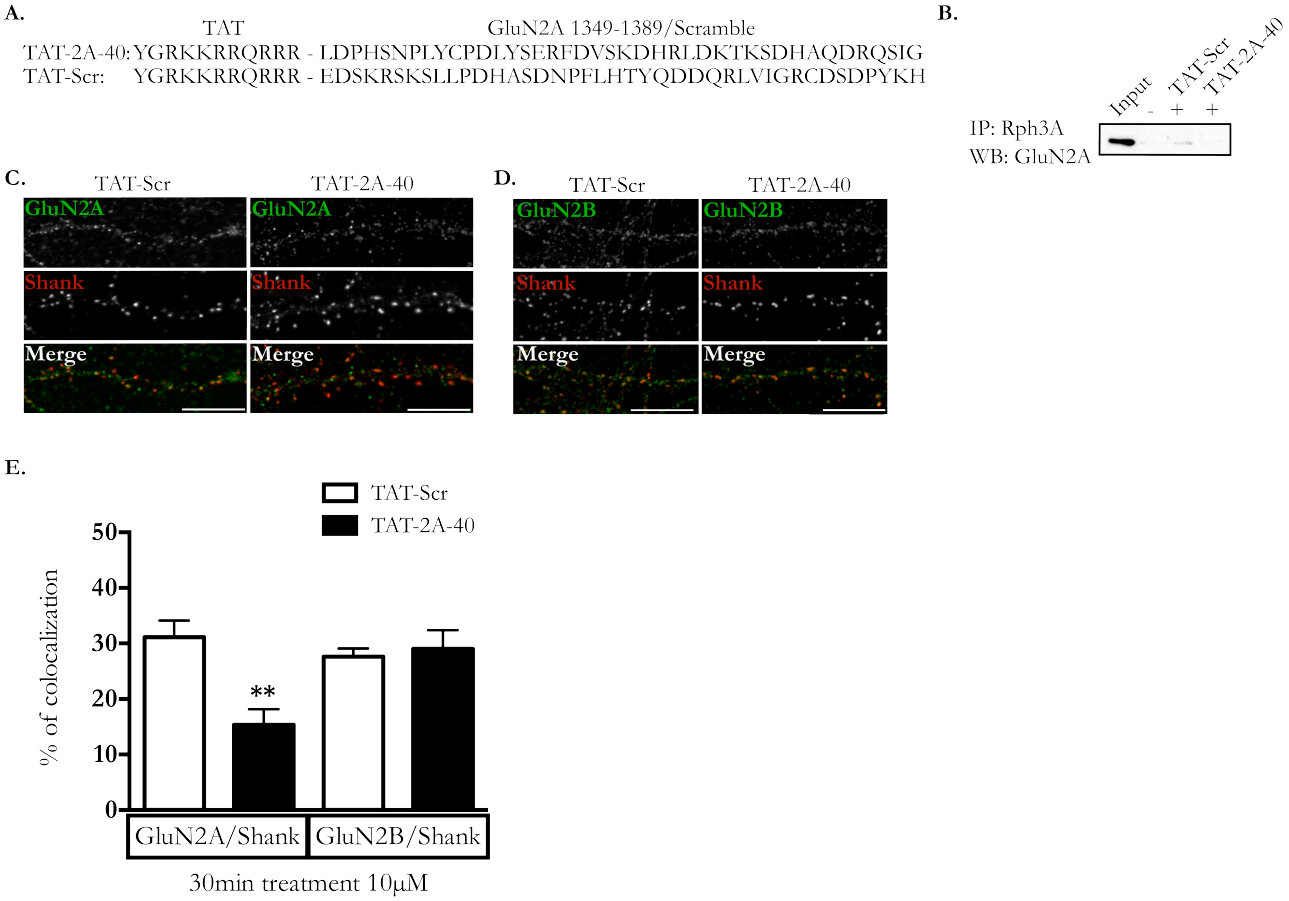

Fig. 13: Rph3A/GluN2A interaction is important for the synaptic localization of GluN2A. (A) Sequence of TAT-2A-40, CPP capable of disrupting Rph3A/GluN2A interaction, and its control TAT-Scr, containing a scramble sequence of the 40 aa coresponding to the Rph3A interaction domain of GluN2A. (B) Co-Immunoprecipitation assay of Rph3A from mice brain P2 fractions treated with CPP at 3nmol/g i.p. for 1h. WB revealing GluN2A. (C) Fluorescent immunocytochemistry of GluN2A (left panel, green) or GluN2B (right panel, green) and Shank (PSD marker, red) in DIV15 rat primary hippocampal neurons treated with either TAT-2A-40 or TAT-Scr 10µM for 30min. Scale bar = 10µm. (D) Bar graph representing GluN2A/Shank or GluN2B/Shank co-localization percentage in DIV15 rat primary hippocampal neurons treated with either TAT-2A-40 or TAT-Scr 10µM for 30min (GluN2A/Shank: two-tailed t test, p=0.0012 ** n=10-12 cells; GluN2B/Shank: two-tailed t test, p=0.6568 n=7-14 cells).

Furthermore, TAT-2A-40 significantly reduces the surface versus total expression ratio of GluN2A in DIV15 rat primary hippocampal neurons compared to the TAT-Scr control, of approxi-

mately 40% of control mean (Fig. 14A & B; two-tailed t test $p<0.0001$ *** n=119-144 dendrites). Similar results were found when treating DIV15 rat primary hippocampal neurons with another CPP called TAT-2A that disrupts the interaction between GluN2A and PSD-95 (Vastagh et al., 2012) although the reduction was of a lesser amplitude, approximately 15% of control mean (Fig. 14C & D, two-tailed t test $p=0.0003$ *** n=33 dendrites). Not only Rph3A/GluN2A interaction is important for the synaptic localization of GluN2A but also for its surface expression in the same way as PSD-95/GluN2A interaction is. This is also shown by comparing the surface expression of GluN2A with a PSD marker, PSD-95. We found that TAT-2A-40 reduces significantly the surface synaptic expression of GluN2A of approximately 20% (Fig. 14E & F, two-tailed t test $p<0.0001$ *** n=119-144 dendrites). Disrupting Rph3A/GluN2A interaction affects the surface availability of GluN2A at the synapse, which should in turn affect the overall amplitude of the NMDA response at glutamatergic synapses.

To assess NMDA response after modulation of Rph3A/GluN2A interaction, we performed patch-clamp recording of pharmacologically isolated NMDA excitatory postsynaptic currents (EPSCs) of CA1 neurons from DIV 12 cultured hippocampal organotypic slices using the 2A-40 peptide (and Scr control), but without the TAT sequence that gives the cell-permeability to the peptide, directly implemented into the patch pipette with the intracellular solution giving us a single-cell postsynaptic targeting. We observed that in presence of the 2A-40 peptide the NMDA EPSC was significantly decreased after 30 min of recording (Fig. 14G & H; two-tailed t test, $p=0.0015$ ** n=9 neurons), with no effect on decay time of the receptor (Fig. 14I; Scr 27'-30' vs 2A-40 27'-30' two-tailed t test, $p=0.7558$ n=9 neurons). Therefore, disrupting Rph3A/GluN2A interaction affects the overall amplitude of NMDA EPSCs but not the kinetics of the receptor suggesting that there is less NMDAR available for activation at the synaptic plasma membrane.

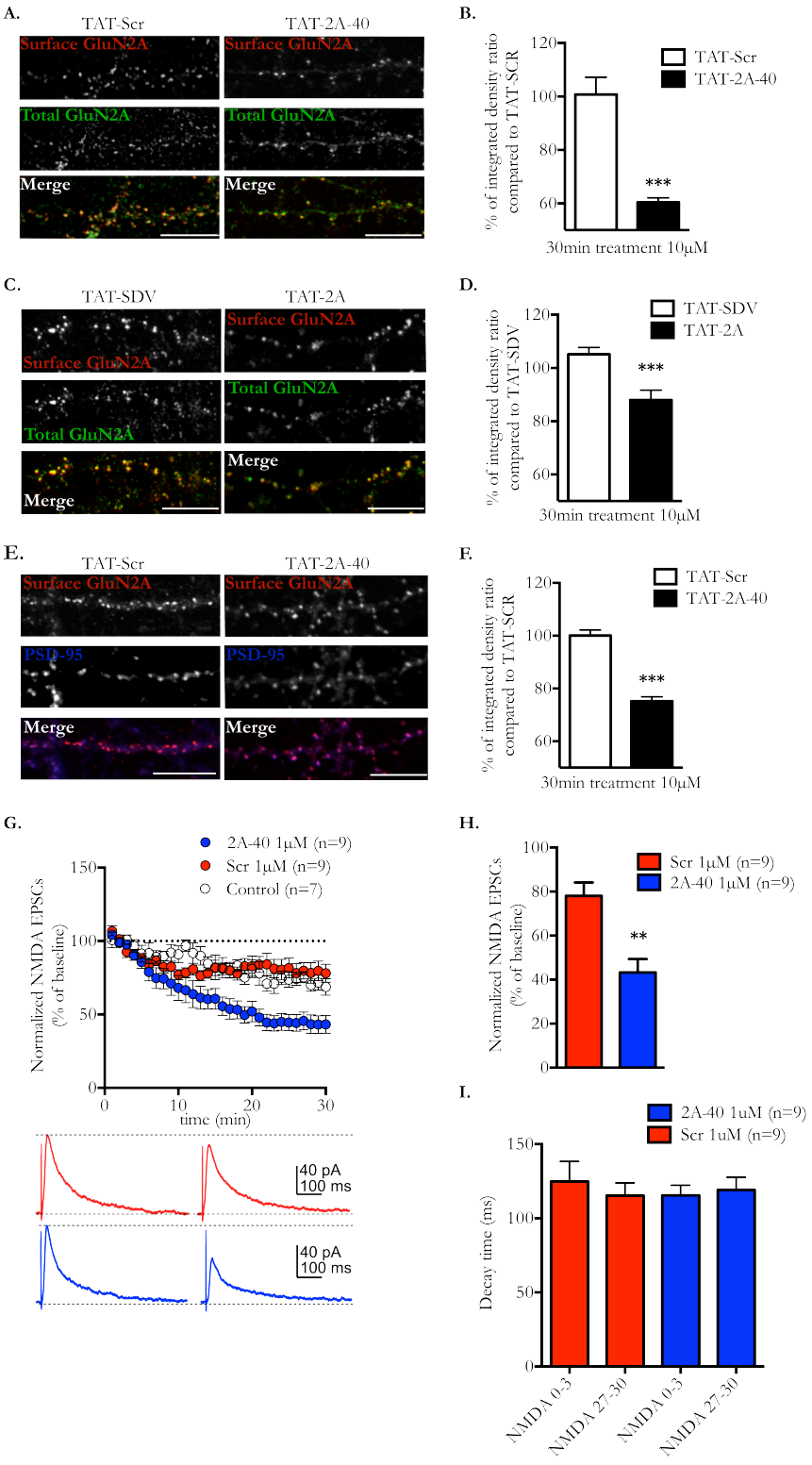

Fig. 14: Rph3A/GluN2A interaction is important for GluN2A surface availability at the synapse. (A) Fluorescence immunocytochemistry of surface (red) and total (green) GluN2A after 30min CPP 10 µM treatment of DIV15 primary hippocampal neurons. Scale bar: 10 µm. (B) Bar graph representation of surface/total ratio percentage of mean TAT-Scr (two-tailed t test, $p<0.0001$ *** n=119-144 dendrites). (C) Fluorescence immunocytochemistry of surface (red) and total (green) GluN2A after 30min CPP 10 µM treatment of DIV15 primary hippocampal neurons. Scale bar: 10 µm. (D) Bar graph representation of surface/total ratio percentage of mean TAT-SDV (two-tailed t test, $p<0.0001$ *** n=119-144 dendrites). (E) Fluorescent immunocytochemistry of surface GluN2A (red) and PSD-95 (blue) after 30min CPP 10 µM treatment of DIV15 primary hippocampal neurons. Scale bar: 10 µm. (F) Bar graph representation of surface GluN2A/ PSD-95 ratio percentage of mean TAT-Scr (two-tailed t test, $p<0.0001$ *** n=119-144 dendrites). (G) Normalized NMDA EPSCs over time in patch-clamp recordings with intracellular 2A-40 (blue) or Scr (red) peptides 1 µM or control without peptide (white) with representation of NMDA EPSCs at first stimulation and last (180^{th}). (H) Bar graph representation of the normalized NMDA EPSCs at the last stimulation (Two-tailed t test, $p=0.0015$ ** n=9 neurons). (I) Bar graph representation of the decay time of NMDA EPSCs in the first 3min and last 3min of recording.

The effects of the TAT-2A-40 (or 2A-40) are specific to NMDAR, as it did not affect the AMPA EPSCs (Fig. 15C) nor the surface versus total expression ratio of GluA1, an AMPAR subunit (Fig. 15A & B; two-tailed t test, p=0.4062 n=39-51 dendrites). Moreover, the TAT-2A-40 peptide is specific to GluN2A subunit as it did not affect the surface versus total expression ration of GluN2B (Fig. 15D; two-tailed t test, p=0.1683 n=53-58 dendrites).

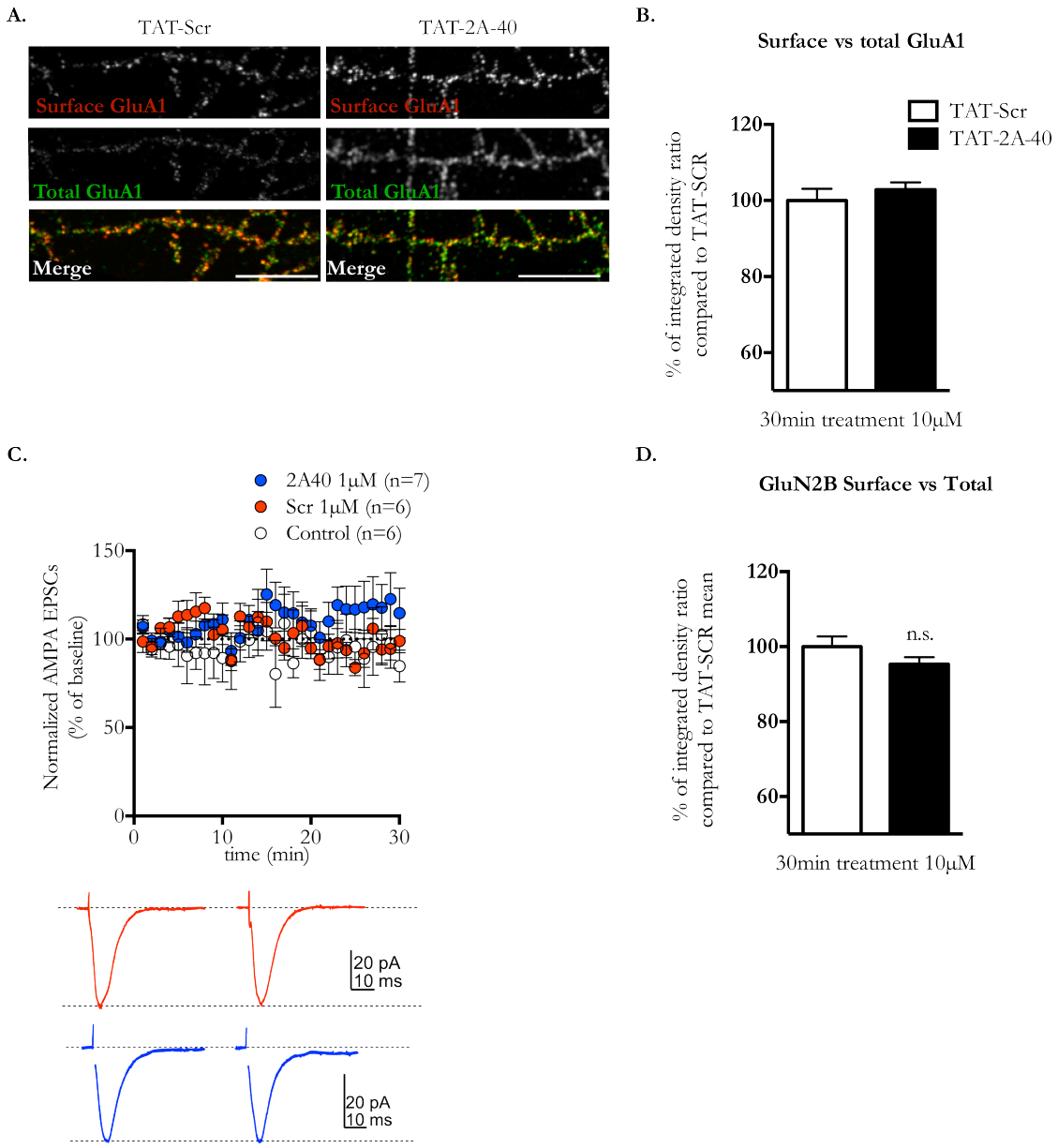

Fig. 15: Specificity of TAT-2A-40 on GluN2A-containing NMDARs. (A) Fluorescent immunocytochemistry of surface (red) and total (green) GluA1 after 30min CPP 10 µM treatment of DIV15 primary hippocampal neurons. Scale bar: 10 µm. (B) Bar graph representation of the GluA1 surface/total ratio percentage of mean TAT-Scr (two-tailed t test, p=0.4062 n=39-51 dendrites). (C) Normalized AMPA EPSCs over time in patch-clamp recordings with intracellular 2A-40 (blue) or Scr (red) peptides 1 µM or control without peptide (white) with representation of AMPA EPSCs at first stimulation and last (180th). (D) Bar graph representation of the GluN2B surface/total ratio percentage of mean TAT-Scr (two-tailed t test, p=0.1683 n=53-58 dendrites).

NMDAR subunit composition regulates receptor function and pharmacological responses. However, the role of distinct GluN2 subunits in dendritic spine remodeling has not yet been profoundly investigated. Accordingly, we investigated the onset of a possible effect of TAT-2A-40 on dendritic

spine morphology and density (Fig. 16A-D). As shown in Fig. 16A & B, treatment of mice with TAT-2A-40 at 3 nmol/g i.p. for 2 h decreased significantly spine density in the hippocampus (~4 spines/10 µm) compared to mice treated with the control peptide (~7 spines/10 µm; Fig. 16B; two-tailed t test, p=0.0184 * n=5 neurons, 780-860 µm). For a more detailed morphological analysis, the length, head width and neck width of the dendritic spines were measured and then, the spines were categorized according to their shape (mushroom, thin and stubby; see Fig. 16D) using a highly validated classification method (K. M. Harris, Jensen, & Tsao, 1992). Although, we didn't find any significant difference in the total proportions of spines (data not shown) and of spine classes (Fig. 16D; two-tailed t tests n=5 neurons, spines: p=0.3466, mushroom: p=0.6548, stubby: p=0.6908; thin: p=0.2329), we have highlighted a significant increase in spines head and neck widths of the TAT-2A-40 treated mice compared to TAT-Scr controls, and no difference in length (Fig. 16C; two-tailed t tests n=350-524 spines, length: p=0.3032, head width: p<0.0001 ***, neck width: p<0.0001 ***).

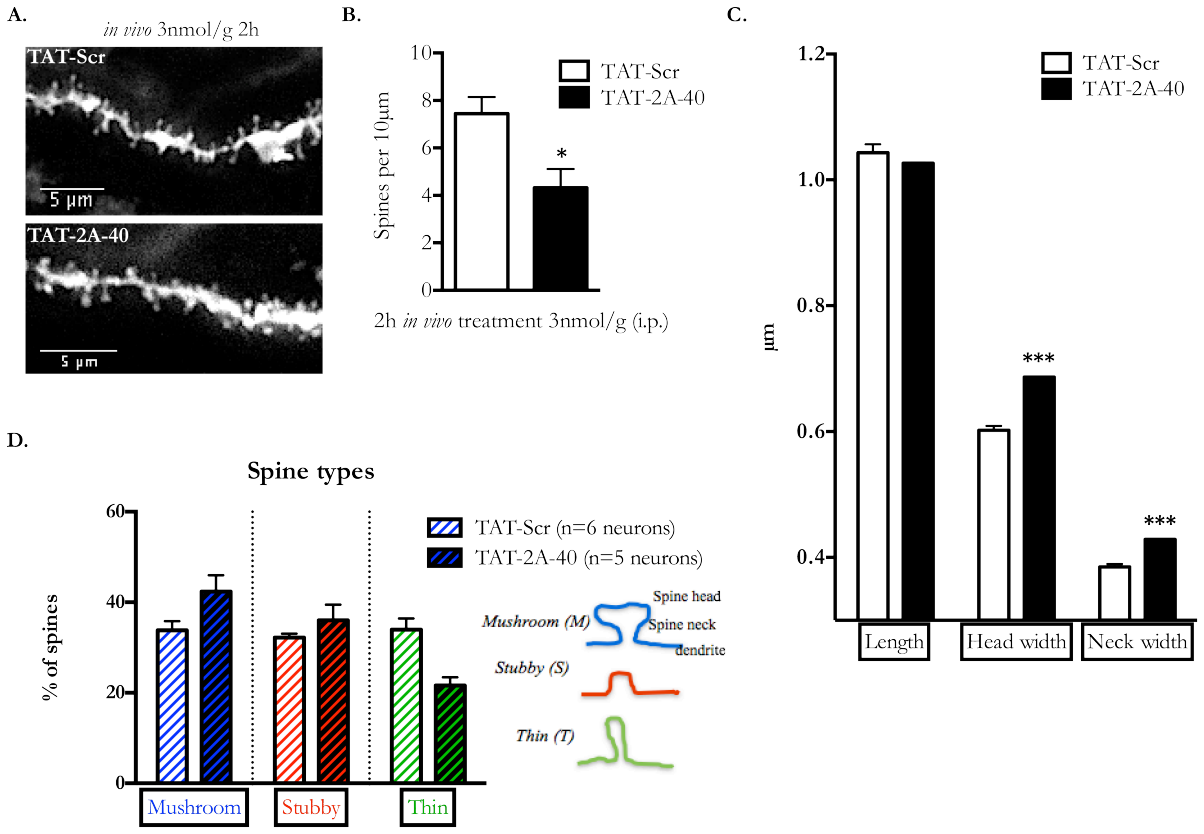

Fig. 16: Effect of TAT-2A-40 on dendritic spine density and morphology in the hippocampus. (A) DiI labeling of hippocampal neurons of CPP 3nmol/g i.p. treated mice for 2h. Scale bar: 5 µm. (B) Bar graph representation of spine density in these animals. (two-tailed t test, p=0.0184 * n=5 neurons, 780-860 µm of dendrite). (C) Bar graph representation of the measurements of spine length, head and neck width of CPP treated mice hippocampus. (D) Bar graph representation of the proportion of different spine classes of these animals and schematic of the spine classes.

Similar data was found when down regulating the expression of Rph3A with an shRNA (shRph3A). Special attention was put in isolating a postsynaptic effect of this knockdown to the maximum of our abilities by using very low transfection efficacy of shRph3A and its scramble control (shScramble) allowing only a few transfected cells very distant from one another, with no visible con-

tact. Primary hippocampal neurons transfected with the shRph3A at DIV 9 showed a decreased of GluN2A synaptic localization (GluN2A/Shank co-localization) at DIV 15 compared to shScramble transfected neurons (Fig. 17A; two-tailed t test, p=0.0011 ** n=17-19 neurons). No difference was found in GluN2B synaptic localization (Fig. 17A; two-tailed t test, p=0.9951 n=10-12 neurons). Moreover, neurons transfected with shRph3A showed a significantly lower spine density (~2 spines/10 μm) than shScramble transfected neurons (~3.5 spines/10 μm; Fig. 17B; two-tailed t test, p=0.0053 *** n=7-8 neurons, ~3.1 mm).

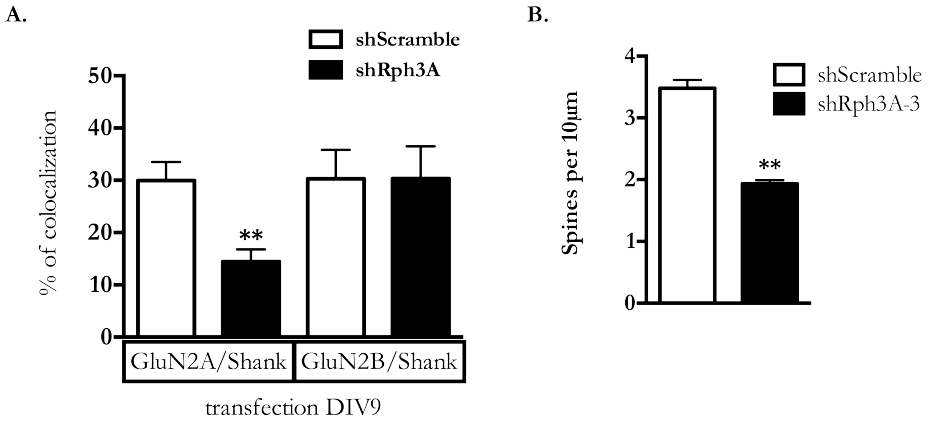

Fig. 17: Knockdown of Rph3A. (A) Bar graph representation of percentage of colocalization of GluN2A or GluN2B with Shank in DIV15 primary hippocampal cultured neurons transfected with shRph3A or its control, shScramble at DIV9. (B) Bar graph representation of spine density in these neurons transfected with shRph3A or shScramble.

Overall, these results show that Rph3A is not a solely presynaptic protein but also a postsynaptic one where it interacts with the GluN2A subunit of NMDAR. They suggest an important role of the Rph3A/GluN2A interaction in the surface availability of GluN2A at the synaptic membrane and therefore in the efficacy of hippocampal NMDAR as well as the overall spine density and morphology. Thus, postsynaptic Rph3A might have an important role in synaptic plasticity.

I.2.3. Modulation of Rph3A/GluN2A interaction and GluN2B/GluN2A developmental switch

As explained previously (refer to paragraph I.3. of introduction), at birth in the hippocampus mainly GluN2B-containing NMDAR are present. This changes over time during development as switch in expression occurs in favor of GluN2A-containing NMDAR. This switch is crucial for the maturation of the excitatory synapse. Since we demonstrated previously that Rph3A/GluN2A interaction is important for maintaining the surface availability of GluN2A-containing NMDAR at dendritic spines, we wondered whether we could affect the developmental switch of expression from GluN2B to GluN2A in the hippocampus by disrupting the Rph3A/GluN2A interaction.

Therefore, we treated with the TAT-2A-40 or its control TAT-Scr three different groups of rat pups. The first group was treated with a single injection of the CPP at 3 nmol/g s.c. at P6, before the switch occurs, and then sacrificed at P15 for molecular analysis. The second group was treated with a chronic injection of the CPP at 3 nmol/g s.c. comprised of 5 injections starting at P6 and ending at

P14, the animals were then sacrificed at P15 for molecular and spine morphology analysis. The third group was treated chronically with the CPP following the same procedure as the second group but the animals were sacrificed at P21 for molecular analysis. After analysis of the hippocampal tissue, we found that there was a significant decrease of GluN2A expression at the PSD (TIF fractions) in TAT-2A-40 treated pups from all groups compared their respective control (Fig. 18A & B; two-tailed t tests, 1st group: TAT-2A-40 vs TAT-Scr $p=0.0212$ * $n=5$, 2nd group: TAT-2A-40 vs TAT-Scr $p=0.0340$ * $n=3$-5, 3rd group: TAT-2A-40 vs TAT-Scr $p=0.0230$ $n=3$) with no changes of level of expression of Rph3A, GluN2B and PSD-95 (Fig. 18A & B; no statistical difference). However, we found a decrease of total PSD-95 expression in the hippocampus of TAT-2A-40 chronically treated pups from the second group compared to their respective TAT-Scr controls (Fig. 18C; two-tailed t test, $p=0.0026$ ** $n=3$) while no such difference was found in the other two groups (data not shown). Moreover, the hippocampal spine morphology analysis of the TAT-2A-40 chronically treated from the second group showed a decreased spine density (~4 spines/10 μm) compared to control (~5.5 spines/10 μm; Fig. 18D; two-tailed t test, $p=0.0055$ ** $n=10$-11 neurons, ~1.5-1.9 mm).

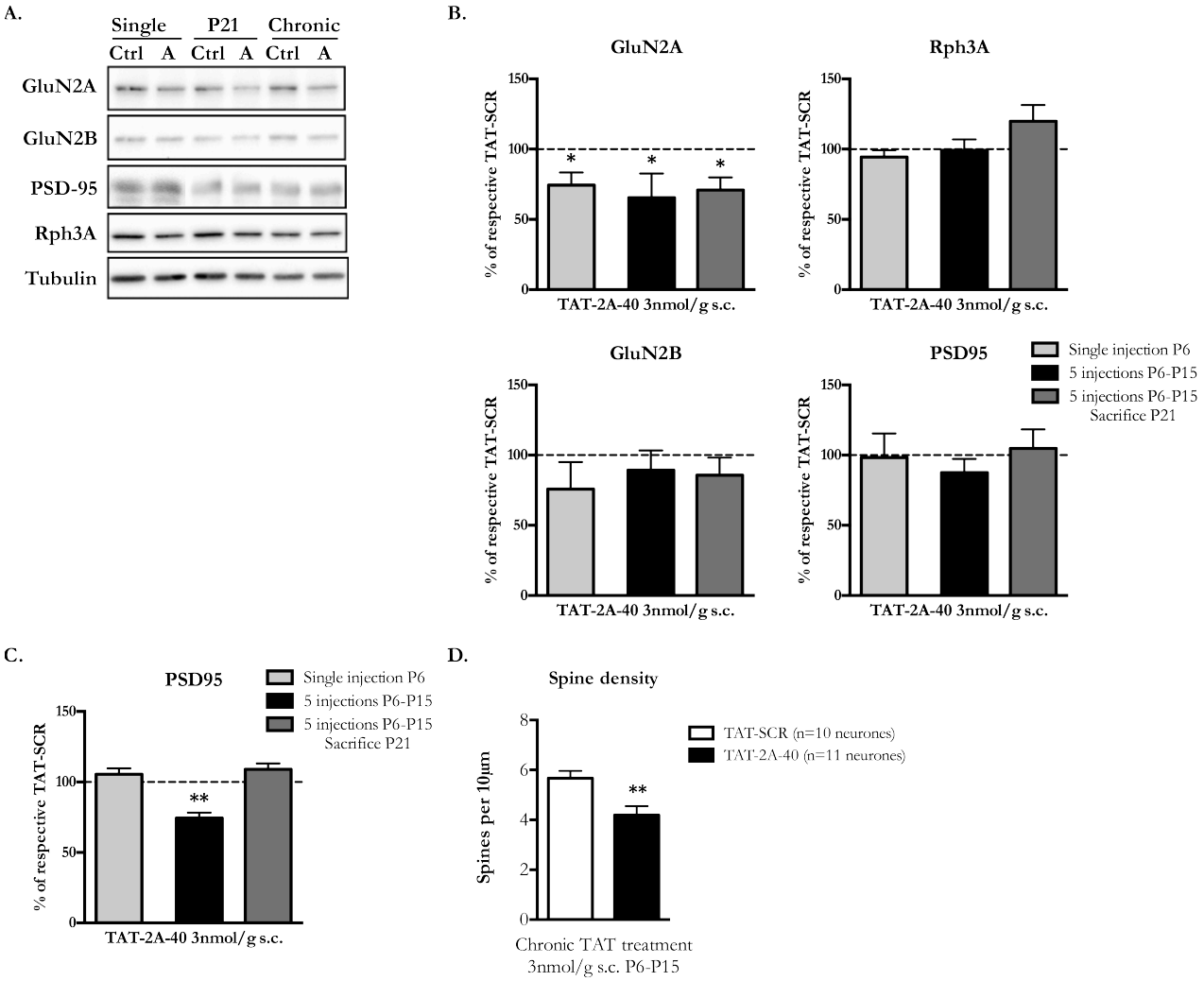

Fig. 18: Modulating Rph3A/GluN2A interaction during GluN2B-to-GluN2A developmental switch in hippocampus.(A) Western blots of GluN2A, GluN2B, PSD-95, Rph3A and tubulin in hippocampal TIF purifications from rat pups traeted with TAT-Scr (Ctrl) or TAT-2A-40 (A) at 3nmol/g in s.c. "Single" corresponds to the group treated with a single injection at P6 and sacrificed at P15; "P21" corresponds to the group treated chronically with 5 injections from P6 to P14 and sacrificed at P21; "Chronic" corresponds to the group treated chronically with 5 injections from P6 to P14 and sacrificed at P15. (B) Bar graph representations of GluN2A, Rph3A, GluN2B and PSD-95 percentage of respective TAT-Scr controls in TIF purifications from the 3 groups of animals treated with TAT-2A-40(GluN2A: two-tailed t tests, Single injection P6: p=0.0212 * n=5; 5 injections P6-P15: p=0.0340 * n=3-5; 5 injections P6-P15 sacrifice P21: p=0.0230 n=3). (C) Bar graph representations of PSD-95 percentage of respective TAT-Scr controls in homogenates from the 3 groups of animals treated with TAT-2A-40(two-tailed t test, 5 injections P6-P15: p=0.0340 * n=3). (D) Bar graph representation of spine density in hippocampus of pups treated chronically with 5 injections from P6 to P14 (sacrifice at P15) with TAT-2A-40 or TAT-Scr 3nmol/g s.c.

These results suggest that disrupting Rph3A/GluN2A interaction affected the synaptic maturity at a crucial developmental stage by reducing the synaptic availability of GluN2A and the overall spine density in the hippocampus. Thus, emphasizing the importance of postsynaptic Rph3A at the excitatory synapse.

I.3. Rph3A/PSD-95 interaction

I.3.1. Characterization of Rph3A/PSD-95 interaction

From the literature, it is known that Rph3A interacts with CASK, a PDZ-containing protein member of the MAGUK family (Y. Zhang et al., 2001). It is believed that the interaction occurs through the C_2 domains of Rph3A. Looking at the sequence of Rph3A, we noticed that its last 4 aa

sequence (-VSSD) resembles a putative PDZ-binding motif which therefore could be the binding domain for CASK through its PDZ-domain but could also enable Rph3A to bind postsynaptic PDZ-containing proteins such PSD-MAGUK family member like PSD-95.

Using co-immunoprecipitation assay, we saw, as previously described *(refer to I.2.1 of results and discussion)*, that Rph3A is capable of interacting with PSD-95 in primary hippocampal neurons (Fig. 12C, left panel). With GST pull-down assay using GST fusion proteins of PDZ1-2 and PDZ3 domains PSD-95, we observed that Rph3A can bind PDZ1-2 and PDZ3 domains of PSD-95 with a higher affinity for PDZ3. It has been suggested before the GluN2 subunits interact with PDZ1-2 domains of PSD-95. Therefore, we hypothesize that GluN2A and Rph3A are not in competition with each other to bind PSD-95 but rather that they can bind simultaneously to form a putative GluN2A/Rph3A/PSD-95 ternary complex.

I.3.2. Modulation of Rph3A/PSD-95

In a similar manner as for the Rph3A/GluN2A interaction, we used two different approaches to verify the role of Rph3A C-tail in the interaction with PSD-95. At first, we transfected COS7 cells with PSD-95 and RFP-Rph3A full-length or RFP-Rph3A(673) (lacking the last 9 aa of the c-tail; see Fig. 19D, top panels). Rph3A(673) showed a very low co-localization value with PSD-95 suggesting the loss of interaction with the PSD-MAGUK protein (Fig. 19E; two-tailed t test, p=0.0014 ** n=8-9 cells). To confirm this result, we designed a cell-permeable TAT peptide containing the last 9 aa of Rph3A C-tail (TAT-Rph3A-9c) to compete with Rph3A for the binding to PSD-95. TAT-Rph3A(-VSSD) lacking the PDZ-interacting domain (VSSD), was used as control peptide (see sequences in Fig. 20A).

We tested the effectiveness of the TAT-Rph3A-9c peptide in COS7 cells transfected with PSD-95 and RFP-Rph3A at 10 μM for 1 h (Fig. 19D, bottom panels, & E). TAT-Rph3A-9c reduced significantly the PSD-95/RFP-Rph3A co-localization score when compared with cells treated with control peptide (Fig. 19E; two-tailed t test, p=0.006 *** n=5-10 cells). These results indicate that Rph3A c-terminal domain is responsible for Rph3A binding to PSD-95.

To verify whether disruption of Rph3A/PSD-95 binding could also affect GluN2A binding to Rph3A and/or PSD-95, we treated triple transfected COS7 cells with TAT-Rph3A-9c or TAT-Rph3a(-VSSD) peptides at 10 μM for 1 h. Interestingly, treatment with the active peptide was sufficient to decrease co-clustering of GluN2A-eGFP with both PSD-95 and RFP-Rph3A (Fig. 19F; two-tailed t tests, GluN2A-eGFP/RFP-Rph3A: p=0.0056 ** n=5 cells, PSD-95/RFP-Rph3A: p=0.0001 *** n=5 cells, GluN2A-eGFP/PSD95: p=0.0110 * n=5 cells), thus indicating a role of Rph3A in modulating GluN2A/PSD-95 interaction.

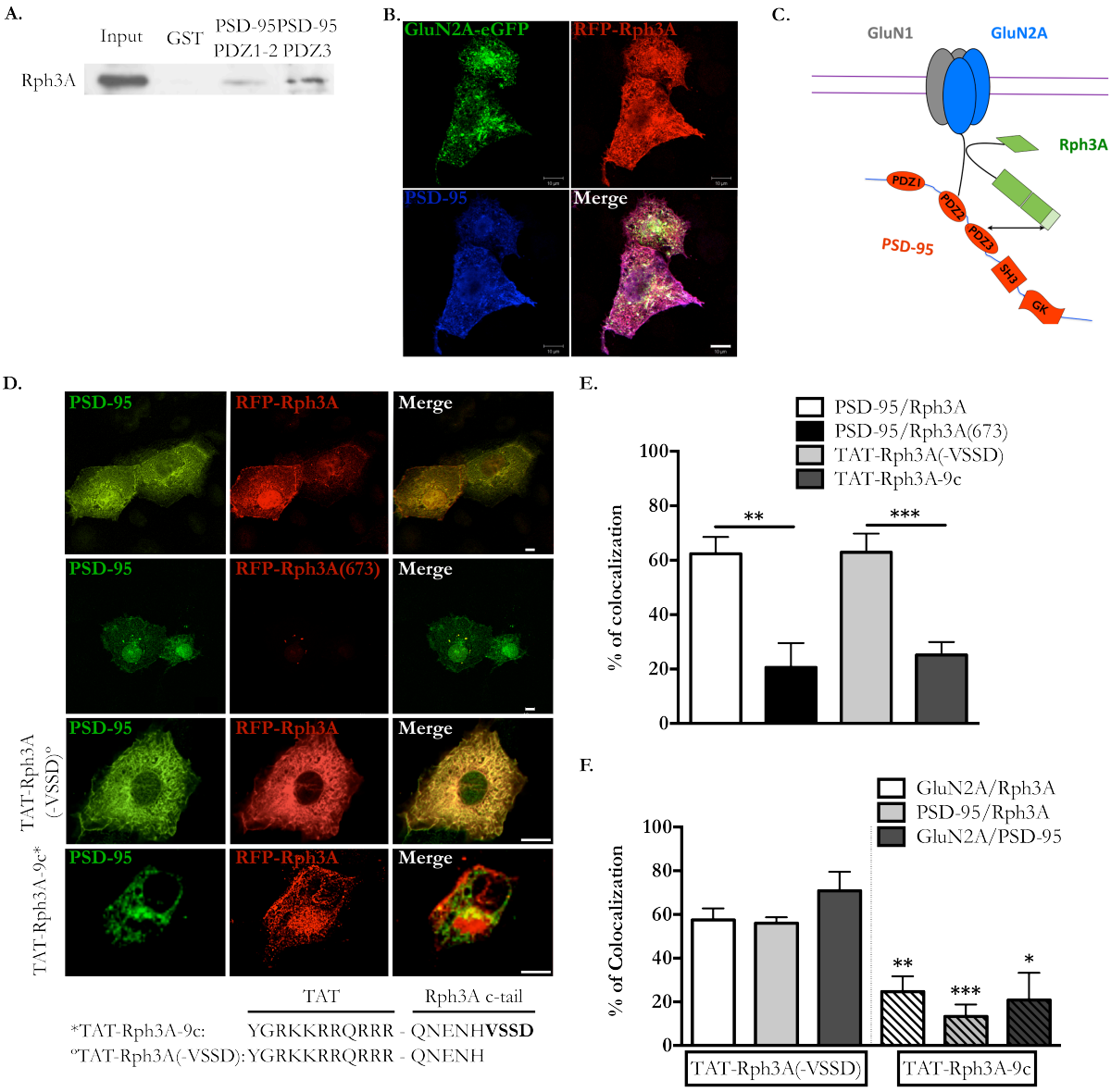

Fig. 19:Rph3A interacts with PSD-95 and GluN2A. (A) GST pull down assay of Rph3A using GST fusion protein of PDZ1-2 and PDZ3 domains of PSD-95. (B) Confocal image of COS7 cell co-transfected with GluN2A-eGFP (green), RFP-Rph3A (red) and PSD95 (blue). Scale bar: 10 µm.(C) Schema of GluN2A/Rph3A/PSD-95 triple complex. (D) Clustering assays in heterologous COS7 cells co-transfected with PSD-95 and RFP-Rph3A or RFP-Rph3A(673), not treated or treated with TAT-Rph3A-9c or TAT-Rph3A(-VSSD). Scale bar: 10 µm. Sequences of CPPs are shown below images. (E) Bar graph representation of percentage of co-localization of PSD-95 and RFP-Rph3A with or without treatment with TAT-Rph3A-9c or TAT-Rph3A(-VSSD), 10 µM 1h, or PSD-95 and RFP-Rph3A(673). (F) Bar graph representation of percentage of co-localization GluN2A-eGFP and RFP-Rph3A, PSD-95 and RFP-Rph3A or GluN2A-eGFP and PSD-95 in COS7 transfected with all three plasmids and treated with TAT-Rph3A-9c or TAT-Rph3A(-VSSD) 10 µM 1h (two-tailed t tests, two-tailed t tests, GluN2A-eGFP/RFP-Rph3A: p=0.0056 ** n=5 cells, PSD-95/RFP-Rph3A: p=0.0001 *** n=5 cells, GluN2A-eGFP/PSD95: p=0.0110 * n=5 cells.

In order to extend these observations to neuronal cells, we performed *in vitro* (cultured DIV15 hippocampal neurons, 10 µM, 30min) as well as *in vivo* (6 week old C57BL6 mice, 3 nmol/g *i.p.*, 1 h) treatments with TAT-Rph3A-9C or TAT-Rph3a(-VSSD) peptides. Subsequently biochemical and imaging experiments were performed. *In vivo* treatment with TAT-Rph3A-9C reduces Rph3A co-immunoprecipitation with both GluN2A and PSD-95 in forebrain P2 fractions (Fig. 20A & B; two-tailed t tests, for GluN2A/Rph3A: p<0.0001 *** n=5 animals, for PSD95/Rph3A: p<0.0001 *** n=3 animals and for PSD-95/GluN2A: p=0.0010 *** n=3 animals). The same treatment *in vitro* leads to a

significant decrease of GluN2A levels at synaptic sites, as indicated by the reduction of GluN2A co-localization with the post-synaptic marker Shank (Fig. 20C & D; two-tailed t test, p=0.0069 ** n=10 neurons). In addition, confocal analysis of GluN2A surface staining at synapses (ratio of integrated density of surface GluN2A in PSD-95 positive clusters) revealed a significant decrease induced by 30min treatment with TAT-Rph3A-9c 10 μM (Fig. 20E & F; two-tailed t test, p=0.0005 *** n=51-100 dendrites). Similarly, TAT-Rph3A-9C reduced total GluN2A surface staining (Fig. 20G & H; two-tailed t test, p=0.0130 * n=50 dendrites) indicating that the interaction of Rph3A with GluN2A/PSD-95 complex is needed for a correct localization of GluN2A in the synaptic membrane. As expected, the same effect was obtained after treatment of hippocampal neurons with a peptide (TAT-2A) disrupting GluN2A/PSD-95 complex (*refer to I.2.2 and Fig. 14C & D of results & discussion*).

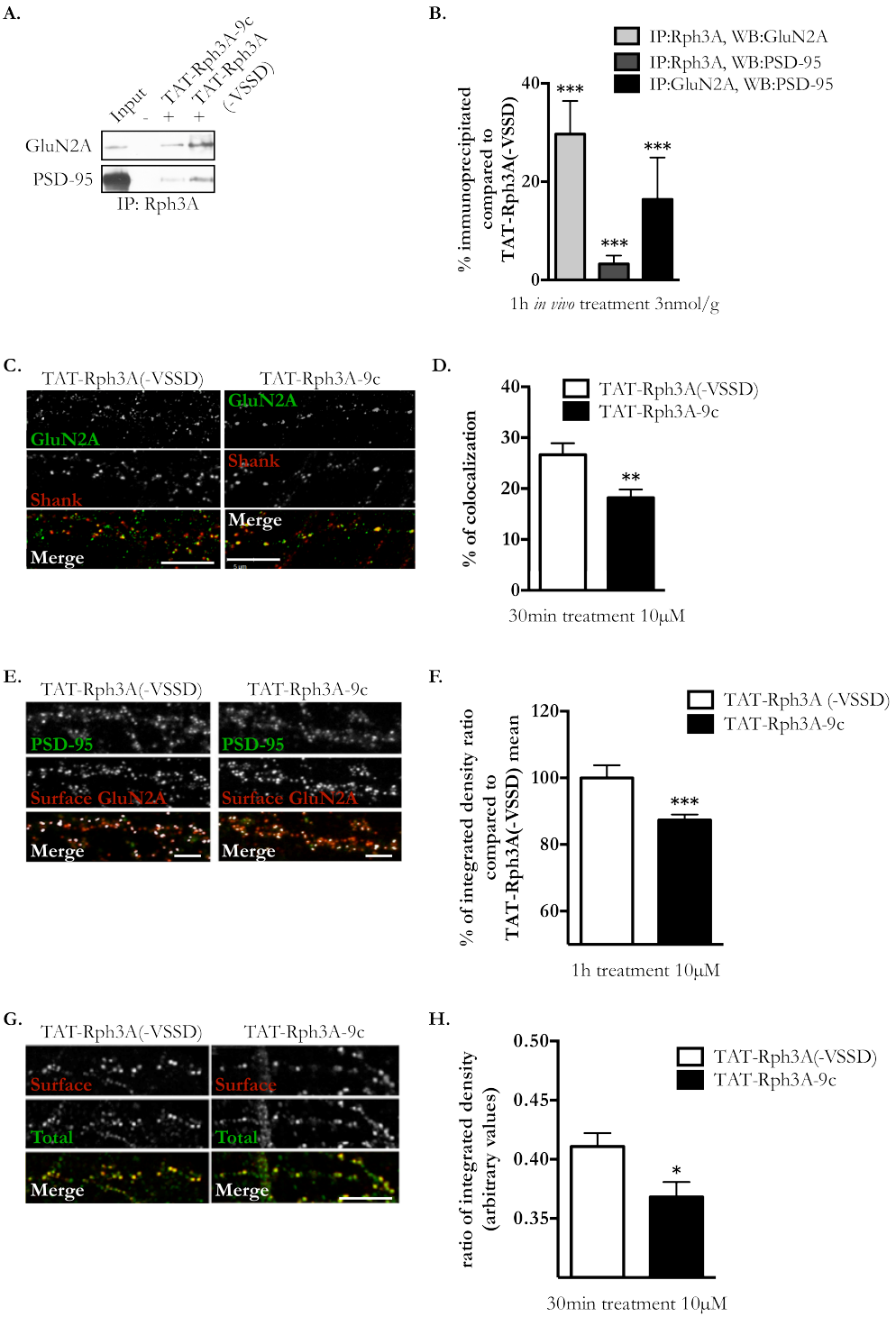

Fig. 20: Modulation of Rph3A/PSD-95 interaction. (A) Co-immunoprecipitation assay of Rph3A revealing as interacting proteins GluN2A and PSD-95 of forebrain P2 fractions of mice treated with CPPs 3 nmol/g i.p. for 1h. (B) Bar graph representation of percentage of immunoprecipitated Rph3A with GluN2A or PSD-95 and immunoprecipitated GluN2A and PSD-95 in TAT-Rph3A-9c treated mice compared to TAT-Rph3A(-VSSD) treated animals (two-tailed t tests, for GluN2A/Rph3A: $p<0.0001$ *** n=5 animals, for PSD95/Rph3A: $p<0.0001$ *** n=3 animals and for PSD-95/GluN2A: $p=0.0010$ *** n=3 animals). (C) Fluorescent immunocytochemistry of GluN2A (green) and Shank (PSD marker, red) in DIV15 rat primary hippocampal neurons treated with either TAT-Rph3A-9c or TAT-Rph3A(-VSSD) 10µM for 30min. Scale bar = 10µm. (D) Bar graph representing GluN2A/Shank co-localization percentage in DIV15 rat primary hippocampal neurons treated with either TAT-Rph3A-9c or TAT-Rph3A(-VSSD) 10µM for 30min (two-tailed t test, $p=0.0069$ ** n=10 neurons). (E) Fluorescent immunocytochemistry of surface GluN2A (red) and PSD-95 (blue) after 30min CPP 10 µM treatment of DIV15 primary hippocampal neurons. Scale bar: 10 µm. (F) Bar graph representation of surface GluN2A/PSD-95 ratio percentage of mean TAT-Rph3A(-VSSD) (two-tailed t test, $p=0.0005$ *** n=51-100 dendrites) (G) Fluorescence immunocytochemistry of surface (red) and total (green) GluN2A after 30min CPP 10 µM treatment of DIV15 primary hippocampal neurons. Scale bar: 10 µm. (H) Bar graph representation of surface/total ratio of CPP treated DIV15 primary hippocampal neurons (two-tailed t test, $p<0.0130$ * n=50 dendrites).

Furthermore, we investigated the onset of a possible effect of TAT-Rph3A-9c on hippocampal dendritic spines. *In vitro* treatment of GFP transfected primary hippocampal neurons with TAT-Rph3A-9c (10 μM, 1 h) induced a significant reduction in dendritic spine density (Fig. 21; two-tailed t test, p=0.0019 ***).

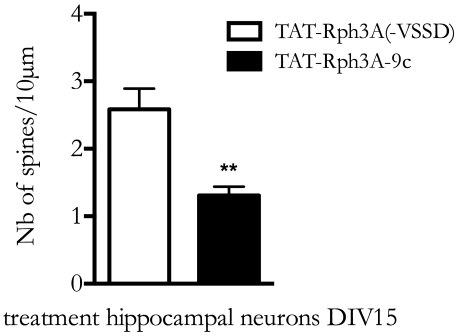

Fig. 21: Dendritic spine density in TAT-Rph3A-9c treated primary hippocampal neurons. Bar grap representation of spine density DIV15 GFP transfected (DIV9) primary hippocampal neurons treated with TAT-Rph3A-9c or TAT-Rph3A(-VSSD) 10 μM 1h.

These results suggest that Rph3A/PSD-95 interaction has an important role in the surface availability of GluN2A at the synaptic membrane and the overall spine density similarly as Rph3A/GluN2A interaction. Moreover, Rph3A/PSD-95 interaction is important for GluN2A/PSD-95 interaction emphasizing that the synaptic availability of GluN2A is dependent on the strength of GluN2A/Rph3A/PSD-95 ternary complex.

II. Pathological conditions: Parkinson's disease and L-DOPA-Induced Dyskinesia

In the striatum, glutamatergic cortical afferents converge with dopaminergic terminals from the *substantia nigra pars compacta* onto the dendritic spines of medium spiny neurons (MSNs). In particular, dopaminergic terminals form synaptic contacts in the neck of MSNs spines, whereas the head of the spine receives inputs from glutamatergic terminals (Surmeier et al., 2007). Consequently, dendritic spines of striatal MSNs are an essential site of information processing between glutamate and dopamine both in physiological conditions and in neurodegenerative events, i.e. in Parkinson's Disease (PD) (Gardoni et al., 2010). In addition, several studies described the co-localization of D1 and NMDA receptors in the MSNs dendritic spine indicating the existence of a direct molecular interaction and a functional cross-talk between the two receptor signaling pathways (Fiorentini, Gardoni, Spano, Di Luca, & Missale, 2003; Jocoy et al., 2011; Kruusmägi et al., 2009). As described earlier, NMDAR composition and localization is affected in PD and LID where an increased GluN2A/GluN2B ratio at synapses and extrasynaptic GluN2B expression at striatal MSNs have been reported (*refer to paragraph II.5 of Introduction*) as well as changes of expression of Rph3A at different time points preceding overt neuronal degeneration in PD and α-synucleinopathy (*refer to paragraph V of introduction*).

Therefore, we believed the Rph3A/GluN2A interaction would be of significance in pathological conditions.

Along with the alterations of NMDAR composition, we have found that the Rph3A/GluN2A interaction was significantly increased in both full 6-OHDA unilaterally lesioned (model of PD) and dyskinetic full 6-OHDA unilaterally lesioned treated with L-DOPA (model of LID) rats (Fig. 22A & B; two-tailed t tests: PD vs control p=0.012 @ n=6 animals, LID vs control p=0.0179 * n=6 animals) although no changes in Rph3A expression in TIF purifications were seen in these animals (Fig. 22C & D). These results suggest a role of Rph3A/GluN2A complex in the pathology and therefore this interaction could be a good target to reduce dyskinesia in parkinsonian patients.

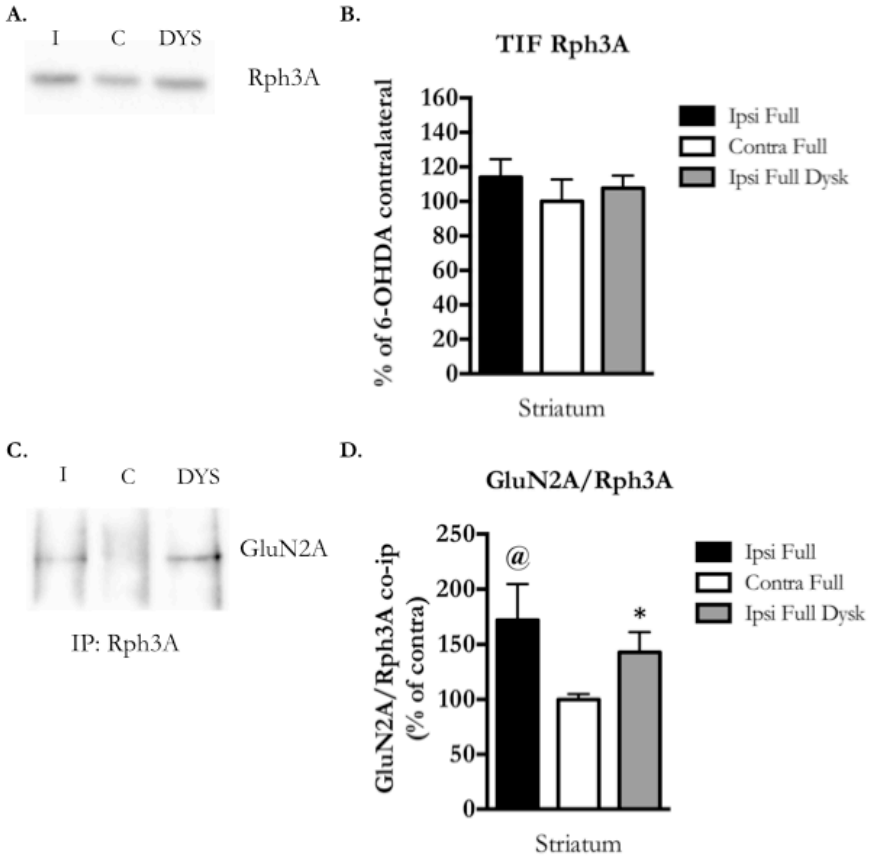

Fig. 22: Rph3A in Parkinson's disease and L-DOPA-induced dyskinesia. (A) Western blot of Rph3A from TIF purifications of the ipsilateral striatum from full 6-OHDA unilaterally lesioned rats (I), contralateral striatum of same animal (C, used as control) and ipsilateral striatum from dyskinetic full 6-OHDA lesioned rat treated with L-DOPA (DYS). (B) Bar graph representation of Rph3A expression percentage of mean Rph3A expression in contralateral striatum from full 6-OHDA unilaterally lesioned rats, from different animal: ipsilateral striatum from full 6-OHDA unilaterally lesioned rats (Ipsi Full), contralateral striatum from full 6-OHDA unilaterally lesioned rats (Contra Full) and ipsilateral striatum from dyskinetic full 6-OHDA unilaterally lesioned rats treated with L-DOPA (Ipsi Full Dusk). (C) Co-immunoprecipitation assay of Rph3A revealing GluN2A by western blot from P2 purifications of the ipsilateral striatum from full 6-OHDA unilaterally lesioned rats (I), contralateral striatum of same animal (C, used as control) and ipsilateral striatum from dyskinetic full 6-OHDA lesioned rat treated with L-DOPA (DYS). (D) Bar graph representation GluN2A/Rph3A co-immunoprecipitate percentage contralateral striatum in P2 fractions of ipsilateral striatum from full 6-OHDA unilaterally lesioned rats (Ipsi Full), contralateral striatum from full 6-OHDA unilaterally lesioned rats (Contra Full) and ipsilateral striatum from dyskinetic full 6-OHDA unilaterally lesioned rats treated with L-DOPA (Ipsi Full Dusk). (two-tailed t tests: Ipsi Full vs Contra Full p=0.012 @ n=6 animals, Ipsi Full Dysk vs Contra Full p=0.0179 * n=6 animals).

We have begun to test this hypothesis with an experiment where we measured the abnormal involuntary movements score (AIMS) throughout the L-DOPA treatment of the full 6-OHDA unilaterally lesioned rats to assess the development and stabilization of LID (AIMS>~20). After 2 weeks of treatment, when the animals were considered to have developed LID, we stereotaxically injected the TAT-2A-40 peptide in dopamine-depleted striatum. The same day as the intrastriatal injection of TAT-2A-40, the animals showed an almost complete disappearance of abnormal involuntary movements following L-DOPA treatment, characterizing those animals as no longer dyskinetics (Fig. 23; two-tailed t test, p=0.0028 ** n=4 animals). This effect was still observed following L-DOPA treatment one day after injection (Fig. 23, two-tailed t test, p=0.0043 ** n=4 animals), three days after injection (Fig. 23; two-tailed t test, p=0.0093 ** n=4 animals) and six days after injection (Fig. 23; two-tailed t test, p=0.0066 ** n=4 animals). Even if other experiments are needed to substantiate this TAT-2A-40 behavioral effect, these results already solidify the notion that postsynaptic Rph3A is involved in the synaptic availability of GluN2A and therefore their interaction might be an interesting new target to tackle LID.

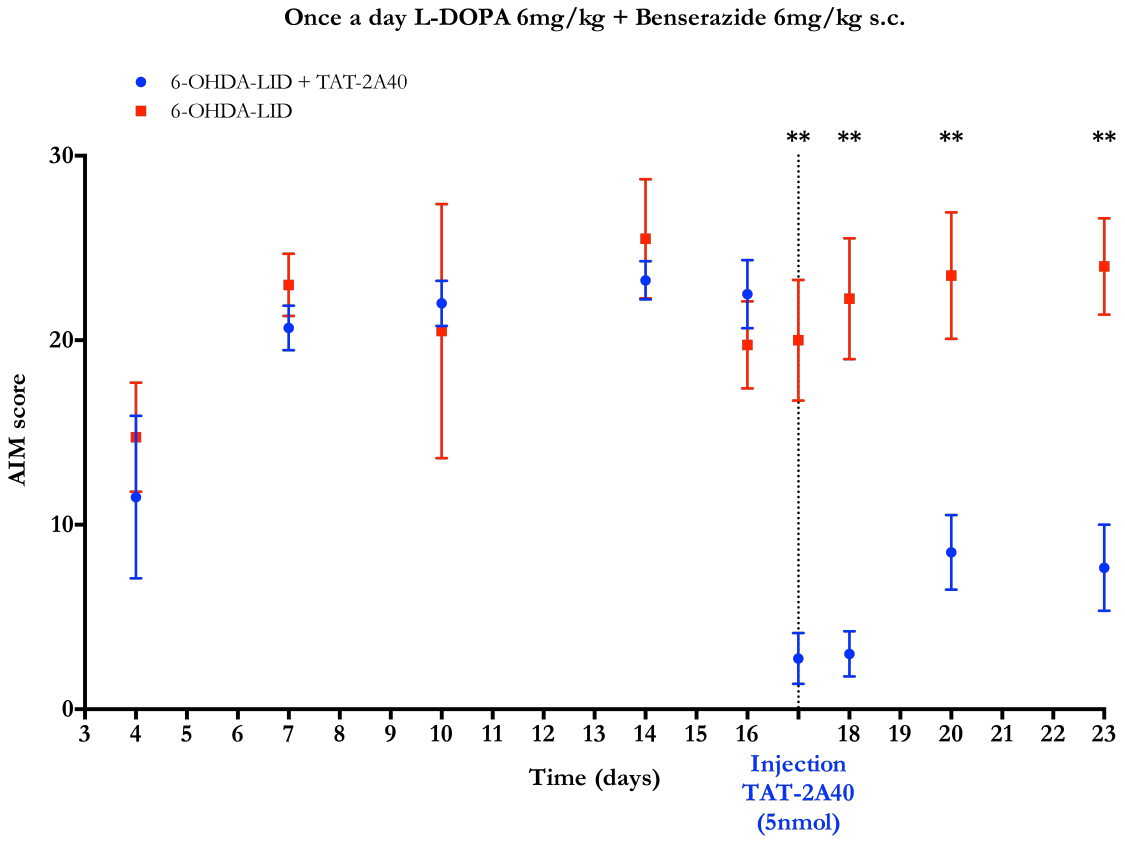

Fig. 23: Intrastriatal injection of TAT-2A-40 and LID. Graph representing AIM score of LID rats (6-OHDA-LID) and LID rats injected with TAT-2A-40 (5nmol) in ipsilateral striatum (6-OHDA-LID + TAT-2A-40) during L-DOPA treatment (once a day L-DOPA 6mg/kg + Benserazide 6mg/kg s.c.) before and after intrastriatal injection of TAT-2A-40 peptide (two-tailed t tests; day 17: p=0.0028 ** n=4 animals, day 18: p=0.0043 ** n=4 animals, day 20: p=0.0093 ** n=4 animals, day 23: p=0.0066 ** n=4 animals). Scoring was performed in double-blind conditions.

CONCLUSION

It is known that GluN2A-containing NMDARs are stable at synapses. On the other hand, GluN2B-containing NMDARs are known to be a more mobile pool of NMDAR at the synapse but also mobile from and to extrasynaptic sites (Groc et al., 2006). However, only the interaction with PSD-95 has been clearly demonstrated to favor GluN2A surface expression and stabilization within the synaptic membrane. Indeed, in search of the molecular mechanism(s) that mediate these differential GluN2-NMDAR distributions in synapses, PSD-95 family proteins emerged as primary candidates. SAP102 co-localizes with GluN2B subunit at the periphery of the synapse whereas PSD-95 co-localizes preferentially with the GluN2A subunit (J. Zhang & Diamond, 2009). Moreover, immunoprecipitation experiments from hippocampus extracts revealed that GluN2B subunit preferentially interacts with SAP102 and the GluN2A subunit with PSD-95 (Sans et al., 2000). However, this view is challenged by a biochemical study showing that the isolated di-heteromeric receptors GluN1/GluN2A and GluN1/GluN2B interact with similar affinities with PSD-95, SAP102 and PSD-93 (Al-Hallaq et al., 2007). Therefore, preferential associations between GluN2 subunits and specific PSD proteins in synapses may not only depend on their affinities but also to other molecular processes that remain to be identified. In this context, even if the literature reported extensive studies describing the differential role of GluN2B-containing receptors at synaptic and extrasynaptic sites and identified relevant protein partners regulating their synaptic localization, much less is known for GluN2A-containing receptors.

For this reason, our lab was interested in studying the molecular mechanisms regulating the synaptic targeting of GluN2A-containing receptors that are far from being understood. Based on these considerations, we decided to study the modulation of the GluN2A subunit in the synapse starting from the identification of new GluN2A-interacting proteins. Our lab recently performed a yeast two hybrid screening of a brain cDNA library using GluN2A(839-1461) as bait, without the last 3 aa (SDV) of the PDZ-binding domain. Among the new putative GluN2A-binding proteins, we found Rph3A. Co-clustering assays in COS-7 cells, co-immunoprecipitation and pull-down assays confirmed Rph3A interaction with GluN2A(1349-1389) C-terminal domain. Incubation of primary neurons with a CPP containing the GluN2A domain aa 1349-1389 (TAT-2A-40) and competing with the endogenous GluN2A subunit for Rph3A binding, led to a significant reduction in the levels of surface and synaptic GluN2A and consequently to a reduction of NMDAR activity. Notably, no effects on the synaptic localization of the GluN2B subunit were observed, nor did we see any effect on AMPAR synaptic availability or activity. Analysis of Rph3A C-terminal domain revealed the presence of a putative PDZ-interacting domain (-VSSD). Co-clustering assays in COS-7 cells and co-immunoprecipitation experiments from neuronal lysates confirmed that Rph3A i) binds also to the scaffolding protein PSD-95 and ii) forms a triple complex with GluN2A and PSD-95 at the excitatory postsynaptic density. Disruption of GluN2A/Rph3A or PSD-95/Rph3A interactions led to a similar decrease in the synaptic levels but also the surface levels of GluN2A-containing NMDARs with a concomitant disruption of GluN2A/PSD-95 complexes.

Altogether these results suggest that GluN2A/PSD-95/Rph3A complex formation is required for a correct localization and stabilization of GluN2A-containing NMDARs at the synapse. However, the fact that Rph3A binds to Myosin Va cargo protein (Brozzi et al., 2012), known to catalyze the transport of AMPARs into dendritic spines during activity-dependent synaptic plasticity, does not exclude Rph3A from being involved in the trafficking of GluN2A. This remains an important issue to be addressed. Overall, even if previous studies report only a presynaptic role for Rph3A in the regulation of vesicle trafficking via interaction small GTPases of the Rab family, cytoskeletal proteins, MAGUK scaffolding proteins and phospholipids (Shirataki et al., 1992; Shirataki et al., 1994; Yamaguchi et al., 1993; Fukuda et al., 2004; Kato et al., 1996; Südhof, 1997; Burns et al., 1998), our work has highlighted the presence of Rph3A at postsynaptic terminal and a role in synaptic availability of GluN2A NMDAR subunit.

The subunit composition of NMDARs is not static but changes during development in response to neuronal activity or sensory experiences. This plasticity, which was long thought to occur exclusively during development, can also occur at adult synapses. Changes in subunit composition can be rapid (timescale of minutes) and can have profound influences on the functioning of synapses and networks. Several studies *in vitro* and *in vivo* indicate that a change in the ratio of GluN2A to GluN2B, as occurs during sensory experience, affects subsequent NMDAR-dependent synaptic modifications. Manipulations of the GluN2A-to-GluN2B ratio, either through pharmacological means (Xu et al., 2009) or activity-dependent alterations (Philpot, Cho, & Bear, 2007; M.-C. Lee, Yasuda, & Ehlers, 2010), regulate both the magnitude and sign of subsequent plasticity, leading to a shift in the LTP and LTD threshold.

Here, we have used the developmentally driven changes in the GluN2A-to-GluN2B ratio as a paradigm to study the functional role of Rph3A in regulating the abundance of GluN2A available at postsynaptic terminals. The chronic treatment (from P6 to P14) with TAT-2A-40, disrupting Rph3A/GluN2A interaction, has led to a decrease of GluN2A present in the PSD preventing the developmental change in NMDAR composition; thus emphasizing on the role of Rph3A in the synaptic localization of GluN2A.

Moreover, in all our experimental paradigms we have observed an effect of the disruption of Rph3A/GluN2A complexes or even the knockdown of Rph3A on the dendritic spine density in hippocampal neurons. This is a comparable result to another study on IQGAP1, a GluN2A binding protein, and more precisely on IQGAP1$^{-/-}$ primary hippocampal neurons where researchers observed a reduced expression of surface GluN2A as well as a reduction in spine density (Gao et al., 2011). Other studies have also shown that synaptic NMDAR activation is also a trigger for genomic processes that increase the transcription of neuroprotective genes like BDNF (Schulz, Siemer, Krug, & Höllt, 1999; Cammarota et al., 2000; Hardingham et al., 2002) that leads to the sprouting of dendrites in many areas of the brain, such as CA1 in the hippocampus (Grande, Fries, Kunz, & Kapczinski, 2010; Tyler &

Pozzo-Miller, 2003) and that inhibition of either GluN2A- or GluN2B-containing NMDARs significantly decreases BDNF expression (X. Zhou, Ding, Chen, Yun, & Wang, 2013). Also a decrease in BDNF expression reduces spine density in these areas (Rothman & Mattson, 2013). Although, there is no real understanding of the role of GluN2A in spine density or spine morphology in the hippocampus.

In the last decade, several studies indicated that dysfunction of the glutamatergic transmission plays a key role in both Parkinson's disease (PD) and L-DOPA-induced dyskinesia (LID) (Calabresi et al., 2011). Particularly, changes in the corticostriatal glutamatergic transmission have been reported in animal models of PD and LID (Sgambato-Faure & Cenci, 2012; Mellone & Gardoni, 2013), as well as in PD patients at different disease stages (Ahmed et al., 2011). After chronic L-DOPA treatment, the glutamatergic signaling from the cortex to the striatum undergoes adaptive changes, which result in the aberrant functioning of NMDAR at the dendritic spines of striatal medium spiny neurons (Sgambato-Faure & Cenci, 2012). In the past ten years, clinical trials focused on the classical pharmacological approach based on NMDAR antagonists to reduce the receptor activity. Among others, amantadine exhibits anti-dyskinetic activity (Sawada et al., 2010), even if its beneficial effect is attenuated after a few months. A recent meta-analysis confirmed the short-term benefits of amantadine in the treatment of dyskinesia (Elahi et al., 2012). Besides NMDAR overactivation, abnormal NMDAR trafficking, which results in the modification of the receptor subunit composition at the synapse, has been involved in the pathogenesis of several brain disorders (Sanz-Clemente, Nicoll, & Roche, 2012). In particular, a great amount of studies have addressed the role of expression, phosphorylation state, and synaptic distribution of the specific subtypes of NMDARs in LID (Sanz-Clemente et al., 2012; Gardoni et al., 2010). Our group demonstrated the alterations in synaptic NMDAR GluN2A/GluN2B subunit ratio in the striatum correlates with the motor behavior abnormalities observed in rat models of PD and LID (Gardoni et al., 2006; Gardoni et al., 2011). Notably, these findings have been confirmed in the striatum of dyskinetic monkeys (Gardoni et al., manuscript in preparation) and in dyskinetic PD patients compared to age-matched control subjects (Gardoni et al., manuscript in preparation). Importantly, we showed that prevention of the aberrant NMDAR GluN2A/GluN2B subunit ratio at the striatal excitatory synapse is sufficient to significantly reduce the onset of LID in L-DOPA-treated parkinsonian animals (Gardoni et al., 2011). In particular, the concomitant systemic treatment with L-DOPA and TAT-2A, a CPP able to interfere with the interaction between GluN2A subunit and the scaffolding protein PSD-95, reduces the percentage of parkinsonian rats developing LID (Gardoni et al., 2011) and ameliorates the dyskinetic behavior in L-DOPA treated MPTP-monkeys (Gardoni et al., manuscript in preparation). Altogether these data support the importance of a correct balance NMDAR subunits at the striatal synapse to counteract the phenotype/molecular changes in PD and LID.

Based on the above-mentioned considerations and taking into account the well-known limitations in the use of classical NMDAR antagonists, we are aiming at restoring the physiological ratio between

GluN2A and GluN2B subunits to reduce dyskinetic behaviors by acting on the synaptic surface availability of GluN2A-containing NMDARs through its interaction with Rph3A. This approach has the advantage of manipulating the subunit composition of synaptic NMDARs, meaning a reduction of synaptic GluN2A-containing NMDARs, rather than a more generalized antagonism of both synaptic and extrasynaptic receptors.

As described in this work, we have found an increased between Rph3A and GluN2A in 6-OHDA-lesioned rats and L-DOPA treated dyskinetic animals. These data are consistent with the previously described increase in synaptic GluN2A-containing NMDARs in the same animal models (Gardoni et al., 2010; Gardoni et al., 2006). Finally, a pilot experiment in a small group of animals demonstrated that intrastriatal injection of TAT-2A-40 peptide in L-DOPA-treated rats resulted in a highly significant decrease of their dyskinetic behavior. Accordingly, it would be of relevance to test TAT-2A-40 in chronic treatments for long-term effects but also in systemic treatments with L-DOPA to reduce the onset of LID itself in order to go towards a clinical application. In addition, it would be relevant to test Rph3A as target not only in LID but also in PD itself, considering that we saw a huge increase of Rph3A/GluN2A interaction also in untreated parkinsonian animals. Interestingly, a significant increase of GluN2A-containing NMDAR was found in animals with a partial lesion, model of early stages of PD, thus supporting the use of peptides disrupting Rph3A/GluN2A at this stage of the disease. For example, it has been shown recently that an analogous peptide (TAT-2A targeting GluN2A-containing NMDARs interaction with PSD-95) improved the motor skills in these rats (Paillé et al., 2010).

Thus, our work has put forward a possible novel therapeutic strategy to counteract LID by reducing the synaptic levels of GluN2A-containing NMDARs at the corticostriatal synapses. Interestingly, an analogous peptide (TAT-2A targeting GluN2A-containing NMDARs interaction with PSD-95) when applied to animal models of LIDs, in concomitant treatment with L-DOPA reduced the onset of dyskinesia (Gardoni et al., 2011; Gardoni et al., manuscript in preparation). Despite the debated clinical applicability of CPPs due to pharmacokinetic and pharmacoeconomic reasons, key results on CPPs have been recently obtained both at preclinical and clinical stages (Gardoni et al., 2011; Hill et al., 2012), clearly supporting the therapeutic relevance of this innovative pharmacological approach. In particular, a peptide differing from only 2 aminoacids (aa) (TAT-GluN2B9c, targeting GluN2B-containing NMDARs interaction with PSD-95) has been used successfully in phase 2 randomized double-blinded placebo-controlled clinical trial for stroke (Hill et al., 2012). Such findings reinforce the applicability of interference peptides in central nervous system disorders and pave the way for future applications in clinical trials. In addition, the production of small and potent plasma-stable peptidomimetic compounds deriving from CPPs can represent the possibility of a further improvement and a more favorable and affordable clinical applicability of this therapeutic intervention strategy (Bach et al., 2011).

REFERENCES

Ahmed, I., Bose, S. K., Pavese, N., Ramlackhansingh, A., Turkheimer, F., Hotton, G., et al. (2011). Glutamate NMDA receptor dysregulation in Parkinson's disease with dyskinesias. *Brain*, *134*(4), 979–986.

Akazawa, C., Shigemoto, R., Bessho, Y., Nakanishi, S., & Mizuno, N. (1994). Differential expression of five N-methyl-D-aspartate receptor subunit mRNAs in the cerebellum of developing and adult rats. *The Journal of Comparative Neurology*, *347*(1), 150–160.

Al-Hallaq, R. A., Conrads, T. P., Veenstra, T. D., & Wenthold, R. J. (2007). NMDA di-heteromeric receptor populations and associated proteins in rat hippocampus. *Journal of Neuroscience*, *27*(31), 8334–8343.

Ascher, P., & Nowak, L. (1988). The role of divalent cations in the N-methyl-D-aspartate responses of mouse central neurones in culture. *The Journal of physiology*, *399*, 247–266.

Bach, A., Eildal, J. N. N., Stuhr-Hansen, N., Deeskamp, R., Gottschalk, M., Pedersen, S. W., et al. (2011). Cell-permeable and plasma-stable peptidomimetic inhibitors of the postsynaptic density-95/N-methyl-D-aspartate receptor interaction. *Journal of medicinal chemistry*, *54*(5), 1333–1346.

Barria, A., & Malinow, R. (2002). Subunit-specific NMDA receptor trafficking to synapses. *Neuron*, *35*(2), 345–353.

Barria, A., & Malinow, R. (2005). NMDA receptor subunit composition controls synaptic plasticity by regulating binding to CaMKII. *Neuron*, *48*(2), 289–301.

Bayer, K. U., De Koninck, P., Leonard, A. S., Hell, J. W., & Schulman, H. (2001). Interaction with the NMDA receptor locks CaMKII in an active conformation. *Nature*, *411*(6839), 801–805.

Bellone, C., & Nicoll, R. A. (2007). Rapid bidirectional switching of synaptic NMDA receptors. *Neuron*, *55*(5), 779–785.

BIRKMAYER, W., & HORNYKIEWICZ, O. (1961). [The L-3,4-dioxyphenylalanine (DOPA)-effect in Parkinson-akinesia]. *Wiener klinische Wochenschrift*, *73*, 787–788.

Bordji, K., Becerril-Ortega, J., Nicole, O., & Buisson, A. (2010). Activation of extrasynaptic, but not synaptic, NMDA receptors modifies amyloid precursor protein expression pattern and increases amyloid-ß production. *Journal of Neuroscience*, *30*(47), 15927–15942.

Brothwell, S. L. C., Barber, J. L., Monaghan, D. T., Jane, D. E., Gibb, A. J., & Jones, S. (2008). NR2B- and NR2D-containing synaptic NMDA receptors in developing rat substantia nigra pars compacta dopaminergic neurones. *The Journal of physiology*, *586*(3), 739–750.

Brozzi, F., Diraison, F., Lajus, S., Rajatileka, S., Philips, T., Regazzi, R., et al. (2012). Molecular Mechanism of Myosin Va Recruitment to Dense Core Secretory Granules. *Traffic (Copenhagen, Denmark)*, *13*(1), 54–69.

Burnashev, N., Schoepfer, R., Monyer, H., Ruppersberg, J. P., Günther, W., Seeburg, P. H., & Sakmann, B. (1992). Control by asparagine residues of calcium permeability and magnesium blockade in the NMDA receptor. *Science*, *257*(5075), 1415–1419.

Burnashev, N., Zhou, Z., Neher, E., & Sakmann, B. (1995). Fractional calcium currents through recombinant GluR channels of the NMDA, AMPA and kainate receptor subtypes. *The Journal of physiology*, *485 (Pt 2)*, 403–418.

Burns, M. E., Sasaki, T., Takai, Y., & Augustine, G. J. (1998). Rabphilin-3A: a multifunctional regulator of synaptic vesicle traffic. *The Journal of general physiology*, *111*(2), 243–255.

Burzomato, V., Frugier, G., Pérez-Otaño, I., Kittler, J. T., & Attwell, D. (2010). The receptor subunits generating NMDA receptor mediated currents in oligodendrocytes. *The Journal of physiology*, *588*(Pt 18), 3403–3414.

Calabresi, P., Di Filippo, M., Ghiglieri, V., Tambasco, N., & Picconi, B. (2010). Levodopa-induced dyskinesias in patients with Parkinson's disease: filling the bench-to-bedside gap. *Lancet neurology*, *9*(11), 1106–1117.

Cammarota, M., Bevilaqua, L. R., Ardenghi, P., Paratcha, G., Levi de Stein, M., Izquierdo, I., & Medina, J. H. (2000). Learning-associated activation of nuclear MAPK, CREB and Elk-1, along with Fos production, in the rat hippocampus after a one-trial avoidance learning: abolition by NMDA receptor blockade. *Brain research. Molecular brain research*, *76*(1), 36–46.

Carmignoto, G., & Vicini, S. (1992). Activity-dependent decrease in NMDA receptor responses during development of the visual cortex. *Science*, *258*(5084), 1007–1011.

Carpenter-Hyland, E. P., Woodward, J. J., & Chandler, L. J. (2004). Chronic ethanol induces synaptic but not extrasynaptic targeting of NMDA receptors. *Journal of Neuroscience*, *24*(36), 7859–7868.

Cenci, M. A., Lee, C. S., & Björklund, A. (1998). L-DOPA-induced dyskinesia in the rat is associated with striatal overexpression of prodynorphin- and glutamic acid decarboxylase mRNA. *The European journal of neuroscience*, *10*(8), 2694–2706.

Cepeda, C., Ariano, M. A., Calvert, C. R., Flores-Hernández, J., Chandler, S. H., Leavitt, B. R., et al. (2001). NMDA receptor function in mouse models of Huntington disease. *Journal of neuroscience research*, *66*(4), 525–539.

Chen, B.-S., & Roche, K. W. (2007). Regulation of NMDA receptors by phosphorylation. *Neuropharmacology*, *53*(3), 362–368.

Chen, B.-S., & Roche, K. W. (2009). Growth factor-dependent trafficking of cerebellar NMDA receptors via protein kinase B/Akt phosphorylation of NR2C. *Neuron*, *62*(4), 471–478.

Chen, B.-S., Thomas, E. V., Sanz-Clemente, A., & Roche, K. W. (2011). NMDA receptor-dependent regulation of dendritic spine morphology by SAP102 splice variants. *Journal of Neuroscience*, *31*(1), 89–96.

Chen, G. Q., Cui, C., Mayer, M. L., & Gouaux, E. (1999). Functional characterization of a potassium-selective prokaryotic glutamate receptor. *Nature*, *402*(6763), 817–821.

Chung, C. Y., Koprich, J. B., Siddiqi, H., & Isacson, O. (2009). Dynamic changes in presynaptic and axonal transport proteins combined with striatal neuroinflammation precede dopaminergic neuronal loss in a rat model of AAV alpha-synucleinopathy. *Journal of Neuroscience*, *29*(11), 3365–3373.

Chung, H. J., Huang, Y. H., Lau, L.-F., & Huganir, R. L. (2004). Regulation of the NMDA receptor complex and trafficking by activity-dependent phosphorylation of the NR2B subunit PDZ ligand. *Journal of Neuroscience*, *24*(45), 10248–10259.

Chung, S. H., Song, W. J., Kim, K., Bednarski, J. J., Chen, J., Prestwich, G. D., & Holz, R. W. (1998). The C2 domains of Rabphilin3A specifically bind phosphatidylinositol 4,5-bisphosphate containing vesicles in a Ca2+-dependent manner. In vitro characteristics and possible significance. *The Journal of biological chemistry*, *273*(17), 10240–10248.

Clarke, R. J., & Johnson, J. W. (2006). NMDA receptor NR2 subunit dependence of the slow component of magnesium unblock. *Journal of Neuroscience*, *26*(21), 5825–5834.

Corlew, R., Brasier, D. J., Feldman, D. E., & Philpot, B. D. (2008). Presynaptic NMDA receptors: newly appreciated roles in cortical synaptic function and plasticity. *The Neuroscientist : a review journal bringing neurobiology, neurology and psychiatry*, *14*(6), 609–625.

Correia, S. S., Bassani, S., Brown, T. C., Lisé, M.-F., Backos, D. S., El-Husseini, A., et al. (2008). Motor protein-dependent transport of AMPA receptors into spines during long-term potentiation. *Nature Neuroscience*, *11*(4), 457–466.

Cotzias, G. C., Papavasiliou, P. S., & Gellene, R. (1969). Modification of Parkinsonism--chronic treatment with L-dopa. *The New England journal of medicine*, *280*(7), 337–345.

Cousins, S. L., Kenny, A. V., & Stephenson, F. A. (2009). Delineation of additional PSD-95 binding domains within NMDA receptor NR2 subunits reveals differences between NR2A/PSD-95 and NR2B/PSD-95 association. *Neuroscience*, *158*(1), 89–95.

Cull-Candy, S. G., & Leszkiewicz, D. N. (2004). Role of distinct NMDA receptor subtypes at central synapses. *Science's STKE : signal transduction knowledge environment*, *2004*(255), re16–re16.

Cull-Candy, S., Brickley, S., & Farrant, M. (2001). NMDA receptor subunits: diversity, development and disease. *Current Opinion in Neurobiology*, *11*(3), 327–335.

da Silva-Júnior, F. P., Braga-Neto, P., Sueli Monte, F., & de Bruin, V. M. S. (2005). Amantadine reduces the duration of levodopa-induced dyskinesia: a randomized, double-blind, placebo-controlled study. *Parkinsonism & related disorders*, *11*(7), 449–452.

Dalva, M. B., Takasu, M. A., Lin, M. Z., Shamah, S. M., Hu, L., Gale, N. W., & Greenberg, M. E. (2000). EphB receptors interact with NMDA receptors and regulate excitatory synapse formation. *Cell*, *103*(6), 945–956.

DeBello, W. M., Betz, H., & Augustine, G. J. (1993). Synaptotagmin and neurotransmitter release. *Cell*, *74*(6), 947–950.

Dingledine, R., Borges, K., Bowie, D., & Traynelis, S. F. (1999). The glutamate receptor ion channels. *Pharmacological reviews*, *51*(1), 7–61.

Dravid, S. M., Prakash, A., & Traynelis, S. F. (2008). Activation of recombinant NR1/NR2C NMDA receptors. *The Journal of physiology*, *586*(Pt 18), 4425–4439.

Dunah, A. W., Wang, Y., Yasuda, R. P., Kameyama, K., Huganir, R. L., Wolfe, B. B., & Standaert, D. G. (2000). Alterations in subunit expression, composition, and phosphorylation of striatal N-methyl-D-aspartate glutamate receptors in a rat 6-hydroxydopamine model of Parkinson's disease. *Molecular pharmacology*, *57*(2), 342–352.

Ehlers, M. D. (2003). Activity level controls postsynaptic composition and signaling via the ubiquitin-proteasome system. *Nature Neuroscience*, *6*(3), 231–242.

Elahi, B., Phielipp, N., & Chen, R. (2012). N-Methyl-D-Aspartate antagonists in levodopa induced dyskinesia: a meta-analysis. *The Canadian journal of neurological sciences. Le journal canadien des sciences neurologiques*, *39*(4), 465–472.

Erisir, A., & Harris, J. L. (2003). Decline of the critical period of visual plasticity is concurrent with the reduction of NR2B subunit of the synaptic NMDA receptor in layer 4. *Journal of Neuroscience*, *23*(12), 5208–5218.

Erreger, K., Dravid, S. M., Banke, T. G., Wyllie, D. J. A., & Traynelis, S. F. (2005). Subunit-specific gating controls rat NR1/NR2A and NR1/NR2B NMDA channel kinetics and synaptic signalling profiles. *The Journal of physiology*, *563*(Pt 2), 345–358.

Fan, J., Cowan, C. M., Zhang, L. Y. J., Hayden, M. R., & Raymond, L. A. (2009). Interaction of postsynaptic density protein-95 with NMDA receptors influences excitotoxicity in the yeast artificial chromosome mouse model of Huntington's disease. *Journal of Neuroscience*, *29*(35), 10928–10938.

Fan, M. M. Y., Fernandes, H. B., Zhang, L. Y. J., Hayden, M. R., & Raymond, L. A. (2007). Altered NMDA receptor trafficking in a yeast artificial chromosome transgenic mouse model of Huntington's disease. *Journal of Neuroscience*, *27*(14), 3768–3779.

Fernandes, H. B., Baimbridge, K. G., Church, J., Hayden, M. R., & Raymond, L. A. (2007). Mitochondrial sensitivity and altered calcium handling underlie enhanced NMDA-induced apoptosis in YAC128 model of Huntington's disease. *Journal of Neuroscience*, *27*(50), 13614–13623.

Fiorentini, C., Gardoni, F., Spano, P., Di Luca, M., & Missale, C. (2003). Regulation of dopamine D1 receptor trafficking and desensitization by oligomerization with glutamate N-methyl-D-aspartate receptors. *The Journal of biological chemistry*, *278*(22), 20196–20202.

Fukuda, M. (2005). Versatile role of Rab27 in membrane trafficking: focus on the Rab27 effector families. *Journal of biochemistry*, *137*(1), 9–16.

Fukuda, M., Kanno, E., & Yamamoto, A. (2004). Rabphilin and Noc2 are recruited to dense-core vesicles through specific interaction with Rab27A in PC12 cells. *The Journal of biological chemistry*, *279*(13), 13065–13075.

Furukawa, Hiroyasu, Singh, S. K., Mancusso, R., & Gouaux, E. (2005). Subunit arrangement and function in NMDA receptors. *Nature*, *438*(7065), 185–192.

Fykse, E. M., Li, C., & Südhof, T. C. (1995). Phosphorylation of rabphilin-3A by Ca2+/calmodulin- and cAMP-dependent protein kinases in vitro. *The Journal of neuroscience : the official journal of the Society for Neuroscience*, *15*(3 Pt 2), 2385–2395.

Gao, C., Frausto, S. F., Guedea, A. L., Tronson, N. C., Jovasevic, V., Leaderbrand, K., et al. (2011). IQGAP1 regulates NR2A signaling, spine density, and cognitive processes. *Journal of Neuroscience*, *31*(23), 8533–8542.

Gardoni, F., Caputi, A., Cimino, M., Pastorino, L., Cattabeni, F., & Di Luca, M. (1998). Calcium/calmodulin-dependent protein kinase II is associated with NR2A/B subunits of NMDA receptor in postsynaptic densities. *Journal of Neurochemistry*, *71*(4), 1733–1741.

Gardoni, F., Ghiglieri, V., Luca, M. D., & Calabresi, P. (2010). Assemblies of glutamate receptor subunits with post-synaptic density proteins and their alterations in Parkinson's disease. *Progress in brain research*, *183*, 169–182.

Gardoni, F., Marcello, E., & Di Luca, M. (2009). Postsynaptic density-membrane associated guanylate kinase proteins (PSD-MAGUKs) and their role in CNS disorders. *NSC*, *158*(1), 324–333.

Gardoni, F., Picconi, B., Ghiglieri, V., Polli, F., Bagetta, V., Bernardi, G., et al. (2006). A critical interaction between NR2B and MAGUK in L-DOPA induced dyskinesia. *Journal of Neuroscience*, *26*(11), 2914–2922.

Gardoni, F., Sgobio, C., Pendolino, V., Calabresi, P., Di Luca, M., & Picconi, B. (2011). Targeting NR2A-containing NMDA receptors reduces L-DOPA-induced dyskinesias. *Neurobiology of aging*.

Gielen, M., Le Goff, A., Stroebel, D., Johnson, J. W., Neyton, J., & Paoletti, P. (2008). Structural rearrangements of NR1/NR2A NMDA receptors during allosteric inhibition. *Neuron*, *57*(1), 80–93.

Gielen, M., Siegler Retchless, B., Mony, L., Johnson, J. W., & Paoletti, P. (2009). Mechanism of differential control of NMDA receptor activity by NR2 subunits. *Nature*, *459*(7247), 703–707.

Gladding, C. M., & Raymond, L. A. (2011). Mechanisms underlying NMDA receptor synaptic/extrasynaptic distribution and function. *Molecular and cellular neurosciences*, *48*(4), 308–320.

Graham, R. K., Pouladi, M. A., Joshi, P., Lu, G., Deng, Y., Wu, N.-P., et al. (2009). Differential susceptibility to excitotoxic stress in YAC128 mouse models of Huntington disease between initiation and progression of disease. *Journal of Neuroscience*, *29*(7), 2193–2204.

Grande, I., Fries, G. R., Kunz, M., & Kapczinski, F. (2010). The role of BDNF as a mediator of neuroplasticity in bipolar disorder. *Psychiatry investigation*, *7*(4), 243–250.

Gray, J. A., Shi, Y., Usui, H., During, M. J., Sakimura, K., & Nicoll, R. A. (2011). Distinct Modes of AMPA Receptor Suppression at Developing Synapses by GluN2A and GluN2B: Single-Cell NMDA Receptor Subunit Deletion In Vivo. *Neuron*, *71*(6), 1085–1101.

Groc, L., Bard, L., & Choquet, D. (2009). Surface trafficking of N-methyl-D-aspartate receptors: physiological and pathological perspectives. *NSC*, *158*(1), 4–18.

Groc, L., Choquet, D., Stephenson, F. A., Verrier, D., Manzoni, O. J., & Chavis, P. (2007). NMDA receptor surface trafficking and synaptic subunit composition are developmentally regulated by the extracellular matrix protein Reelin. *Journal of Neuroscience*, *27*(38), 10165–10175.

Groc, L., Heine, M., Cousins, S. L., Stephenson, F. A., Lounis, B., Cognet, L., & Choquet, D. (2006). NMDA receptor surface mobility depends on NR2A-2B subunits. *Proceedings of the National Academy of Sciences of the United States of America*, *103*(49), 18769–18774.

Hadj Tahar, A., Grégoire, L., Darré, A., Bélanger, N., Meltzer, L., & Bédard, P. J. (2004). Effect of a selective glutamate antagonist on L-dopa-induced dyskinesias in drug-naive parkinsonian monkeys. *Neurobiology of Disease*, *15*(2), 171–176.

Hardingham, G. E., & Bading, H. (2010). Synaptic versus extrasynaptic NMDA receptor signalling: implications for neurodegenerative disorders. *Nature Publishing Group*, *11*(10), 682–696.

Hardingham, G. E., Fukunaga, Y., & Bading, H. (2002). Extrasynaptic NMDARs oppose synaptic NMDARs by triggering CREB shut-off and cell death pathways. *Nature Neuroscience*.

Harper, P. S. (1992). The epidemiology of Huntington's disease. *Human genetics*, *89*(4), 365–376.

Harris, A. Z., & Pettit, D. L. (2007). Extrasynaptic and synaptic NMDA receptors form stable and uniform pools in rat hippocampal slices. *The Journal of physiology*, *584*(Pt 2), 509–519.

Harris, K. M., Jensen, F. E., & Tsao, B. (1992). Three-dimensional structure of dendritic spines and synapses in rat hippocampus (CA1) at postnatal day 15 and adult ages: implications for the maturation of synaptic physiology and long-term potentiation. *The Journal of neuroscience : the official journal of the Society for Neuroscience*, *12*(7), 2685–2705.

Haucke, V. (2005). Phosphoinositide regulation of clathrin-mediated endocytosis. *Biochemical Society transactions*, *33*(Pt 6), 1285–1289.

Henneberger, C., Papouin, T., Oliet, S. H. R., & Rusakov, D. A. (2010). Long-term potentiation depends on release of D-serine from astrocytes. *Nature*, *463*(7278), 232–236.

Henson, M. A., Roberts, A. C., Pérez-Otaño, I., & Philpot, B. D. (2010). Influence of the NR3A subunit on NMDA receptor functions. *Progress in neurobiology*, *91*(1), 23–37.

Hill, M. D., Martin, R. H., Mikulis, D., Wong, J. H., Silver, F. L., Terbrugge, K. G., et al. (2012). Safety and efficacy of NA-1 in patients with iatrogenic stroke after endovascular aneurysm repair (ENACT): a phase 2, randomised, double-blind, placebo-controlled trial. *Lancet neurology*, *11*(11), 942–950.

Horak, M., & Wenthold, R. J. (2009). Different roles of C-terminal cassettes in the trafficking of full-length NR1 subunits to the cell surface. *The Journal of biological chemistry*, *284*(15), 9683–9691.

Hughes, C. A., & Bennett, V. (1995). Adducin: a physical model with implications for function in assembly of spectrin-actin complexes. *The Journal of biological chemistry*, *270*(32), 18990–18996.

Hynd, M. R., Scott, H. L., & Dodd, P. R. (2004). Glutamate-mediated excitotoxicity and neurodegeneration in Alzheimer's disease. *Neurochemistry international*, *45*(5), 583–595.

Ivarsson, R., Jing, X., Waselle, L., Regazzi, R., & Renström, E. (2005). Myosin 5a controls insulin granule recruitment during late-phase secretion. *Traffic (Copenhagen, Denmark)*, *6*(11), 1027–1035.

Jarabek, B. R., Yasuda, R. P., & Wolfe, B. B. (2004). Regulation of proteins affecting NMDA receptor-induced excitotoxicity in a Huntington's mouse model. *Brain*, *127*(Pt 3), 505–516.

Jocoy, E. L., André, V. M., Cummings, D. M., Rao, S. P., Wu, N., Ramsey, A. J., et al. (2011). Dissecting the contribution of individual receptor subunits to the enhancement of N-methyl-d-aspartate currents by dopamine D1 receptor activation in striatum. *Frontiers in systems neuroscience*, *5*, 28.

Johnson, J. W., & Ascher, P. (1987). Glycine potentiates the NMDA response in cultured mouse brain neurons. *Nature*, *325*(6104), 529–531.

Jones, M. L., & Leonard, J. P. (2005). PKC site mutations reveal differential modulation by insulin of NMDA receptors containing NR2A or NR2B subunits. *Journal of Neurochemistry*, *92*(6), 1431–1438.

Jung, S.-Y., Kim, J., Kwon, O. B., Jung, J. H., An, K., Jeong, A. Y., et al. (2010). Input-specific synaptic plasticity in the amygdala is regulated by neuroligin-1 via postsynaptic NMDA receptors. *Proceedings of the National Academy of Sciences*, *107*(10), 4710–4715.

Karakas, E., Simorowski, N., & Furukawa, H. (2011). Subunit arrangement and phenylethanolamine binding in GluN1/GluN2B NMDA receptors. *Nature*, *475*(7355), 249–253.

Kato, M., Sasaki, T., Ohya, T., Nakanishi, H., Nishioka, H., Imamura, M., & Takai, Y. (1996). Physical and functional interaction of rabphilin-3A with alpha-actinin. *The Journal of biological chemistry*, *271*(50), 31775–31778.

Kennedy, M. B. (2000). Signal-processing machines at the postsynaptic density. *Science*, *290*(5492), 750–754.

Kennedy, M. B., Beale, H. C., Carlisle, H. J., & Washburn, L. R. (2005). Integration of biochemical signalling in spines. *Nature Reviews Neuroscience*, *6*(6), 423–434.

Kew, J. N., Richards, J. G., Mutel, V., & Kemp, J. A. (1998). Developmental changes in NMDA receptor glycine affinity and ifenprodil sensitivity reveal three distinct populations of NMDA receptors in individual rat cortical neurons. *The Journal of neuroscience : the official journal of the Society for Neuroscience*, *18*(6), 1935–1943.

Kim, B. G., Dai, H.-N., McAtee, M., Vicini, S., & Bregman, B. S. (2007). Labeling of dendritic spines with the carbocyanine dye DiI for confocal microscopic imaging in lightly fixed cortical slices. *Journal of Neuroscience Methods*, *162*(1-2), 237–243.

Kim, J. H., Liao, D., Lau, L. F., & Huganir, R. L. (1998). SynGAP: a synaptic RasGAP that associates with the PSD-95/SAP90 protein family. *Neuron*, *20*(4), 683–691.

Kirson, E. D., & Yaari, Y. (1996). Synaptic NMDA receptors in developing mouse hippocampal neurones: functional properties and sensitivity to ifenprodil. *The Journal of physiology*, *497 (Pt 2)*, 437–455.

Kishida, S., Shirataki, H., Sasaki, T., Kato, M., Kaibuchi, K., & Takai, Y. (1993). Rab3A GTPase-activating protein-inhibiting activity of Rabphilin-3A, a putative Rab3A target protein. *The Journal of biological chemistry*, *268*(30), 22259–22261.

Kornhuber, J., Bormann, J., Hübers, M., Rusche, K., & Riederer, P. (1991). Effects of the 1-amino-adamantanes at the MK-801-binding site of the NMDA-receptor-gated ion channel: a human postmortem brain study. *European Journal of Pharmacology*, *206*(4), 297–300.

Köhr, G. (2007). NMDA receptor mobility: cultures versus acute brain slices or neonatal versus mature synapses? *The Journal of physiology*, *584*(Pt 2), 367–367.

Krapivinsky, G., Krapivinsky, L., Manasian, Y., Ivanov, A., Tyzio, R., Pellegrino, C., et al. (2003). The NMDA receptor is coupled to the ERK pathway by a direct interaction between NR2B and RasGRF1. *Neuron*, *40*(4), 775–784.

Kruusmägi, M., Kumar, S., Zelenin, S., Brismar, H., Aperia, A., & Scott, L. (2009). Functional differences between D(1) and D(5) revealed by high resolution imaging on live neurons. *Neuroscience*, *164*(2), 463–469.

Kuner, T., & Schoepfer, R. (1996). Multiple structural elements determine subunit specificity of Mg2+ block in NMDA receptor channels. *The Journal of neuroscience : the official journal of the Society for Neuroscience*, *16*(11), 3549–3558.

Kuner, T., Wollmuth, L. P., Karlin, A., Seeburg, P. H., & Sakmann, B. (1996). Structure of the NMDA receptor channel M2 segment inferred from the accessibility of substituted cysteines. *Neuron*, *17*(2), 343–352.

Kurup, P., Zhang, Y., Xu, J., Venkitaramani, D. V., Haroutunian, V., Greengard, P., et al. (2010). Abeta-mediated NMDA receptor endocytosis in Alzheimer's disease involves ubiquitination of the tyrosine phosphatase STEP61. *Journal of Neuroscience*, *30*(17), 5948–5957.

Landles, C., & Bates, G. P. (2004). Huntingtin and the molecular pathogenesis of Huntington's disease. Fourth in molecular medicine review series. *EMBO reports*, *5*(10), 958–963.

Lau, C. G., & Zukin, R. S. (2007). NMDA receptor trafficking in synaptic plasticity and neuropsychiatric disorders. *Nature Reviews Neuroscience*, *8*(6), 413–426.

Laurie, D. J., & Seeburg, P. H. (1994). Regional and developmental heterogeneity in splicing of the rat brain NMDAR1 mRNA. *The Journal of neuroscience : the official journal of the Society for Neuroscience*, *14*(5 Pt 2), 3180–3194.

Lavezzari, G., McCallum, J., Dewey, C. M., & Roche, K. W. (2004). Subunit-specific regulation of NMDA receptor endocytosis. *Journal of Neuroscience*, *24*(28), 6383–6391.

Lavezzari, G., McCallum, J., Lee, R., & Roche, K. W. (2003). Differential binding of the AP-2 adaptor complex and PSD-95 to the C-terminus of the NMDA receptor subunit NR2B regulates surface expression. *Neuropharmacology*, *45*(6), 729–737.

Lee, M.-C., Yasuda, R., & Ehlers, M. D. (2010). Metaplasticity at single glutamatergic synapses. *Neuron*, *66*(6), 859–870.

Leonard, A. S., Lim, I. A., Hemsworth, D. E., Horne, M. C., & Hell, J. W. (1999). Calcium/calmodulin-dependent protein kinase II is associated with the N-methyl-D-aspartate receptor. *Proceedings of the National Academy of Sciences of the United States of America*, *96*(6), 3239–3244.

Levine, M. S., Cepeda, C., & André, V. M. (2010). Location, location, location: contrasting roles of synaptic and extrasynaptic NMDA receptors in Huntington's disease. *Neuron*, *65*(2), 145–147.

Li, C., Takei, K., Geppert, M., Daniell, L., Stenius, K., Chapman, E. R., et al. (1994). Synaptic targeting of rabphilin-3A, a synaptic vesicle Ca2+/phospholipid-binding protein, depends on rab3A/3C. *Neuron*, *13*(4), 885–898.

Li, J. H., Wang, Y. H., Wolfe, B. B., Krueger, K. E., Corsi, L., Stocca, G., & Vicini, S. (1998). Developmental changes in localization of NMDA receptor subunits in primary cultures of cortical neurons. *The European journal of neuroscience*, *10*(5), 1704–1715.

Li, J.-Y., Plomann, M., & Brundin, P. (2003). Huntington's disease: a synaptopathy? *Trends in molecular medicine*, *9*(10), 414–420.

Li, L., Murphy, T. H., Hayden, M. R., & Raymond, L. A. (2004). Enhanced striatal NR2B-containing N-methyl-D-aspartate receptor-mediated synaptic currents in a mouse model of Huntington disease. *Journal of neurophysiology*, *92*(5), 2738–2746.

Lisman, J., Schulman, H., & Cline, H. (2002). The molecular basis of CaMKII function in synaptic and behavioural memory. *Nature Reviews Neuroscience*, *3*(3), 175–190.

Liu, X.-B., Murray, K. D., & Jones, E. G. (2004). Switching of NMDA receptor 2A and 2B subunits at thalamic and cortical synapses during early postnatal development. *Journal of Neuroscience*, *24*(40), 8885–8895.

Lonart, G., & Südhof, T. C. (1998). Region-specific phosphorylation of rabphilin in mossy fiber nerve terminals of the hippocampus. *The Journal of neuroscience : the official journal of the Society for Neuroscience*, *18*(2), 634–640.

Löschmann, P.-A., De Groote, C., Smith, L., Wüllner, U., Fischer, G., Kemp, J. A., et al. (2004). Antiparkinsonian activity of Ro 25-6981, a NR2B subunit specific NMDA receptor antagonist, in animal models of Parkinson's disease. *Experimental neurology*, *187*(1), 86–93.

Luginger, E., Wenning, G. K., Bösch, S., & Poewe, W. (2000). Beneficial effects of amantadine on L-dopa-induced dyskinesias in Parkinson's disease. *Movement Disorders*, *15*(5), 873–878.

Lundblad, M., Andersson, M., Winkler, C., Kirik, D., Wierup, N., & Cenci, M. A. (2002). Pharmacological validation of behavioural measures of akinesia and dyskinesia in a rat model of Parkinson's disease. *The European journal of neuroscience*, *15*(1), 120–132.

Luthi-Carter, R., Apostol, B. L., Dunah, A. W., DeJohn, M. M., Farrell, L. A., Bates, G. P., et al. (2003). Complex alteration of NMDA receptors in transgenic Huntington's disease mouse brain: analysis of mRNA and protein expression, plasma membrane association, interacting proteins, and phosphorylation. *Neurobiology of Disease*, *14*(3), 624–636.

Lynch, D. R., & Guttmann, R. P. (2002). Excitotoxicity: perspectives based on N-methyl-D-aspartate receptor subtypes. *The Journal of pharmacology and experimental therapeutics*, *300*(3), 717–723.

Madry, C., Mesic, I., Bartholomäus, I., Nicke, A., Betz, H., & Laube, B. (2007). Principal role of NR3 subunits in NR1/NR3 excitatory glycine receptor function. *Biochemical and biophysical research communications*, *354*(1), 102–108.

Mangiarini, L., Sathasivam, K., Seller, M., Cozens, B., Harper, A., Hetherington, C., et al. (1996). Exon 1 of the HD gene with an expanded CAG repeat is sufficient to cause a progressive neurological phenotype in transgenic mice. *Cell*, *87*(3), 493–506.

Matsui, T., Sekiguchi, M., Hashimoto, A., Tomita, U., Nishikawa, T., & Wada, K. (1995). Functional comparison of D-serine and glycine in rodents: the effect on cloned NMDA receptors and the extracellular concentration. *Journal of Neurochemistry*, *65*(1), 454–458.

Matta, J. A., Ashby, M. C., Sanz-Clemente, A., Roche, K. W., & Isaac, J. T. R. (2011). mGluR5 and NMDA receptors drive the experience- and activity-dependent NMDA receptor NR2B to NR2A subunit switch. *Neuron*, *70*(2), 339–351.

Mayer, M. L. (2011). Emerging models of glutamate receptor ion channel structure and function. *Structure (London, England : 1993)*, *19*(10), 1370–1380.

Mayer, M. L., & Westbrook, G. L. (1987). Permeation and block of N-methyl-D-aspartic acid receptor channels by divalent cations in mouse cultured central neurones. *The Journal of physiology*, *394*, 501–527.

McKiernan, C. J., Stabila, P. F., & Macara, I. G. (1996). Role of the Rab3A-binding domain in targeting of rabphilin-3A to vesicle membranes of PC12 cells. *Molecular and cellular biology*, *16*(9), 4985–4995.

Mellone, M., & Gardoni, F. (2013). Modulation of NMDA receptor at the synapse: Promising therapeutic interventions in disorders of the nervous system. *European Journal of Pharmacology*.

Mercuri, N. B., & Bernardi, G. (2005). The 'magic' of L-dopa: why is it the gold standard Parkinson's disease therapy? *Trends in pharmacological sciences*, *26*(7), 341–344.

Milnerwood, A. J., & Raymond, L. A. (2007). Corticostriatal synaptic function in mouse models of Huntington's disease: early effects of huntingtin repeat length and protein load. *The Journal of physiology*, *585*(Pt 3), 817–831.

Miyazaki, M., Shirataki, H., Kohno, H., Kaibuchi, K., Tsugita, A., & Takai, Y. (1994). Identification as beta-adducin of a protein interacting with rabphilin-3A in the presence of Ca2+ and phosphatidylserine. *Biochemical and biophysical research communications*, *205*(1), 460–466.

Mizoguchi, A., Yano, Y., Hamaguchi, H., Yanagida, H., Ide, C., Zahraoui, A., et al. (1994). Localization of Rabphilin-3A on the synaptic vesicle. *Biochemical and biophysical research communications*, *202*(3), 1235–1243.

Mohrmann, R., Köhr, G., Hatt, H., Sprengel, R., & Gottmann, K. (2002). Deletion of the C-terminal domain of the NR2B subunit alters channel properties and synaptic targeting of

N-methyl-D-aspartate receptors in nascent neocortical synapses. *Journal of neuroscience research*, *68*(3), 265–275.

Montaville, P., Coudevylle, N., Radhakrishnan, A., Leonov, A., Zweckstetter, M., & Becker, S. (2008). The PIP2 binding mode of the C2 domains of rabphilin-3A. *Protein science : a publication of the Protein Society*, *17*(6), 1025–1034.

Mony, L., Kew, J. N. C., Gunthorpe, M. J., & Paoletti, P. (2009). Allosteric modulators of NR2B-containing NMDA receptors: molecular mechanisms and therapeutic potential. *British journal of pharmacology*, *157*(8), 1301–1317.

Monyer, H., Burnashev, N., Laurie, D. J., Sakmann, B., & Seeburg, P. H. (1994). Developmental and regional expression in the rat brain and functional properties of four NMDA receptors. *Neuron*, *12*(3), 529–540.

Mori, H., & Mishina, M. (1995). Structure and function of the NMDA receptor channel. *Neuropharmacology*, *34*(10), 1219–1237.

Mori, H., Masaki, H., Yamakura, T., & Mishina, M. (1992). Identification by mutagenesis of a Mg(2+)-block site of the NMDA receptor channel. *Nature*, *358*(6388), 673–675.

Morissette, M., Dridi, M., Calon, F., Hadj Tahar, A., Meltzer, L. T., Bédard, P. J., & Di Paolo, T. (2006). Prevention of levodopa-induced dyskinesias by a selective NR1A/2B N-methyl-D-aspartate receptor antagonist in parkinsonian monkeys: implication of preproenkephalin. *Movement Disorders*, *21*(1), 9–17.

Moriyoshi, K., Masu, M., Ishii, T., Shigemoto, R., Mizuno, N., & Nakanishi, S. (1991). Molecular cloning and characterization of the rat NMDA receptor. *Nature*, *354*(6348), 31–37.

Mothet, J. P., Parent, A. T., Wolosker, H., Brady, R. O., Linden, D. J., Ferris, C. D., et al. (2000). D-serine is an endogenous ligand for the glycine site of the N-methyl-D-aspartate receptor. *Proceedings of the National Academy of Sciences of the United States of America*, *97*(9), 4926–4931.

Nakazawa, T., Komai, S., Watabe, A. M., Kiyama, Y., Fukaya, M., Arima-Yoshida, F., et al. (2006). NR2B tyrosine phosphorylation modulates fear learning as well as amygdaloid synaptic plasticity. *The EMBO journal*, *25*(12), 2867–2877.

Nase, G., Weishaupt, J., Stern, P., Singer, W., & Monyer, H. (1999). Genetic and epigenetic regulation of NMDA receptor expression in the rat visual cortex. *The European journal of neuroscience*, *11*(12), 4320–4326.

Nash, J. E., Fox, S. H., Henry, B., Hill, M. P., Peggs, D., McGuire, S., et al. (2000). Antiparkinsonian actions of ifenprodil in the MPTP-lesioned marmoset model of Parkinson's disease. *Experimental neurology*, *165*(1), 136–142.

Nash, J. E., Johnston, T. H., Collingridge, G. L., Garner, C. C., & Brotchie, J. M. (2005). Subcellular redistribution of the synapse-associated proteins PSD-95 and SAP97 in animal models of Parkinson's disease and L-DOPA-induced dyskinesia. *FASEB journal : official publication of the Federation of American Societies for Experimental Biology*, *19*(6), 583–585.

Nash, J. E., Ravenscroft, P., McGuire, S., Crossman, A. R., Menniti, F. S., & Brotchie, J. M. (2004). The NR2B-selective NMDA receptor antagonist CP-101,606 exacerbates L-DOPA-induced dyskinesia and provides mild potentiation of anti-parkinsonian effects of L-DOPA in the MPTP-lesioned marmoset model of Parkinson's disease. *Experimental neurology*, *188*(2), 471–479.

Nutt, J. G., Gunzler, S. A., Kirchhoff, T., Hogarth, P., Weaver, J. L., Krams, M., et al. (2008). Effects of a NR2B selective NMDA glutamate antagonist, CP-101,606, on dyskinesia and Parkinsonism. *Movement Disorders*, *23*(13), 1860–1866.

Omkumar, R. V., Kiely, M. J., Rosenstein, A. J., Min, K. T., & Kennedy, M. B. (1996). Identification of a phosphorylation site for calcium/calmodulindependent protein kinase II in the NR2B subunit of the N-methyl-D-aspartate receptor. *The Journal of biological chemistry*, *271*(49), 31670–31678.

Osborne, S. L., Wen, P. J., & Meunier, F. A. (2006). Phosphoinositide regulation of neuroexocytosis: adding to the complexity. *Journal of Neurochemistry*, *98*(2), 336–342.

Pachernegg, S., Strutz-Seebohm, N., & Hollmann, M. (2012). GluN3 subunit-containing NMDA receptors: not just one-trick ponies. *Trends in Neurosciences*, *35*(4), 240–249.

Paillé, V., Picconi, B., Bagetta, V., Ghiglieri, V., Sgobio, C., Di Filippo, M., et al. (2010). Distinct levels of dopamine denervation differentially alter striatal synaptic plasticity and NMDA receptor subunit composition. *Journal of Neuroscience*, *30*(42), 14182–14193.

Paoletti, P. (2011). Molecular basis of NMDA receptor functional diversity. *The European journal of neuroscience*, *33*(8), 1351–1365.

Paoletti, P., Bellone, C., & Zhou, Q. (2013). NMDA receptor subunit diversity: impact on receptor properties, synaptic plasticity and disease. *Nature Reviews Neuroscience*, *14*(6), 383–400.

Papouin, T., Ladepeche, L., Ruel, J., Sacchi, S., Labasque, M., Hanini, M., et al. (2012). Synaptic and extrasynaptic NMDA receptors are gated by different endogenous coagonists. *Cell*, *150*(3), 633–646.

Park, J. J., & Loh, Y. P. (2008). How peptide hormone vesicles are transported to the secretion site for exocytosis. *Molecular endocrinology (Baltimore, Md.)*, *22*(12), 2583–2595. doi:10.1210/me.2008-0209

Philpot, B. D., Cho, K. K. A., & Bear, M. F. (2007). Obligatory role of NR2A for metaplasticity in visual cortex. *Neuron*, *53*(4), 495–502.

Philpot, B. D., Sekhar, A. K., Shouval, H. Z., & Bear, M. F. (2001). Visual experience and deprivation bidirectionally modify the composition and function of NMDA receptors in visual cortex. *Neuron*, *29*(1), 157–169.

Piccoli, G., Verpelli, C., Tonna, N., Romorini, S., Alessio, M., Nairn, A. C., et al. (2007). Proteomic analysis of activity-dependent synaptic plasticity in hippocampal neurons. *Journal of proteome research*, *6*(8), 3203–3215.

Picconi, B., Centonze, D., Håkansson, K., Bernardi, G., Greengard, P., Fisone, G., et al. (2003). Loss of bidirectional striatal synaptic plasticity in L-DOPA-induced dyskinesia. *Nature Neuroscience*, *6*(5), 501–506.

Picconi, B., Gardoni, F., Centonze, D., Mauceri, D., Cenci, M. A., Bernardi, G., et al. (2004). Abnormal Ca2+-calmodulin-dependent protein kinase II function mediates synaptic and motor deficits in experimental parkinsonism. *Journal of Neuroscience*, *24*(23), 5283–5291.

Piña-Crespo, J. C., Talantova, M., Micu, I., States, B., Chen, H.-S. V., Tu, S., et al. (2010). Excitatory glycine responses of CNS myelin mediated by NR1/NR3 "NMDA" receptor subunits. *Journal of Neuroscience*, *30*(34), 11501–11505.

Priestley, T., Laughton, P., Myers, J., Le Bourdellés, B., Kerby, J., & Whiting, P. J. (1995). Pharmacological properties of recombinant human N-methyl-D-aspartate receptors

comprising NR1a/NR2A and NR1a/NR2B subunit assemblies expressed in permanently transfected mouse fibroblast cells. *Molecular pharmacology*, *48*(5), 841–848.

Prybylowski, K., Chang, K., Sans, N., Kan, L., Vicini, S., & Wenthold, R. J. (2005). The synaptic localization of NR2B-containing NMDA receptors is controlled by interactions with PDZ proteins and AP-2. *Neuron*, *47*(6), 845–857.

Qian, A., & Johnson, J. W. (2006). Permeant ion effects on external Mg2+ block of NR1/2D NMDA receptors. *Journal of Neuroscience*, *26*(42), 10899–10910.

Qian, A., Antonov, S. M., & Johnson, J. W. (2002). Modulation by permeant ions of Mg(2+) inhibition of NMDA-activated whole-cell currents in rat cortical neurons. *The Journal of physiology*, *538*(Pt 1), 65–77.

Qian, A., Buller, A. L., & Johnson, J. W. (2005). NR2 subunit-dependence of NMDA receptor channel block by external Mg2+. *The Journal of physiology*, *562*(Pt 2), 319–331.

Quinlan, E. M., Olstein, D. H., & Bear, M. F. (1999a). Bidirectional, experience-dependent regulation of N-methyl-D-aspartate receptor subunit composition in the rat visual cortex during postnatal development. *Proceedings of the National Academy of Sciences of the United States of America*, *96*(22), 12876–12880.

Quinlan, E. M., Philpot, B. D., Huganir, R. L., & Bear, M. F. (1999b). Rapid, experience-dependent expression of synaptic NMDA receptors in visual cortex in vivo. *Nature Neuroscience*, *2*(4), 352–357.

Raveendran, R., Devi Suma Priya, S., Mayadevi, M., Steephan, M., Santhoshkumar, T. R., Cheriyan, J., et al. (2009). Phosphorylation status of the NR2B subunit of NMDA receptor regulates its interaction with calcium/calmodulin-dependent protein kinase II. *Journal of Neurochemistry*, *110*(1), 92–105.

Riou, M., Stroebel, D., Edwardson, J. M., & Paoletti, P. (2012). An alternating GluN1-2-1-2 subunit arrangement in mature NMDA receptors. *PloS one*, *7*(4), e35134.

Rosé, S. D., Lejen, T., Casaletti, L., Larson, R. E., Pene, T. D., & Trifaró, J.-M. (2003). Myosins II and V in chromaffin cells: myosin V is a chromaffin vesicle molecular motor involved in secretion. *Journal of Neurochemistry*, *85*(2), 287–298.

Rothman, S. M., & Mattson, M. P. (2013). Activity-dependent, stress-responsive BDNF signaling and the quest for optimal brain health and resilience throughout the lifespan. *Neuroscience*, *239*, 228–240.

Rudolf, R., Kögel, T., Kuznetsov, S. A., Salm, T., Schlicker, O., Hellwig, A., et al. (2003). Myosin Va facilitates the distribution of secretory granules in the F-actin rich cortex of PC12 cells. *Journal of cell science*, *116*(Pt 7), 1339–1348.

Rudolf, R., Salm, T., Rustom, A., & Gerdes, H. H. (2001). Dynamics of immature secretory granules: role of cytoskeletal elements during transport, cortical restriction, and F-actin-dependent tethering. *Molecular Biology of the Cell*, *12*(5), 1353–1365.

Rumbaugh, G., Prybylowski, K., Wang, J. F., & Vicini, S. (2000). Exon 5 and spermine regulate deactivation of NMDA receptor subtypes. *Journal of neurophysiology*, *83*(3), 1300–1306.

Rylander, D., Recchia, A., Mela, F., Dekundy, A., Danysz, W., & Cenci, M. A. (2009). Pharmacological modulation of glutamate transmission in a rat model of L-DOPA-induced dyskinesia: effects

on motor behavior and striatal nuclear signaling. *The Journal of pharmacology and experimental therapeutics*, *330*(1), 227–235.

Sakurada, K., Masu, M., & Nakanishi, S. (1993). Alteration of Ca2+ permeability and sensitivity to Mg2+ and channel blockers by a single amino acid substitution in the N-methyl-D-aspartate receptor. *The Journal of biological chemistry*, *268*(1), 410–415.

Salussolia, C. L., Prodromou, M. L., Borker, P., & Wollmuth, L. P. (2011). Arrangement of subunits in functional NMDA receptors. *Journal of Neuroscience*, *31*(31), 11295–11304.

Sanhueza, M., Fernandez-Villalobos, G., Stein, I. S., Kasumova, G., Zhang, P., Bayer, K. U., et al. (2011). Role of the CaMKII/NMDA receptor complex in the maintenance of synaptic strength. *Journal of Neuroscience*, *31*(25), 9170–9178.

Sans, N., Petralia, R. S., Wang, Y. X., Blahos, J., Hell, J. W., & Wenthold, R. J. (2000). A developmental change in NMDA receptor-associated proteins at hippocampal synapses. *Journal of Neuroscience*, *20*(3), 1260–1271.

Sanz-Clemente, A., Matta, J. A., Isaac, J. T. R., & Roche, K. W. (2010). Casein kinase 2 regulates the NR2 subunit composition of synaptic NMDA receptors. *Neuron*, *67*(6), 984–996.

Sanz-Clemente, A., Nicoll, R. A., & Roche, K. W. (2012). Diversity in NMDA Receptor Composition: Many Regulators, Many Consequences. *The Neuroscientist : a review journal bringing neurobiology, neurology and psychiatry*.

Sawada, H., Oeda, T., Kuno, S., Nomoto, M., Yamamoto, K., Yamamoto, M., et al. (2010). Amantadine for dyskinesias in Parkinson's disease: a randomized controlled trial. *PloS one*, *5*(12), e15298.

Schlüter, O. M., Schnell, E., Verhage, M., Tzonopoulos, T., Nicoll, R. A., Janz, R., et al. (1999). Rabphilin knock-out mice reveal that rabphilin is not required for rab3 function in regulating neurotransmitter release. *Journal of Neuroscience*, *19*(14), 5834–5846.

Schneggenburger, R. (1996). Simultaneous measurement of Ca2+ influx and reversal potentials in recombinant N-methyl-D-aspartate receptor channels. *Biophysical journal*, *70*(5), 2165–2174.

Schulz, S., Siemer, H., Krug, M., & Höllt, V. (1999). Direct evidence for biphasic cAMP responsive element-binding protein phosphorylation during long-term potentiation in the rat dentate gyrus in vivo. *The Journal of neuroscience : the official journal of the Society for Neuroscience*, *19*(13), 5683–5692.

Schwarting, R. K., & Huston, J. P. (1996). The unilateral 6-hydroxydopamine lesion model in behavioral brain research. Analysis of functional deficits, recovery and treatments. *Progress in neurobiology*, *50*(2-3), 275–331.

Selkoe, D. J. (2002). Alzheimer's disease is a synaptic failure. *Science*, *298*(5594), 789–791.

Sgambato-Faure, V., & Cenci, M. A. (2012). Glutamatergic mechanisms in the dyskinesias induced by pharmacological dopamine replacement and deep brain stimulation for the treatment of Parkinson's disease. *Progress in neurobiology*, *96*(1), 69–86.

Shankar, G. M., Bloodgood, B. L., Townsend, M., Walsh, D. M., Selkoe, D. J., & Sabatini, B. L. (2007). Natural oligomers of the Alzheimer amyloid-beta protein induce reversible synapse loss by modulating an NMDA-type glutamate receptor-dependent signaling pathway. *Journal of Neuroscience*, *27*(11), 2866–2875.

Shehadeh, J., Fernandes, H. B., Zeron Mullins, M. M., Graham, R. K., Leavitt, B. R., Hayden, M. R., & Raymond, L. A. (2006). Striatal neuronal apoptosis is preferentially enhanced by NMDA receptor activation in YAC transgenic mouse model of Huntington disease. *Neurobiology of Disease*, *21*(2), 392–403.

Sheng, M., Cummings, J., Roldan, L. A., Jan, Y. N., & Jan, L. Y. (1994). Changing subunit composition of heteromeric NMDA receptors during development of rat cortex. *Nature*, *368*(6467), 144–147.

Shinohara, Y., Hirase, H., Watanabe, M., Itakura, M., Takahashi, M., & Shigemoto, R. (2008). Left-right asymmetry of the hippocampal synapses with differential subunit allocation of glutamate receptors. *Proceedings of the National Academy of Sciences*, *105*(49), 19498–19503.

Shirataki, H., Kaibuchi, K., Yamaguchi, T., Wada, K., Horiuchi, H., & Takai, Y. (1992). A possible target protein for smg-25A/rab3A small GTP-binding protein. *The Journal of biological chemistry*, *267*(16), 10946–10949.

Shirataki, H., Yamamoto, T., Hagi, S., Miura, H., Oishi, H., Jin-no, Y., et al. (1994). Rabphilin-3A is associated with synaptic vesicles through a vesicle protein in a manner independent of Rab3A. *The Journal of biological chemistry*, *269*(52), 32717–32720.

Shulman, J. M., De Jager, P. L., & Feany, M. B. (2011). Parkinson's disease: genetics and pathogenesis. *Annual review of pathology*, *6*(1), 193–222. doi:10.1146/annurev-pathol-011110-130242

Simons, K., & Zerial, M. (1993). Rab proteins and the road maps for intracellular transport. *Neuron*, *11*(5), 789–799.

Smith, R., Klein, P., Koc-Schmitz, Y., Waldvogel, H. J., Faull, R. L. M., Brundin, P., et al. (2007). Loss of SNAP-25 and rabphilin 3a in sensory-motor cortex in Huntington's disease. *Journal of Neurochemistry*, *103*(1), 115–123.

Smith, R., Petersén, Å., Bates, G. P., Brundin, P., & Li, J.-Y. (2005). Depletion of rabphilin 3A in a transgenic mouse model (R6/1) of Huntington's disease, a possible culprit in synaptic dysfunction. *Neurobiology of Disease*, *20*(3), 673–684.

Snow, B. J., Macdonald, L., Mcauley, D., & Wallis, W. (2000). The effect of amantadine on levodopa-induced dyskinesias in Parkinson's disease: a double-blind, placebo-controlled study. *Clinical neuropharmacology*, *23*(2), 82–85.

Snyder, E. M., Nong, Y., Almeida, C. G., Paul, S., Moran, T., Choi, E. Y., et al. (2005). Regulation of NMDA receptor trafficking by amyloid-beta. *Nature Neuroscience*, *8*(8), 1051–1058.

Sobolevsky, A. I., Rosconi, M. P., & Gouaux, E. (2009). X-ray structure, symmetry and mechanism of an AMPA-subtype glutamate receptor. *Nature*, *462*(7274), 745–756.

Sprengel, R., Suchanek, B., Amico, C., Brusa, R., Burnashev, N., Rozov, A., et al. (1998). Importance of the intracellular domain of NR2 subunits for NMDA receptor function in vivo. *Cell*, *92*(2), 279–289.

Stahl, B., Chou, J. H., Li, C., Südhof, T. C., & Jahn, R. (1996). Rab3 reversibly recruits rabphilin to synaptic vesicles by a mechanism analogous to raf recruitment by ras. *The EMBO journal*, *15*(8), 1799–1809.

Steece-Collier, K., Chambers, L. K., Jaw-Tsai, S. S., Menniti, F. S., & Greenamyre, J. T. (2000). Antiparkinsonian actions of CP-101,606, an antagonist of NR2B subunit-containing N-methyl-d-aspartate receptors. *Experimental neurology*, *163*(1), 239–243.

Steigerwald, F., Schulz, T. W., Schenker, L. T., Kennedy, M. B., Seeburg, P. H., & Köhr, G. (2000). C-Terminal truncation of NR2A subunits impairs synaptic but not extrasynaptic localization of NMDA receptors. *The Journal of neuroscience : the official journal of the Society for Neuroscience*, *20*(12), 4573–4581.

Stern, P., Béhé, P., Schoepfer, R., & Colquhoun, D. (1992). Single-channel conductances of NMDA receptors expressed from cloned cDNAs: comparison with native receptors. *Proceedings. Biological sciences / The Royal Society*, *250*(1329), 271–277.

Steyer, J. A., & Almers, W. (1999). Tracking single secretory granules in live chromaffin cells by evanescent-field fluorescence microscopy. *Biophysical journal*, *76*(4), 2262–2271.

Stocca, G., & Vicini, S. (1998). Increased contribution of NR2A subunit to synaptic NMDA receptors in developing rat cortical neurons. *The Journal of physiology*, *507 (Pt 1)*, 13–24.

Strack, S., & Colbran, R. J. (1998). Autophosphorylation-dependent targeting of calcium/calmodulin-dependent protein kinase II by the NR2B subunit of the N-methyl- D-aspartate receptor. *The Journal of biological chemistry*, *273*(33), 20689–20692.

Sugars, K. L., & Rubinsztein, D. C. (2003). Transcriptional abnormalities in Huntington disease. *Trends in genetics : TIG*, *19*(5), 233–238.

Sun, Y., Savanenin, A., Reddy, P. H., & Liu, Y. F. (2001). Polyglutamine-expanded huntingtin promotes sensitization of N-methyl-D-aspartate receptors via post-synaptic density 95. *The Journal of biological chemistry*, *276*(27), 24713–24718.

Surmeier, D. J., Ding, J., Day, M., Wang, Z., & Shen, W. (2007). D1 and D2 dopamine-receptor modulation of striatal glutamatergic signaling in striatal medium spiny neurons. *Trends in Neurosciences*, *30*(5), 228–235.

Suvarna, N., Borgland, S. L., Wang, J., Phamluong, K., Auberson, Y. P., Bonci, A., & Ron, D. (2005). Ethanol alters trafficking and functional N-methyl-D-aspartate receptor NR2 subunit ratio via H-Ras. *The Journal of biological chemistry*, *280*(36), 31450–31459.

Südhof, T. C. (1995). The synaptic vesicle cycle: a cascade of protein-protein interactions. *Nature*, *375*(6533), 645–653.

Südhof, T. C. (1997). Function of Rab3 GDP-GTP exchange. *Neuron*, *18*(4), 519–522.

Südhof, T. C., & Rizo, J. (1996). Synaptotagmins: C2-domain proteins that regulate membrane traffic. *Neuron*, *17*(3), 379–388.

Swanwick, C. C., Shapiro, M. E., Yi, Z., Chang, K., & Wenthold, R. J. (2009). NMDA receptors interact with flotillin-1 and -2, lipid raft-associated proteins. *FEBS letters*, *583*(8), 1226–1230.

Takai, Y., Sasaki, T., Shirataki, H., & Nakanishi, H. (1996). Rab3A small GTP-binding protein in Ca(2+)-dependent exocytosis. *Genes to cells : devoted to molecular & cellular mechanisms*, *1*(7), 615–632.

Tan, M. G. K., Lee, C., Lee, J. H., Francis, P. T., Williams, R. J., Ramírez, M. J., et al. (2013). Decreased rabphilin 3A immunoreactivity in Alzheimer's disease is associated with Aβ burden. *Neurochemistry international*, *64C*, 29–36.

Tang, T. T.-T., Badger, J. D., Roche, P. A., & Roche, K. W. (2010). Novel approach to probe subunit-specific contributions to N-methyl-D-aspartate (NMDA) receptor trafficking reveals a

dominant role for NR2B in receptor recycling. *Journal of Biological Chemistry*, *285*(27), 20975–20981.

Thomas, A., Iacono, D., Luciano, A. L., Armellino, K., Di Iorio, A., & Onofrj, M. (2004). Duration of amantadine benefit on dyskinesia of severe Parkinson's disease. *Journal of neurology, neurosurgery, and psychiatry*, *75*(1), 141–143.

Thomas, C. G., Miller, A. J., & Westbrook, G. L. (2006). Synaptic and extrasynaptic NMDA receptor NR2 subunits in cultured hippocampal neurons. *Journal of neurophysiology*, *95*(3), 1727–1734.

Tovar, K. R., & Westbrook, G. L. (1999). The incorporation of NMDA receptors with a distinct subunit composition at nascent hippocampal synapses in vitro. *Journal of Neuroscience*, *19*(10), 4180–4188.

Tovar, K. R., & Westbrook, G. L. (2002). Mobile NMDA receptors at hippocampal synapses. *Neuron*, *34*(2), 255–264.

Townsend, M., Yoshii, A., Mishina, M., & Constantine-Paton, M. (2003). Developmental loss of miniature N-methyl-D-aspartate receptor currents in NR2A knockout mice. *Proceedings of the National Academy of Sciences of the United States of America*, *100*(3), 1340–1345.

Traynelis, S. F., Wollmuth, L. P., McBain, C. J., Menniti, F. S., Vance, K. M., Ogden, K. K., et al. (2010). Glutamate receptor ion channels: structure, regulation, and function. *Pharmacological reviews*, *62*(3), 405–496.

Tsuboi, T., & Fukuda, M. (2005). The C2B domain of rabphilin directly interacts with SNAP-25 and regulates the docking step of dense core vesicle exocytosis in PC12 cells. *The Journal of biological chemistry*, *280*(47), 39253–39259.

Tu, W., Xu, X., Peng, L., Zhong, X., Zhang, W., Soundarapandian, M. M., et al. (2010). DAPK1 interaction with NMDA receptor NR2B subunits mediates brain damage in stroke. *Cell*, *140*(2), 222–234.

Tyler, W. J., & Pozzo-Miller, L. (2003). Miniature synaptic transmission and BDNF modulate dendritic spine growth and form in rat CA1 neurones. *The Journal of physiology*, *553*(Pt 2), 497–509. doi:10.1113/jphysiol.2003.052639

Ubach, J., García, J., Nittler, M. P., Südhof, T. C., & Rizo, J. (1999). Structure of the Janus-faced C2B domain of rabphilin. *Nature cell biology*, *1*(2), 106–112. doi:10.1038/10076

Ungerstedt, U., & Arbuthnott, G. W. (1970). Quantitative recording of rotational behavior in rats after 6-hydroxy-dopamine lesions of the nigrostriatal dopamine system. *Brain Research*, *24*(3), 485–493.

Vance, K. M., Hansen, K. B., & Traynelis, S. F. (2012). GluN1 splice variant control of GluN1/GluN2D NMDA receptors. *The Journal of physiology*, *590*(Pt 16), 3857–3875.

Varadi, A., Ainscow, E. K., Allan, V. J., & Rutter, G. A. (2002). Involvement of conventional kinesin in glucose-stimulated secretory granule movements and exocytosis in clonal pancreatic beta-cells. *Journal of cell science*, *115*(Pt 21), 4177–4189.

Varadi, A., Tsuboi, T., & Rutter, G. A. (2005). Myosin Va transports dense core secretory vesicles in pancreatic MIN6 beta-cells. *Molecular Biology of the Cell*, *16*(6), 2670–2680.

Varadi, A., Tsuboi, T., Johnson-Cadwell, L. I., Allan, V. J., & Rutter, G. A. (2003). Kinesin I and cytoplasmic dynein orchestrate glucose-stimulated insulin-containing vesicle movements in clonal MIN6 beta-cells. *Biochemical and biophysical research communications*, *311*(2), 272–282.

Vastagh, C., Gardoni, F., Bagetta, V., Stanic, J., Zianni, E., Giampa, C., et al. (2012). NMDA receptor composition modulates dendritic spine morphology in striatal medium spiny neurons. *Journal of Biological Chemistry*.

Verhagen Metman, L., Del Dotto, P., van den Munckhof, P., Fang, J., Mouradian, M. M., & Chase, T. N. (1998). Amantadine as treatment for dyskinesias and motor fluctuations in Parkinson's disease. *Neurology*, *50*(5), 1323–1326.

Vicini, S., Wang, J. F., Li, J. H., Zhu, W. J., Wang, Y. H., Luo, J. H., et al. (1998). Functional and pharmacological differences between recombinant N-methyl-D-aspartate receptors. *Journal of neurophysiology*, *79*(2), 555–566.

Vissel, B., Krupp, J. J., Heinemann, S. F., & Westbrook, G. L. (2002). Intracellular domains of NR2 alter calcium-dependent inactivation of N-methyl-D-aspartate receptors. *Molecular pharmacology*, *61*(3), 595–605.

Vonsattel, J. P., & DiFiglia, M. (1998). Huntington disease. *Journal of neuropathology and experimental neurology*, *57*(5), 369–384.

Wang, J., Liu, S., Fu, Y., Wang, J. H., & Lu, Y. (2003). Cdk5 activation induces hippocampal CA1 cell death by directly phosphorylating NMDA receptors. *Nature Neuroscience*, *6*(10), 1039–1047.

Watanabe, M., Inoue, Y., Sakimura, K., & Mishina, M. (1992). Developmental changes in distribution of NMDA receptor channel subunit mRNAs. *Neuroreport*, *3*(12), 1138–1140.

Wessell, R. H., Ahmed, S. M., Menniti, F. S., Dunbar, G. L., Chase, T. N., & Oh, J. D. (2004). NR2B selective NMDA receptor antagonist CP-101,606 prevents levodopa-induced motor response alterations in hemi-parkinsonian rats. *Neuropharmacology*, *47*(2), 184–194.

Williams, K., Pahk, A. J., Kashiwagi, K., Masuko, T., Nguyen, N. D., & Igarashi, K. (1998). The selectivity filter of the N-methyl-D-aspartate receptor: a tryptophan residue controls block and permeation of Mg2+. *Molecular pharmacology*, *53*(5), 933–941.

Wolf, E., Seppi, K., Katzenschlager, R., Hochschorner, G., Ransmayr, G., Schwingenschuh, P., et al. (2010). Long-term antidyskinetic efficacy of amantadine in Parkinson's disease. *Movement Disorders*, *25*(10), 1357–1363.

Wollmuth, L. P., Kuner, T., Seeburg, P. H., & Sakmann, B. (1996). Differential contribution of the NR1- and NR2A-subunits to the selectivity filter of recombinant NMDA receptor channels. *The Journal of physiology*, *491 (Pt 3)*, 779–797.

Wyllie, D. J., Béhé, P., & Colquhoun, D. (1998). Single-channel activations and concentration jumps: comparison of recombinant NR1a/NR2A and NR1a/NR2D NMDA receptors. *The Journal of physiology*, *510 (Pt 1)*, 1–18.

Xu, Z., Chen, R.-Q., Gu, Q.-H., Yan, J.-Z., Wang, S.-H., Liu, S.-Y., & Lu, W. (2009). Metaplastic regulation of long-term potentiation/long-term depression threshold by activity-dependent changes of NR2A/NR2B ratio. *Journal of Neuroscience*, *29*(27), 8764–8773.

Yamaguchi, T., Shirataki, H., Kishida, S., Miyazaki, M., Nishikawa, J., Wada, K., et al. (1993). Two functionally different domains of rabphilin-3A, Rab3A p25/smg p25A-binding and

phospholipid- and Ca(2+)-binding domains. *The Journal of biological chemistry*, *268*(36), 27164–27170.

Yashiro, K., & Philpot, B. D. (2008). Regulation of NMDA receptor subunit expression and its implications for LTD, LTP, and metaplasticity. *Neuropharmacology*, *55*(7), 1081–1094.

Yasuda, M., Johnson-Venkatesh, E. M., Zhang, H., Parent, J. M., Sutton, M. A., & Umemori, H. (2011). Multiple forms of activity-dependent competition refine hippocampal circuits in vivo. *Neuron*, *70*(6), 1128–1142.

Yuan, H., Hansen, K. B., Vance, K. M., Ogden, K. K., & Traynelis, S. F. (2009). Control of NMDA receptor function by the NR2 subunit amino-terminal domain. *Journal of Neuroscience*, *29*(39), 12045–12058.

Zeron, M. M., Hansson, O., Chen, N., Wellington, C. L., Leavitt, B. R., Brundin, P., et al. (2002). Increased sensitivity to N-methyl-D-aspartate receptor-mediated excitotoxicity in a mouse model of Huntington's disease. *Neuron*, *33*(6), 849–860.

Zhang, H., Li, Q., Graham, R. K., Slow, E., Hayden, M. R., & Bezprozvanny, I. (2008). Full length mutant huntingtin is required for altered Ca2+ signaling and apoptosis of striatal neurons in the YAC mouse model of Huntington's disease. *Neurobiology of Disease*, *31*(1), 80–88.

Zhang, J., & Diamond, J. S. (2009). Subunit- and pathway-specific localization of NMDA receptors and scaffolding proteins at ganglion cell synapses in rat retina. *Journal of Neuroscience*, *29*(13), 4274–4286.

Zhang, Y., Luan, Z., Liu, A., & Hu, G. (2001). The scaffolding protein CASK mediates the interaction between rabphilin3a and beta-neurexins. *FEBS letters*, *497*(2-3), 99–102.

Zhou, X., Ding, Q., Chen, Z., Yun, H., & Wang, H. (2013). Involvement of the GluN2A and GluN2B subunits in synaptic and extrasynaptic N-methyl-D-aspartate receptor function and neuronal excitotoxicity. *Journal of Biological Chemistry*, *288*(33), 24151–24159.

Zhu, J. J., Qin, Y., Zhao, M., Van Aelst, L., & Malinow, R. (2002). Ras and Rap control AMPA receptor trafficking during synaptic plasticity. *Cell*, *110*(4), 443–455.

Zuccato, C., Valenza, M., & Cattaneo, E. (2010). Molecular mechanisms and potential therapeutical targets in Huntington's disease. *Physiological reviews*, *90*(3), 905–981.

ABBREVIATIONS

6-OHDA: 6-hydroxydopamine

ABD: agonist binding domain

AD: Alzheimer's disease

AMPA: 3-hydroxy-5-methyl-4-isoxazole proprionic acid

AP: Anterio-posterior coordonates

APP: amyloid precursor protein

Aβ: β-amyloid

BR-MyoVa: brain-spliced isoform of Myosin Va

Ca^{2+}: calcium

CAMKII: Ca^{2+}-calmodulin kinase II

Cb: Cerebellum

CNS: central nervous system

coIP: coImmunoprecipitation

CPP: cell-permeable peptide

CTD: C-terminal domain

Cx: Cortex

DA: dopaminergic/dopamine

DIV: day *in vitro*

DV: dorso-ventral coordinates

E: embryonic stage day

eGFP: enhanced green fluorescent protein

EPSC: excitatory postsynaptic current

ER: endoplasmatic reticulum

fEPSCP: field excitatory postsynaptic potential

GFP: green fluorescent protein

GluN: subunit of NMDAR

H or Homo: homogenate

HD: Huntington's disease

Hp: Hippocampus

htt: huntingtin

i.p.: intraperitoneal

iGluR: ionotropic glutamate receptor

Ip3: inositol-1,4,5-trisphosphate

K^+: potassium

KA: kainate

L: lateral coordinate

L-DOPA: L-3,4-dihydroxyphenylalanine (also levodopa)

LID: L-DOPA-Induced Dyskinesia

LTP: long term potentiation

MAGUK: membrane-associated guanylate kinase

Mg^{2+}: magnesium

mGluR: metabotropic glutamate receptor

mhtt: Mutated htt

MPTP: 1-methyl-4-phenyl-1,2,3,6-tetrahydropyridine

MSN: medium spiny neurons

Na^+: sodium

NMDA: *N*-methyl-D-aspartate

NMDAR: NMDA receptor

nNOS: nitric oxide synthase

NTD: N-terminal domain

P2: crude membrane fraction (pellet 2)

P234-Rph3A: phosphorylated form of Rph3A at Ser234

P: postnatal day

PD: Parkinson's disease

PIP2: Phosphatidylinositol-4,5-bisphosphate

PSD: postsynaptic density

Ras-GRF1: Ras-guanine nucleotide-releasing factor

RasGAP: Ras GTPase activating protein

RFP: red fluorescent protein

Rph3A: Rabphilin3A

s.c.: subcutaneous

SGs: secretory granules

SNARE: soluble N-ethylmaleimide-sensitive factor attachment protein receptor

St: Striatum

STEP: striatal enriched tyrosine phosphatase

Syn: synaptosomes

tGFP: turbo GFP

TIF: Triton-X-100 Insoluble Fraction

TMD: transmembrane domain